Aus dem Institut für Schlaganfall- und Demenzforschung

der Ludwig – Maximilians – Universität München

Direktor: Prof. Dr. M. Dichgans

Effect of bradykinin receptor 1 and acid-sensing ion channel 1a on outcome after experimental traumatic brain injury

Dissertation

zum Erwerb des Doktorgrades der Medizin

an der Medizinischen Fakultät der

LUDWIG – MAXIMILIANS – UNIVERSITÄT ZU MÜNCHEN

VORGELEGT VON

Shiqi Cheng

aus

Nanchang, Jiangxi, China

2020

Mit Genehmigung der Medizinischen Fakultät

der Universität München

Berichterstatter:	Prof. Dr. med. Nikolaus Plesnila
Mitberichterstatter:	Prof. Dr. Uwe Ködel
	Prof. Dr. Jennifer Linn
	Prof. Dr. Sabine Liebscher
Mitbetreuung durch den promovierten Mitarbeiter:	PD Dr. med. Nicole Angela Terpolilli
Dekan:	Prof. Dr. med. dent. Reinhard Hickel
Tag der mündlichen Prüfung:	26.05.2020

Table of Contents

1. Introduction

1.1 Traumatic Brain Injury

1.1.1 Epidemiology

Traumatic brain injury (TBI) is a cerebral insult with high morbidity and mortality. In past decades, TBI imposed a heavy socioeconomic burden on society, leading to relevant public health problems due to high rates of permanent disability and high health care costs [1-4]. There are approximately 69 million people who suffer from TBI each year worldwide. The incidence of TBI differs across different countries and regions. In 2015, the World Health Organization (WHO) reported the highest incidence rate for the USA/Canada (1299/100,000) and the lowest rate for Africa (801/100,000) [5] (Figure 1). In 2013, TBI led to 282,000 hospitalizations and 56,000 deaths, which accounted for 30 percent of all injury-related deaths in the USA [6]. In Europe, the annual mean incidence rate of TBI was reported to be 326 per 100,000 from 1990 to 2014 [7]; the majority of patients are male [7] and either below 25 or above 75 years of age [8]. In the US, the main age-groups affected by TBI are infants (0 to 4 years; 1591/ 100,000), young adults (15 to 24 years; 1081/100,000), and the elderly (≥75 years; 2232/100,000 [9]).

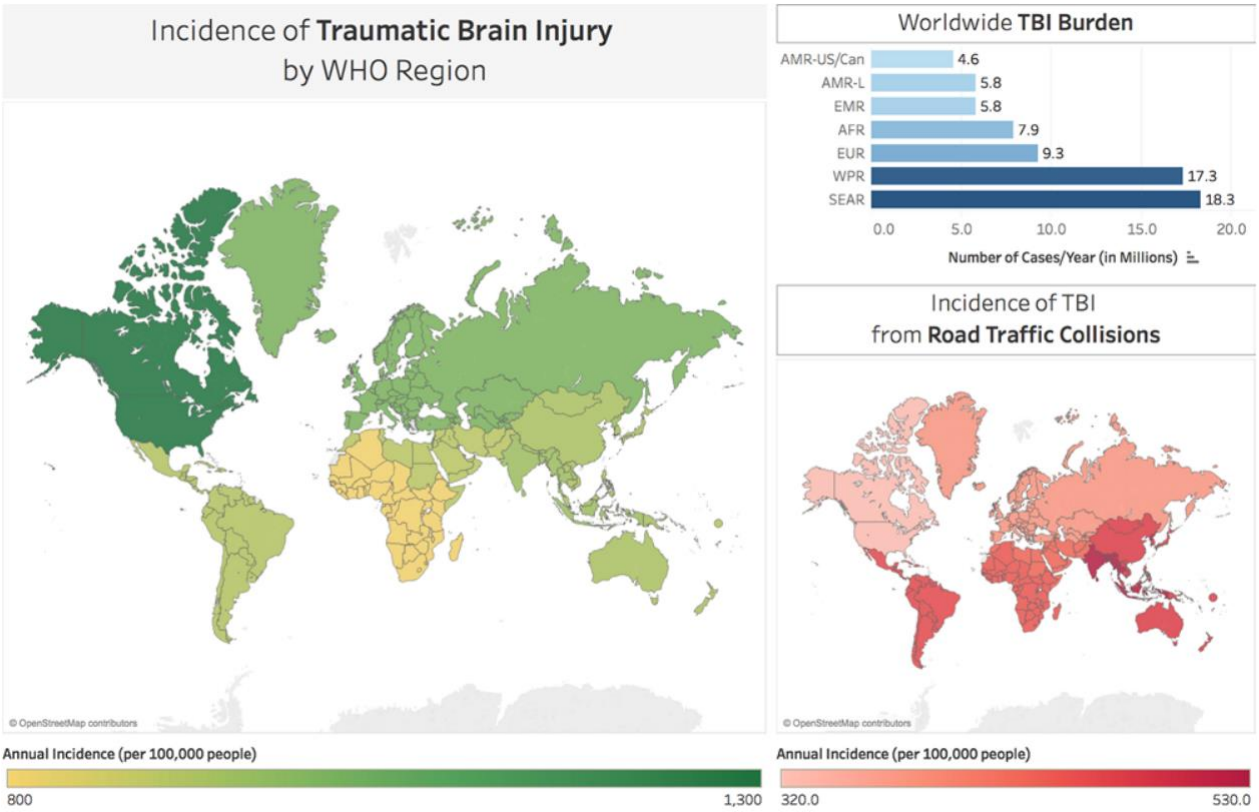

Figure 1: Map illustrating the occurrence of TBI cases per 100,000 people in the worldwide (left). Histogram (upper right) showing the evaluated volume of TBI annually across WHO regions. Map (lower right) indicating the occurrence of TBI (cases per 100,000 people) caused by traffic accidents by WHO region [5]

1.1.2 Etiology

The causes of TBI are multifaceted, including falls, accidents, sports injuries, and ballistic/military trauma. Falls, responsible for approximately 50% of all cases [10, 11], are the major cause of TBI in infants and the elderly with over 13,000 cases every year [12]. About one fourth of TBI cases [13] arises from accidents, either by traffic-related injury [14] or by blunt trauma to the head [15]. Motor vehicle and traffic-related incidents are responsible for most TBI-related deaths [16]. There is an increase in sports-related mild TBI cases (ranging from 1.6 to 3.8 million/a) in the USA [17]. Sports-related and violence-related traumatic brain injury is far more frequent in males than in females [18, 19].

1.1.3 Classification

1.1.3.1 Classification by injury severity – the Glasgow Coma Score

In order to grade injury severity, TBI can be classified in several ways. The most commonly utilized clinical grading system is the Glasgow Coma Scale (GCS) (Figure 2), which correlates well with injury severity and outcome [20].

Behavior	**Response**
Eye Opening (E)	4 = spontaneous 3 = to sound 2 = to pressure 1 = none
Verbal Response (V)	5 = orientated 4 = confused 3 = words, but not coherent 2 = sounds, but no words 1 = none
Motor Response (M)	6 = obeys command 5 = localizing 4 = normal flexion 3 = abnormal flexion 2 = extension 1 = none

Figure 2: Glasgow Coma Scale Score (modified according to Teasdale and Jennett) [20]

The GCS ranges from 3 to 15 points, 3 being the worst and 15 the best score [21]. GCS evaluates three domains: eye response (E, max. 4 points), verbal response (V, max. 5 points), and motor response (M, max. 6 points). The components of the GCS should be recorded individually. A composite score of more than 12 in a TBI patients is classified as mild brain injury, the score from 9 to 12 as a moderate injury, and a score of less than 9 indicates severe brain injury. However, this scoring system has also limitations. For example, a fully conscious patient with severe cervical spinal cord injury may be unable to perform motor tasks. Also, scoring of eye movements in patients with ocular injury or bulbar trauma may not be possible [22]. Age and preexisting conditions and disabilities like dementia and/or aphasia can lead to variance in diagnosis and outcome [13, 23, 24]. Lastly, GCS cannot be reliably obtained in patients who are sedated and/or intubated.

1.1.3.2 Patho-anatomic classification

Apart from clinical variables, TBI can be graded using radiomorphologic features obtained by computed tomography (CT) or magnetic resonance imaging (MRI). This patho-anatomic classification takes into account location and patterns of (structural) injury thus helping to determine possible treatment strategies. Common features occurring in TBI can be either classified as focal lesions such as skull fractures, epidural, subdural, intracerebral hematoma, brain contusions and lacerations, or more diffuse injury patterns, called “diffuse axonal injury” (DAI) [25]. CT scanning is the most widely available and reliable imaging method and therefore the first option for diagnosis of acute TBI in an emergency situation in adults. In 1992, the Marshall Score was first introduced as a CT based classification system (Figure 3) to describe the severity and predict mortality of TBI [26]. A primary disadvantage of the Marshal Score is that patients with multiple injuries cannot be clearly classified and that CT scanning is not standardized thereby making unambiguous grading difficult [27].

Category	Definition
Diffuse injury I	No visible intracranial pathology
Diffuse injury II	Midline shift of 0 to 5 mm; basal cisterns remain visible; no high or mixed density lesions >25 cm^3
Diffuse injury III (swelling)	Midline shift of 0 to 5 mm; basal cisterns compressed or completely effaced; no high or mixed density lesions >25 cm^3
Diffuse injury IV (shift)	Midline shift > 5mm; no high or mixed density lesions >25 cm^3
Evacuated mass lesion V	Any lesion evacuated surgically
Non-evacuated mass lesion VI	High or mixed density lesions >25 cm^3; not surgically evacuated

Figure 3: Marshall Classification of TBI based on CT scan (modified from Marshall scores) [26]

1.1.3.3 Classification of TBI by injury mechanism

TBI can be subdivided according to injury mechanism into closed head injury, open head injury, and acceleration-deceleration injury. In closed head injury, the dura mater remains intact. Still, this type of injury can give rise to long-term physical, cognitive and psychological impairments [28, 29]. Open head injury, especially with penetrating injury (dislocated skull fracture, penetrated dura mater and meninges) usually results in severe and most often permanent tissue damage and, thus, disability.

1.1.4 Pathophysiology of traumatic brain injury

The pathophysiology of TBI develops in a two-staged process, primary and secondary brain injury. Primary brain injury arises from the mechanical impact hitting the head and

develops within seconds. The degree of the primary injury depends solely on the traumatic force itself and therefore cannot be influenced by treatment. Following the initial damage, a plethora of secondary mechanism occurs that eventually leads to an increase in tissue injury. This process starts minutes after trauma and may continue for decades after the initial injury [30].

1.1.4.1 Primary brain injury

Primary brain injury arises from external forces impacting the head, resulting in disruption of anatomic brain structures. Common injury patterns include focal brain contusions, diffuse and focal vascular injuries (extradural hemorrhage, subdural hemorrhage, subarachnoid hemorrhage, intra-parenchymal, and intra-ventricular hemorrhage) and diffuse axonal injury resulting from axonal shearing [31, 32].

1.1.4.1.1 Focal brain contusions

Focal brain contusions are defined as regional abrasions of brain tissue. They commonly occur in frontal and temporal lobes and are caused by collision between brain and bony structures at the skull base. Clinically, they are often characterized by severe headache, varied levels of unconsciousness, and vomiting [33, 34]. Brain contusions are a very common injury pattern and are frequently diagnosed after road traffic incidents [35]. On a histopathological level, brain contusions reveal a variety of pathological changes, including focal brain tissue necrosis and hemorrhage, commonly entailing cortex and subcortical white matter [36].

1.1.4.1.2 Diffuse and focal vascular injuries

Depending on the vessels injured, TBI may result in extradural, subdural, intra-parenchymal, or intra-ventricular hematoma as well as subarachnoid hemorrhage. Extradural (also called epidural) hematoma is most commonly caused by disruption of a meningeal artery, particularly the middle meningeal artery (75%) [37] due to skull fracture [38]. Typically, patients suffer from a short-lasting unconsciousness which is followed by

a period of consciousness and a secondary deterioration of consciousness [39]. Due to their mass effect with consecutive risk of herniation, large epidural hematomas usually need to be surgically removed; if treated in time prognosis is usually favorable [40]. In subdural hematoma (SDH), blood accumulates between the surface of the arachnoid membrane and the inner layer of the dura mater due to the disruption of bridging veins [41]. SDH usually presents with severe headache, focal neurological deficits, loss of consciousness or coma [42, 43]. SDH occurs in approximately 15% of all head trauma cases and is present in up to 30% of fatal TBI cases. Because subdural hematomas may expand quickly and unimpededly, quick surgical intervention is usually necessary in order to avoid massive intracranial hypertension. However, even with swift intervention morbidity and mortality of SDH remain high [44].

Traumatic subarachnoid hemorrhage (tSAH) due to vessel rupture between the pial and the arachnoid membrane [45] is present in up to 53% of TBI cases and is commonly found after road traffic accidents [46]. Greene et al. used CT criteria to grade tSAH. Common complications of tSAH are cerebral vasospasm which may lead to infarctions and hydrocephalus [47].

1.1.4.1.3 Diffuse axonal injury

Diffuse axonal injury (DAI) is a common lesion type in TBI [48]. DAI often results from rapid acceleration and deceleration of the brain leading to shearing of axons [49]. DAI commonly occurs during high-speed collisions [6]. It can be classified in three grades according to location, extent, and severity of white matter changes/ injuries [50]. In DAI, mechanical forces disrupt the cytoskeleton of axons, thus leading to axonal proteolysis and swelling [51] which may result in dysfunction of neuronal interconnection [52].

The diagnosis of DAI is based on CT or MRI scans and the clinical presentation of the patient. Most common clinical symptoms of DAI include headache, dizziness, and nausea. DAI is often the explanation why a patient is unconscious even though the CT scan does

not reveal gross pathology. Severe DAI can lead to loss of consciousness [53] and may result in long-term functional impairments [54].

1.1.4.2 Secondary brain injury

Secondary injury occurs minutes up to several years after the primary injury [55, 56] and involves complex cellular, molecular and vascular mechanisms, including cerebral edema, impaired cerebral metabolism, alterations of cerebral blood flow and autoregulation, free radical formation, excitotoxicity, and neuroinflammation, just to name a few [57].

1.1.4.2.1 Acute Secondary Brain Injury

1.1.4.2.1.1 Oxidative stress

Oxidative stress is defined as an imbalance between antioxidant defense mechanisms and the production of reactive oxygen species (ROS). Reactive oxygen species include peroxides, superoxide, hydroxyl radicals, and singlet oxygen [58], and play a crucial role in acute secondary brain injury [59, 60].

Hypoxia after TBI leads to acidosis which in turn activates pH-dependent calcium channels, resulting in increased production of ROS/reactive nitrogen species (RNS) and a massive activation of phospholipases [61]. Also, ruptured red blood cells (RBC) after TBI may induce ROS formation [62] as the massive release of free hemoglobin and degraded hemoglobin releases iron, which catalyzes ROS production [63].

Under physiological conditions, formation of ROS and free radicals is prevented through antioxidative systems (e.g. glutamine, glutathione) [64, 65]. In experimental TBI, an increase of hydroxyl radicals and superoxide anions is observed in the acute phase post-injury. These harmful molecules impair the mitochondrial electron transport chain (ETC) thereby decreasing the production of ATP and finally leading to necrotic or apoptotic cell death [66].

1.1.4.2.1.2 Excitotoxicity

Excitotoxicity mediated by N-methyl-D-aspartic acid (NMDA) and α-amino-3-hydroxy5-methyl-4-isoxazole-propionic acid (AMPA) glutamate receptors [67] plays a pivotal role in secondary brain injury after TBI. Elevated extracellular glutamate activates NMDA receptors thereby triggering an influx of sodium and calcium ions into neurons. High cytosolic calcium concentrations in turn activate a variety of pathological mechanisms which finally result in injury of the cytoskeleton, DNA lysis, and ultimately necrosis and apoptosis [68]. The most important factor triggered by excess glutamate in neurons is an increase in intracellular calcium [69]. Calcium overload eventually impedes mitochondrial function. The over-activation of the calcium-dependent mitochondrial permeability transition pore (mPTP) disrupts the membrane potential of mitochondria thus disabling ATP production [66, 70].

1.1.4.2.1.3 Inflammatory responses

At the moment of brain injury, danger-associated molecular patterns (DAMPs) and alarmins are released into the extracellular space where they can then be recognized by pattern recognition receptors (PRRs) and cytokine receptors on resident cells of the central nervous system (CNS). This process stimulates the local production of cytokines and chemokines, for example, Interleukin (IL)-1ß, 6,12, and 18, tumor necrosis factor alpha (TNF-α), and Interferon-gamma (IFN-γ), that are involved in coordinating the activation, expansion, and recruitment of leukocytes in the injury region. As the first reactor of inflammatory response after injury, neutrophils arrive within a few hours into the sub-arachnoid and perivascular space surrounding the primary damage/contusion, then enter the brain parenchyma as early as 24 h after injury [71-75]. The peak of neutrophils accumulation appears within the first day and decreases dramatically from days 3 to 5 post-injury [76, 77]. The main function of neutrophils seems to be the cleaning up the cellular debris and damaged cells in the injured region. However, the exact functional relevance of neutrophils post-TBI is inconclusive. A study [78] reports that

neutrophils associated with BBB breakdown and neurodegeneration, but neutrophils do not seem to contribute to posttraumatic blood brain barrier (BBB) disruption as pharmacological depletion did not affect BBB damage [79]. Similarly, another study found neutrophil depletion by an anti-Gr-1 antibody reduced edema formation, microglia activation, and activated caspase-3-positive cells 24 h after controlled cortical injury, but did not affect BBB leakage [80]. Blocking CD11d, a marker of neutrophils, improved behavioral outcome after mild experimental TBI [81]. In a CCI model using neutrophil elastase (NE) knockout mice, Semple *et al*. found significantly decreased brain edema formation as well as a reduction of apoptotic neurons in the hippocampus 24 h after injury. However, NE deficiency did not translate into long-term neuroprotection since it did not ameliorate cortical or hippocampal damage two months post-injury. These results indicate that NE activity contributes to brain edema and early neurodegeneration, but fail to protect against long-term secondary injury after brain injury [82].

Microglia play a pivotal role in the inflammatory response after TBI. Microglia are the first cells responding to brain injury by extending their process towards the injury site within minutes after TBI [83]. When activated, microglia produce pro- and anti-inflammatory factors that result in the recruitment of resident and peripheral cells. The role of microglia in posttraumatic brain damage is often controversial and a lot of studies even suggest that they may be neurotoxic [84]. P38α MAPK regulates the changes in microglia morphology and facilitates the production of pro-inflammatory cytokine from activated microglia [85]. Activated microglia increase expression of IL-1β, CD14, and arginase 24 hours post-trauma [86]. Activation of microglia releases a range of inflammatory triggers, including cytokines (such as IL-1b, TNF-a), metalloproteinase, and reactive oxygen species [87, 88]. The reduction of gap-junction proteins from 6 hours to 4 days after TBI and subsequent edema formation is mediated by microglial activation and chemotaxis [89]. However, microglia may also play neuroprotective roles in the CNS by removing cell debris and maintaining the integrity of the BBB and the glial limitans [90, 91]. Neurotrophins released by microglia

are involved in the reconstruction of the nervous system after injury [92]. Reduction of microglia exacerbates hippocampal neuron death indicating a neuroprotective role of microglia [93]. However, the effect of microglia on the inflammatory response depends on their activation state, which is classified into M1 and M2 polarization states. M1 microglia play a pro-inflammatory role while M2 play an anti-inflammatory role [94]. M1 microglia are mainly presented from 3 to 7 days after TBI, while the number of M2 microglia increases from day 5 after experimental TBI [95]. Elevation of M2 microglia improves histological and functional outcome in experimental TBI [96]. Chronic activation of M2 microglia exert a trophic role in primates after TBI [97]. So far, it is still uncertain how microglia contribute to the development of posttraumatic brain damage.

1.1.4.2.1.4 Cerebral edema

Two types of cerebral edema [98] have been described: cytotoxic edema, characterized by accumulation of intracellular water as a result of cellular damage, and vasogenic edema, characterized by accumulation of extracellular water as a result of vascular leakage due to disruption of the blood brain barrier [99].

In cytotoxic edema, i. e. cellular swelling, water influx into the cell is the result of activation of ion-selective channels, such as the Na^+/H^+ exchanger, the Na^+-K^+-$2Cl^-$ cotransporter (NKCC1), and the $Na^+/HCO3^-$ transporter family, and a subsequent increase in intracellular Na^+ and K^+ [100, 101]. In essence, cytotoxic edema is a physiologic response of astrocytes, which try to maintain the homeostasis of the extracellular space in the brain [102-107].

Vasogenic edema mainly results from the destruction of the structural integrity of the BBB allowing water efflux from the vascular lumen towards the interstitial space [98, 108]. The BBB consists of endothelial cells, astrocyte end-feet, pericytes, and tight junctions (TJ) and separates the blood from cerebral tissue and interstitial space [109]. After TBI, extravasated protein-rich fluid may pass through the disrupted BBB and deposit in the extracellular compartment resulting in increases in oncotic pressure which ultimately

causes water influx and, subsequently, an increase in brain volume [110]. A variety of molecules take part in the secondary disruption of the BBB after mechanical trauma thereby aggravating vasogenic edema, for example inflammatory cytokines (tumor necrosis factor (TNF), interleukins (IL) 6 ,1β) [83, 111], chemokines (CXCL1 and CXCL2, CCL2), inflammatory cells (neutrophil infiltration, microglia) [112, 113], vascular endothelial growth factor A (VEGF-A) [114], matrix metalloproteinase (MMP-2, MMP-9), and aquaporin 4 (AQP4) [107, 110, 115].

1.1.4.2.1.5 Intracranial hypertension

The average intracranial volume is about 1500 ml, which is mainly composed of brain tissue (over 85%), 10% (intravascular) blood, and 5% cerebrospinal fluid [116]. According to the Monro-Kellie doctrine, an increase in intracranial volume can be compensated by decrease of blood and cerebrospinal fluid volume thus keeping intracranial pressure within a physiological limit [117]. However, when an injury induces a volume increase (hemorrhage, edema formation) which exceeds a critical limit (>150 ml), these compensatory mechanisms fail and ICP may increase exponentially and reduce cerebral perfusion.

Cerebral perfusion mainly depends on two elements: mean arterial pressure (MAP) and ICP. The cerebral perfusion pressure (CPP) can therefore be determined as follows: CPP = MAP – ICP [118].

The typical clinical presentations of intracranial hypertension includes headache, vomiting, nausea, and progressive loss of consciousness [119]. If developing over a short period of time, severe brain swelling can induce herniation, a life-threatening condition where the brain stem is compressed against the tentorium cerebelli and may cause respiratory failure [120].

1.1.4.2.2 Chronic secondary brain injury

In the past, clinical and experimental studies concentrated on reducing acute injury progression post-TBI. Recently, more and more researchers note that a variety of neurodegenerative symptoms may be found in patients in the chronic phase, i. e. years and decades after TBI [121-124]. Also, experimental studies demonstrated that moderate, severe TBI and repeated mild TBI result in progressive neurodegeneration associated with neurological changes [125-127].

Neurodegeneration after TBI is hypothesized to be linked to chronic inflammation. Persistent neuroinflammatory changes, e.g. microglial activation, were found in the cortex more than one year after TBI in humans [128]. These changes were associated with hippocampal neurodegeneration, and loss of myelin [129, 130]. Activated microglia and phagocytic macrophages were observed in the corpus callosum up to 18 years following injury, associated with ongoing axonal degeneration and tissue atrophy [30]. Moreover, a one-fourth loss of corpus callosum thickness was observed in patients surviving longer than one year post-injury indicating white matter atrophy. Noticeably, major histocompatibility complex class II (CR3/43), CD68 and NADPH oxidase (NOX2) labeled activated microglia were uncovered at lesion boundary at 1 year post-injury; neuroinflammatory factors and oxidative stress markers notably increased [83]. An increase in translocator protein 18 kDa (TSPO) ligand levels was observed after experimental TBI, which probably was in association with highly activated microglia within secondary inflammatory response [131]. Using TSPO-Positron emission tomography (PET) in patients within years after a brain injury, an increased ligand binding was detected diffusely at spots far from the lesion, suggesting chronic inflammatory response [56]. Erturk et al. used MRI to demonstrate substantial loss of brain tissue within a few weeks after an experimentally closed TBI model. In ensuing months post-TBI, no further anatomical damage was detected in MRI. However, a loss of dendritic spine density in the contralateral hippocampus was detected after one year, which was associated with

progressive neuroinflammation spreading from initial lesion to distant region. Heterozygous deletion of CX3CR1 decreased the recruitment of immune cells, ameliorated chronic neurodegeneration, and promoted functional prognosis post-trauma [132]. Rodgers et al. demonstrated that anti-inflammatory therapy by using the phosphodiesterase inhibitor ibudilast one month after an experimental TBI reduced chronic anxiety-like behavior and gliosis at six months post-trauma [133]. Delayed activation of metabotropic glutamate receptor 5 (mGLuR5) expressed in microglia ameliorated inflammatory response, lesion expansion, and improved functional recovery up to three months post-injury [134]. These findings indicate that inhibiting chronic inflammation may reduce neurodegeneration and thus improve functional and behavioral outcome after TBI.

Apart from inflammation, Tau pathology was also observed in the chronic phase after TBI [135]. Under physiologic conditions, Tau is a protein binding to tubulin in order to stabilize the microtubule structure of neurons. After TBI, tau may separate from tubulin causing phosphorylation of tau, which then is unable to bind to tubulin again [136]. As hyper-phosphorylated tau is insoluble, accumulation of hyper-phosphorylated tau in the intracellular space facilitates the formation of tau oligomers, which eventually form neurofilament tangles (NFT) [137, 138]. As NFTs mature and propagate, patients begin to present with behavioral symptoms and cognitive impairment [136]. Chronic traumatic encephalopathy (CTE), first described as a “punch drunk” syndrome by Martland in 1928 in boxers [139], is associated with repetitive TBI. It has been shown to occur in athletes practicing contact sports such as football and wrestling who suffer frequent and repetitive blows to the head [140, 141]. On a pathological level, CTE is characterized by aggregation of phosphorylated tau (p-tau) in neurons, astrocytes, and cell processes in perivascular spaces within the depths of cortical sulci [142]. Activated microglia can contribute to tau accumulation in CTE and could therefore be a potential risk to promote the development of CTE [143]. Injection of adeno-associated virus (AAV) vector carrying a gene for an anti-

pTau antibody into the hippocampus of mice notably reduced p-Tau levels in a CTE mice model [144]. But until now, the progression and pathomechanisms of the chronic phase after TBI remains to be better understood.

1.2 The Kallikrein-Kinin-System

1.2.1 Introduction

In 1909, Abelous and Bardier first described the Kallikrein-Kinin-System (KKS). They reported that the application of human urine transiently decreased the blood pressure in dogs [145]. Over the next decades, the single components of the KKS system were gradually discovered. In 1930, kallikrein (KLK) was discovered by Heinrich Kraut and Eugen Werle [146]. In 1948, Werle et al. renamed the compound kallidin and its precursor kallidinogen [147]. Later, Rocha e Silva et. al isolated bradykinin (BK) from snake venom [148]. Regoli and his colleagues described the bradykinin B1 receptor (B1R) and the bradykinin B2 receptor (B2R) as well as the physiological function of BK and its analog desArg9-BK [149]. In 1964, Schachter categorized bradykinin and kallidin as kinins and named their precursors kininogens (KNGs) [150].

Prekallikrein (PK), has been described to express in liver, testicles, ovaries, the parotid gland, esophagus, skin, the respiratory tract, prostate, and breast [151]. It is a serine protease with a molecular weight between 85 kDa and 88 kDa [152], which is modified to KLK by activated factor XII [153]. KLKs come in two subtypes: plasma (pKLK) and tissue (tKLK) kallikrein [153]. PKLK is composed of a heavy chain (53 k Da) and a light chain (33–36 kDa) [154]. The heavy chain of pKLK binds to high molecular weight kininogen (HMWK), while the light chain catalyzes the cleavage of HMWK into bradykinin (BK) [152]. TKLK is an acid glycoprotein with a molecular weight between 24 kDa and 45 kDa [155] which is widely expressed in kidney, pancreas, colon, pituitary gland [156], spleen, and the central nervous system [152]. TKLK can liberate kallidin from HMWK and low molecular weight

kininogen (LMWK) [157]. PKLK catalyzes the conversion of plasminogen into plasmin, thereby promoting fibrinolysis [158].

KNGs including HMWK and LMWK are synthesized in hepatic tissues [159] and occur in lung, kidney, neural and cardiac tissues in human and animals [160-162]. HMWK (120 kDa) is a β-globulin with a concentration of nearly 80 mg/ml and LMWK (68–75 kDa) is a polypeptide with a concentration of approximately 60 mg/ml in human plasma [163]. HMWK and LMWK are the precursors of bradykinin and kallidin, respectively [153]. BK, kallidin and their carboxy-terminal des-Arg metabolites are termed kinins [164]. BK is a peptide composed of nine amino acids and plays a physiological role, e.g. in vasodilation and natriuresis [165]. BK has a very short half-life and is rapidly degraded by kininase I, kininase II, and neutral endopeptidase (NEP) in plasma [166]. Kallidin is a decapeptide with an additional lysine amino acid at the N-terminus in comparison to BK [153]. Kinins bind to B1 or B2 receptors, activating signaling cascades to regulate a variety of physiological functions, including blood pressure regulation, mitogenesis [167], and nitric oxide (NO) synthesis [168]. BK and kallidin specifically bind to B2 receptors and are cleaved by kininase I-type into des-Arg^{9} BK and des-Arg^{10} kallidin, which are the specific agonists of B1 receptors [169].

Both the B1 and B2 receptors have seven transmembrane structures and belong to the G-protein coupled receptor family. The human B2R (41 kDa) consists of 359 amino acids and B1R (approximately 40 kDa) is composed of 353 amino acids [170]. The B2 receptor is ubiquitously expressed in various tissues under physiological conditions, e.g. vascular endothelial cells, sensory neurons, smooth muscle cells, and certain leukocyte subtypes [171]. The B1 receptor is hardly expressed under physiological conditions but was demonstrated to be upregulated under pathological conditions such as sepsis, inflammation, or oxidative stress [172]. B2R and B1R are activated by their specific agonists (Bradykinin and des-Arg^{9}-Bradykinin, respectively), which are converted from

KNGS catalyzed by KLK, initiating various effects, e.g. vasodilation, inflammation, and edema formation [169, 173] (Figure 4).

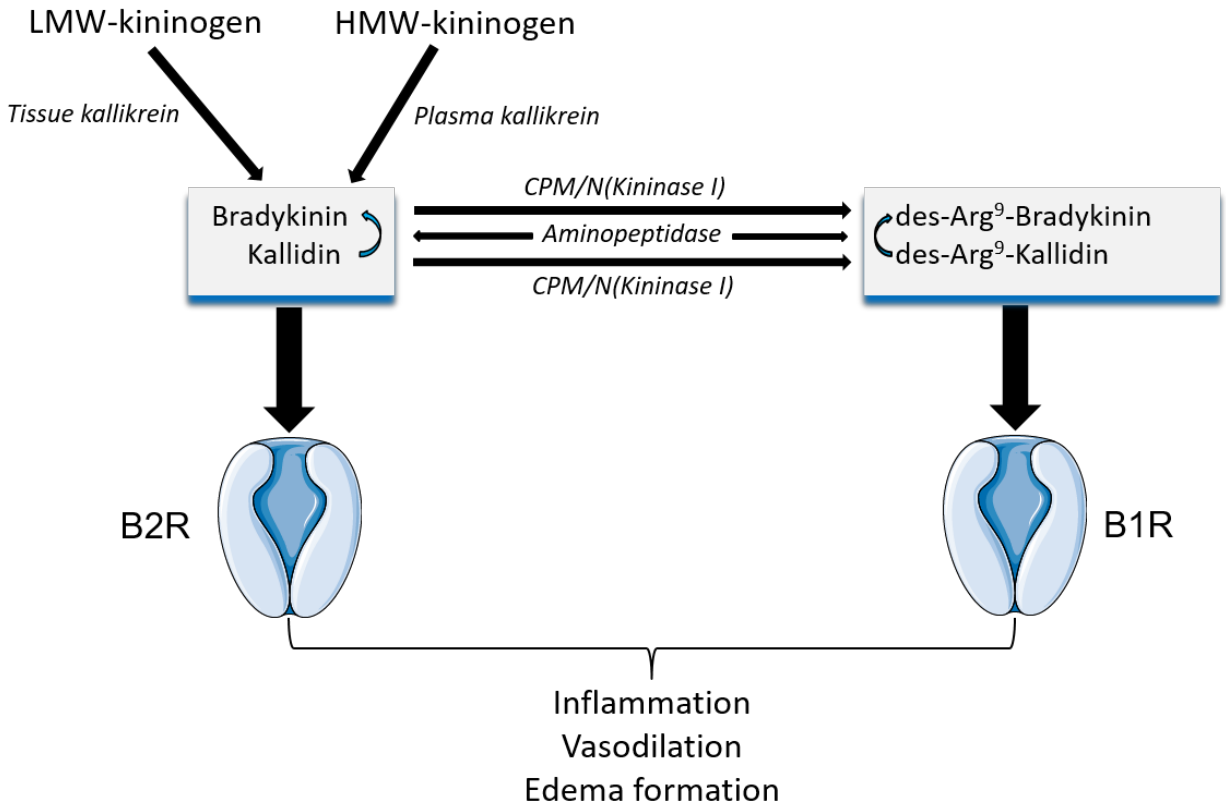

Figure 4: Components and effects of KKS (modified from Albert-Weissenberger) [169]

1.2.2 Role of the KKS in brain injury

Application of protinin, an inhibitor of plasma kallikrein [174], led to a reduction of edema formation in a cold injury TBI model in rabbits [175]. Trabold et al. reported that the concentration of bradykinin in brain tissue significantly increases 2h after controlled cortical impact, and then gradually decreases over time. Deficiency of B2 but not B1 receptors reduces brain edema formation as well as lesion volume and improves neurological outcome in a TBI model in mice [176]. However, Hellal et al. demonstrated that the B2 receptor mediated a neurotoxic effect after TBI, by exacerbating the inflammatory response and neurological deficit in closed head injury in mice [177]. In a

weight-drop traumatic brain injury model, pharmacological inhibition and genetic elimination of B1R induced neuroprotection by ameliorating the inflammatory response and reducing brain edema formation within 7 days after TBI. A B1 receptor deficit reduced functional deficits over 7 days after TBI by reduction of axonal damage, astroglia activation and release of cytokine [178]. Raslan et al. report that pharmacological inhibition or genetic elimination of the B1 receptor reduced lesion volume after TBI by reduction BBB disruption and reduced release of inflammatory cells and cytokines in the acute phase of TBI in mice [179]. Furthermore, the B1 receptor seems to participate in the mediation of memory impairment in the rat hippocampus after experimental TBI [180]. However, presently all studies focus on the effects of the KKS in the acute phase after traumatic brain injury. Its role in the development of chronic posttraumatic brain damage is so far unclear.

1.3 Acid-sensing ion channels

1.3.1 Background

Acid-sensing ion channels (Asic) are proton-gated, voltage-insensitive, cationic channels widely expressed in the nervous system, as well as in various subtypes of epithelial and immune cells [181, 182]. Asics belong to the degenerin/epithelial sodium channel (DEG/ENaC) superfamily [183] which contains Asic 1a, 1b, 2a, 2b, and Asic 4 [181] channel. Asic 1a, Asic 2a, and Asic 2b are extensively expressed in both the central (CNS) and the peripheral nervous system [184-186], while Asic 1b and Asic 3 are only expressed in the peripheral nervous system [187, 188].

Asics consist of a large extracellular loop surrounded by two transmembrane domains (TM1 and TM2) and intracellular N- and C-termini [182, 189]. The functional channel is formed by three subunits, either three homomeric Asic or a composition of heteromeric Asic subtypes [190, 191]. Different Asic subtypes exhibit different electrophysiological properties. The half-maximal activation pH value (pH_{50}) of homomeric Asic 1a channels is

between pH 6.2 and 6.8 [192, 193]. Asic 1b has a lower pH_{50} (5.9) than Asic 1a [194]. When activated by acidosis, the Asic 1a channel is permeable to sodium and partially to calcium. Given the existing gradients this triggers an ion inward current [182, 195]. Asic 2a and 2b are not pivotal for acid-evoked currents [196], but can form heteromeric Asic 1a/2a [196] and Asic 2a/3 [197] channels which – when activated by acidosis - induce inward currents, eventually effecting physiological and pathological functions.

Asic 1a channels are highly expressed on postsynaptic membranes of neurons in the amygdala, somatosensory cortex, posterior cingular cortex, and hippocampus [198] and are involved in synaptic plasticity, learning, memory, and fear conditioning [186, 199]. By activation of Asic 1a protons function as neurotransmitters and mediate neural activity and synaptic plasticity in the CNS [200]. Asic 2 is involved in neurosensory mechanotransduction of cutaneous afferent fibers [201], e. g. serosal colonic, tension, and mucosal types of gastroesophageal afferent fibers [202] as well as in mediating the baroreceptor reflex [203] and the pressure-induced constriction of the middle cerebral artery [204]. Asic 3 plays a pivotal role in mechanotransduction of neurosensory information in the CNS [205].

1.3.2 Role of Asic in brain injury

In a murine cerebral ischemia model, intracerebroventricular injection of a Asic 1a inhibitor (PcTx1) and genetic disruption of Asic 1 function reduced infarct volume [206]. The inhibition of Asic 1a resulted in neuroprotection with an efficient time window of up to 5 hours, persisting for at least 7 days in an ischemia model [207]. Pignataro et al. reported that downregulation of Asic 1a expression enhances neuroprotection induced by ischemic preconditioning and postconditioning in rats [208]. In a rodent model of autoimmune encephalomyelitis (EAE), reduction of functional deficits and axonal degeneration was detected in Asic 1 knock-out mice compared to wild-type littermates. Tissue acidosis was sufficient to open Asic 1 according to pH recordings from the spinal cord. Asic1 deficiency also exhibited protective effects in nerve explants in vitro. Amiloride,

a blocker of Asic, likewise exerted neuroprotection in nerve explants and EAE [209]. Parkinson's disease (PD) is associated with acidosis. In a 1-methyl-4-phenyl-1,2,3,6-tetrahydropyridine (MPTP) induced PD rodent model, Arias et al. showed that amiloride contributed to neuronal protection and preservation of dopaminergic cell bodies in the substantia nigra [210]. Benzamil, a drug with a similar activity as amiloride, remarkably alleviated huntingtin-polyglutamine (htt-polyQ) aggregation in vitro. Furthermore, in an animal model of Huntington's disease (HD), benzamil ameliorated the inhibition of ubiquitin-proteasome system (UPS) activity, leading to enhanced degradation of soluble htt-polyQ. Blocking the expression of Asic 1a with siRNA also contributed to an enhancement of UPS activity and reduction of the htt-polyQ aggregation in the striatum [211].

After TBI, brain edema results in a pathological ICP increase and subsequent reductions of CBF and acidosis. Asic 1a activation by acidosis resulted in depolarization of the neurons and an excitatory response (Figure 5) [212, 213]. Yin et al. demonstrated that deficiency of Asic 1a and administration of sodium hydrogen carbonate ($NaHCO_3$) in order to elevate pH reduced neurodegeneration four days post-TBI. Genetic elimination of Asic 1a reduced spatial memory deficits in rats with TBI in the acute phase [214]. Pharmacological inhibition and disruption of the Asic 1a gene induced neuroprotection in ischemic brain injury in the acute phase [206, 215]. To date, the role of Asic 1a in chronic progression after TBI has not been investigated.

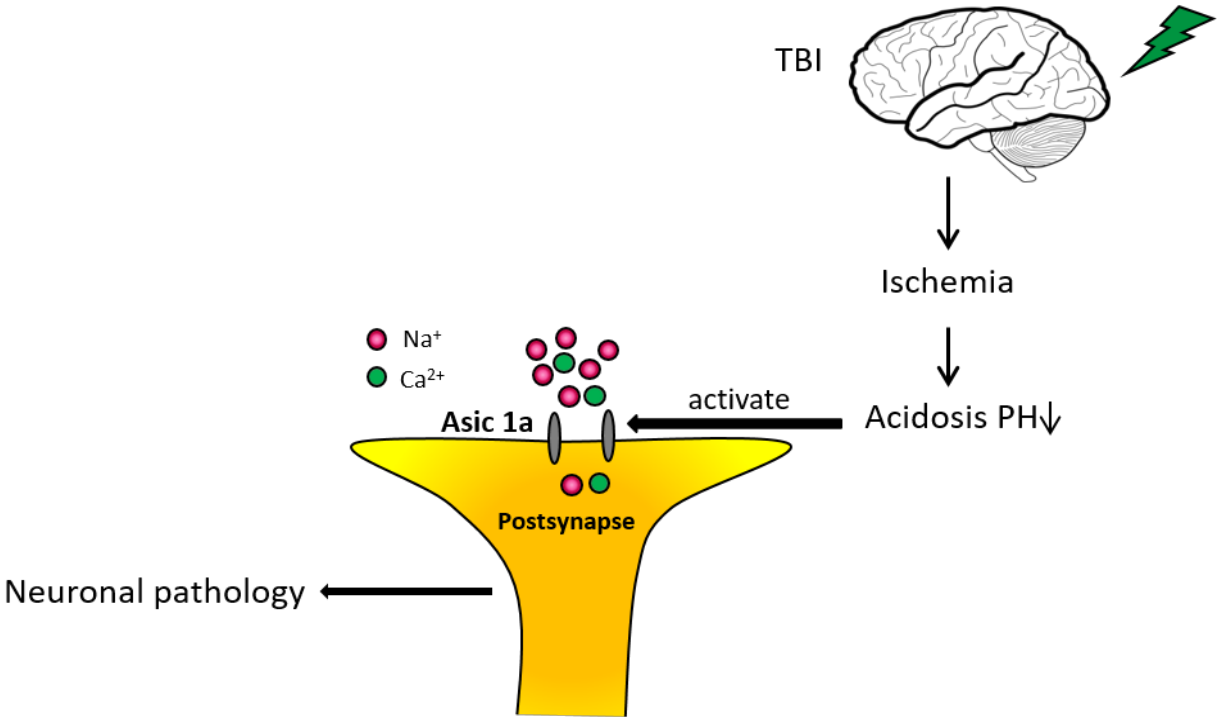

Figure 5: Activation of Asic 1a after TBI

1.4 Aim of study

The present study aims to study the roles of the bradykinin B1 receptor and Asic 1a for the development of chronic brain damage after traumatic brain injury.

2. Materials and methods

2.1 Materials

2.1.1 Equipment

Axio Imager M2 Microscope (12.5 X)	Carl Zeiss Microscopy GmbH (Jena, Germany)
Control Cortical Impact Device (Mouse-Katjuscha 2000)	L. Kopacz (University of Mainz, Germany)
Cryostat NX70	Thermo Fisher Scientific (Waltham, USA)
DC Temperature Control System	FHC (Bowdoin, United States)
High precision drill	Rewatronic Products (Wald Michelbach, Germany)
Drill Tip (GD041R, 6mm/ISO, 2.35X70mm)	Braun (Frankfurt am Main, Germany)
Dumont Forceps (11253-20)	Fine Scientific Tools (Heidelberg, Germany)
Dumont Laminectomy Forceps (11223-20)	Fine Scientific Tools (Heidelberg, Germany)
Extra Fine Bonn Scissor (14084-08)	Fine Scientific Tools (Heidelberg, Germany)
Fume Hood (DS-DG03-1200)	Wesemann (Munich, Germany)
High-resolution Camera (acA1300- 60g mNIR)	Basler (Ahrensburg, Germany)
LED light source (KL2500)	Leica (Wetzlar, Germany)
Leica M80 Stereomicroscope (1 X)	Leica (Wetzlar, Germany)
Medi HEAT Heater	Peco Services (Brough, UK)
Micro-needle holder (12001-13)	Fine Scientific Tools (Heidelberg, Germany)
Model 900 Small Animal Stereotaxic frame	David KOPF Instruments® (California, USA)
Nanoscan PET/MRI 3T	Mediso Medical Imaging Systems (Budapest, Hungary)

Perfusion Machine (628159)	Leica Biosystems Richmond (Richmond, USA)
Vibratome (Leica VT 1200s)	Leica (Wetzlar, Germany)

2.1.2 Software

Axiovision LE 4.8	Carl Zeiss (Oberkochen, Germany)
EthoVision®XT 7	Noldus Information Technology (Wageningen, Netherlands)
InterView™ FUSION - A	Mediso Medical Imaging Systems (Budapest, Hungary)
Graph pad prism 8.0	GraphPad Software (San Diego, California, USA)
Sigma plot 13.0	Systat Software (Chicago, USA)
ZEN 2012	Carl Zeiss (Oberkochen, Germany)

2.1.3 Consumables

Bepathen Eye and Nose Ointment	Bayer Vital (Leverkusen, Germany)
Cotton Swab	Nobamed Paul Danz (Wetter, Germany)
Coverslips (24 x 60 mm)	Thermo Fisher Scientific (Waltham, Massachusetts, USA)
Eukitt Quick-hardening Mounting Medium	O. Kindler (Freiburg, Germany)
Infusion Set	B-Braun (Melsungen, Germany)
Injekt-F Syringe (1ml)	BD Biosciences (San Jose, California, USA)
Prolene Suture (5-0)	Ethicon (Somerville, New Jersey, United States)

Scalpel (No.11)	Feather (SEKI-SHI, GIFU, Japan)
SERAFIT Suture (6-0)	Serag Wiessner (Naila, Germany)
Sugi Sponge Points	Kettenbach (Eschenburg, Germany)
Superfrost Plus Microscope Slides	Thermo Fisher Scientific (Waltham, Massachusetts, USA)
Surflo Winged	Terumo Medical Corporation (Leuven, Belgium)
Vasco Nitril Blue Glove (S)	B-Braun (Melsungen, Germany)

2.1.4 Chemicals

3M™ Vetbond™ Tissue Adhesive	3M (Maplewood, Minnesota, USA)
Agarose	VWR (Ulm, Germany)
Avidin/Biotin Blocking Kit	Vector laboratories (Burlingame, California, USA)
Bovine Serum Albumin	Sigma-Aldrich (Taufkirchen, Germany)
Buprenorphine (Buprenovet 0.3mg/ml)	Bayer (Leverkusen, Germany)
Embedding Medium (Eukitt®)	Kindler (Herzogenaurach, Germany)
Ethanol (EMSURE, ≥99.8%)	Sigma-Aldrich (St. Louis, Missouri, USA)
Ethylene glycol	Sigma-Aldrich (St. Louis, Missouri, USA)
Fentanyl (Fentadon 50mg/ml)	Albrecht (Munich, Germany)
Glycerol	Sigma-Aldrich (St. Louis, Missouri, USA)
Hematoxylin	Sigma-Aldrich (St. Louis, Missouri, USA)
Isoflurane Isp-Vet	Abbott (Chicago, Illinois, USA)
Medetomidine	Zoetis (Parsippany-Troy Hills, New Jersey, USA)

Midazolam	B-Braun (Melsungen, Germany)
NaCl isotonic solution 0.9%	Fresenius Kabi (Bad Homburg, Germany)
Paraformaldehyde (4%)	Morphisto (Frankfurt am Main, Germany)
Phosphate buffer saline (PBS, 10x)	Klinikum Apotheke (Munich, Germany)
Sucrose	Sigma-Aldrich (St. Louis, Missouri, USA)

2.1.5 Buffers and solutions

4% Agarose:

4g	Agarose
100ml	PBS (1x)

PBS, 1x:

100ml	PBS (10x)
900ml	Millipore water

Cryoprotection solution:

250ml	Glycerin
250ml	Ethylenglycol
500ml	PBS (1x)

2.2 Methods

2.2.1 Experimental animals and husbandry

8-12 weeks old male and female B1 and Asic1a knock-out mice and their respective wild type littermates (body weight 23-30 g) were bred in the animal facility of the Institute for Stroke and Dementia Research (Munich, Germany). All health checks and hygiene measures were performed according to FELASA guidelines [227]. Animals were housed with a 12-hour light/dark cycle and free access to food and water in standard cages (207

x 140 x 265 mm, Ehret Life Science Solutions, Freiburg, Germany) before experiments. After surgery, each experimental animal was housed separately for seven days to avoid fighting. After one week, five same-sex mice were housed in a cage until the end of the observation period. All experiments were performed in accordance with the guidelines of the animal care institutions of Munich University and approved by the Government of Upper Bavaria (protocols number 0-27-15 and 44-17).

2.2.2 Targeted disruption of the B1 receptor gene

The cloning of B1-receptor gene used 129/SvJ mice genome as a template. The targeting vector contained a neomycin-resistance gene. Flanking the gene is a 1.0-kb genomic region upstream of the B1 coding sequence (CDS) and a 7.0-kb region downstream of the B1 CDS. The HSV-tk gene was used for negative selection. The NotI digestion was performed to linearize the construct before transfecting into E14 –1 embryonic stem cells (ESCs) via electroporation. Clones resistant to Gancyclovir and G418 were selected and later validated by PCR. Two positive clones were selected to inject into C57BL/6 blastocysts, giving rise to chimeras whose offspring contains heterozygous locus for the targeted mutation [216]. This strain was received from Laboratories' Fournier in 2003 and backcrossed to C57BL/6 for more than 10 generations. Homozygous and heterozygous B1R deficient mice and wild-type littermates were generated by mating heterozygote breeding pairs.

2.2.3 Targeted disruption of the Asic 1a gene

Exon 1 and approximately 400 base pairs of upstream sequence (encoding the first 121 amino acids of the protein) were replaced with a neomycin resistance cassette in (129X1/SvJ x 129S1/Sv) F1-Kitl+-derived R1 embryonic stem (ES) cells. The deleted region includes the intracellular N-terminus, the first transmembrane domain, and a portion of the extracellular domain [186]. This strain was backcrossed to C57BL/6 mice for more than 10 generations. Breeding pairs were purchased from Jackson Laboratories in 2015 and

homozygous and heterozygous Asic 1a mice and wild type littermates were generated by mating heterozygous mice.

2.2.4 Randomization and blinding

Mice were randomly assigned to experimental groups by a third party not involved in the study; group allocation was revealed only after complete analysis of the data. Surgery, behavioral testing, preparation, and evaluation of histological specimens as well as (statistical) analysis of results were performed in a blinded fashion.

2.2.5 Protocol for the assessment of the effect of Bradykinin-1-receptor deficiency on chronic posttraumatic brain damage and outcome after experimental TBI

Experimental groups included wild type (WT), heterozygous, and homozygous B1 mice (n =12/group). Bodyweight was measured at 3 days before surgery, on the day of surgery, and at days 1, 3, 7, 14, 60, 90, 180, 270, and 360 post-trauma. Beam Walk testing was performed 3 days before surgery, then on day 1, 3, 7, 14, 60, 90, 180, 270 and 360 after CCI. Tail Suspension test, Barnes Maze test and MRI were performed at day 60, 90, 180, 270 and 360 after CCI. Histological analysis was performed on brains harvested at the end of the observation time at 360 days after TBI (Figure 6).

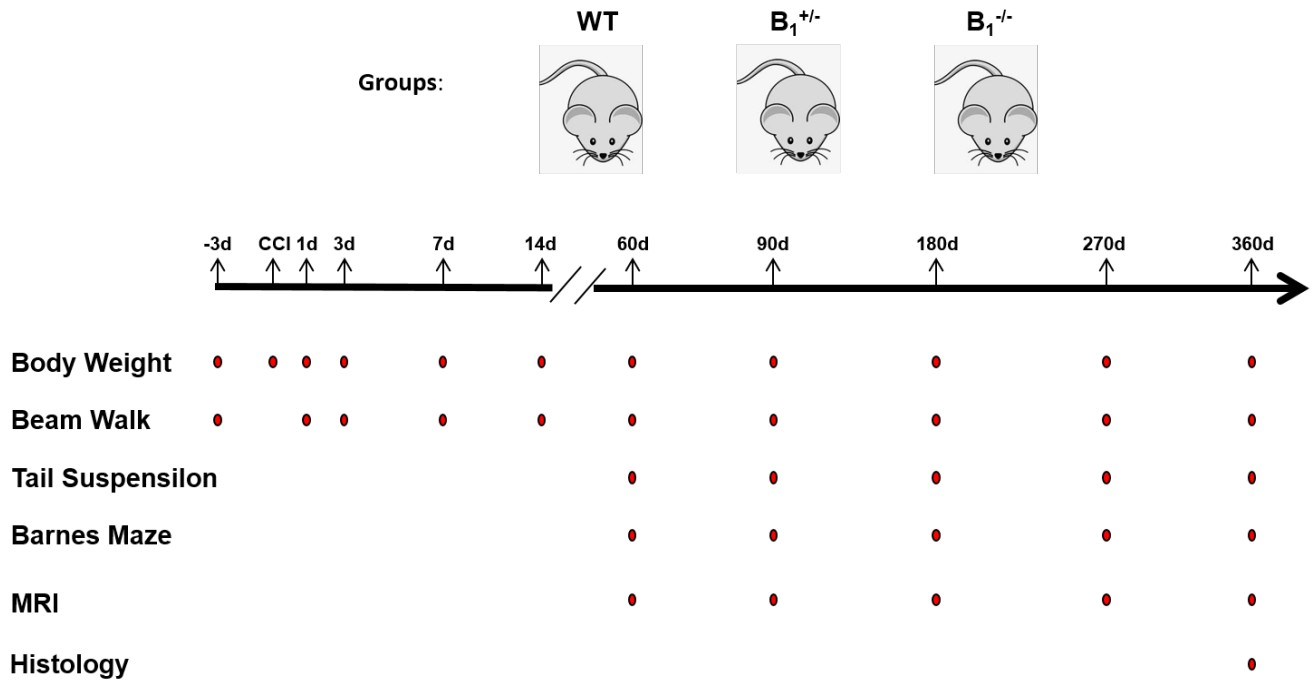

Figure 6: Schematic of B1 project design

2.2.6 Protocol for the assessment of the effect of Asic 1a on chronic posttraumatic brain damage and outcome after experimental TBI

Groups of WT and heterozygous Asic1a knock-out mice were used for brain edema measurements 24 h after CCI (sham = 4, TBI = 8). For the Asic 1a-project, WT, heterozygous, and homozygous Asic 1a mice (n =12/group) were examined. Bodyweight was determined three days before surgery, on surgery day, then at days 1, 3, 7, 14, 60, 90, and 180 post-TBI. Beam Walk testing was conducted 3 days before surgery, then at days 1, 3, 7, 14, 60, 90, and 180 after TBI. The tail Suspension test, the Barnes Maze test and MRI scanning were performed at days 60, 90, and 180 after TBI. Histological analysis was done with brain tissue harvested 180 days post-trauma (Figure 7).

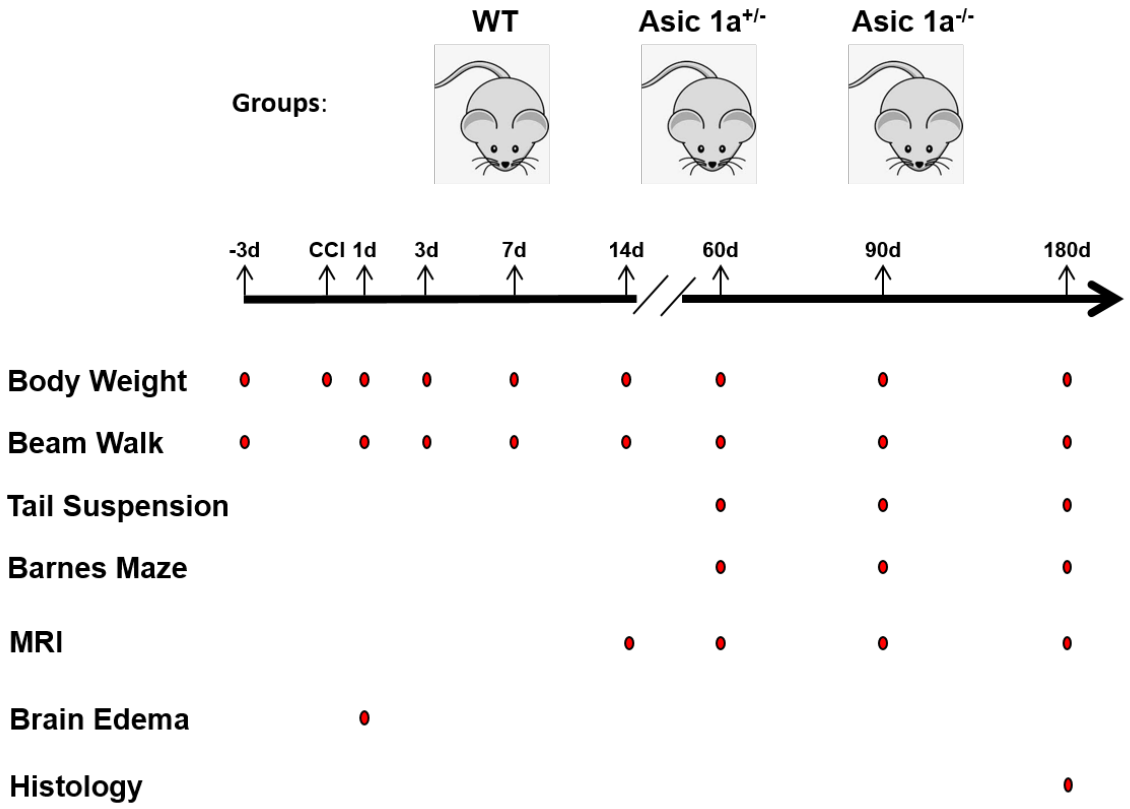

Figure 7: Schematic of Asic 1a project design

2.2.7 Anesthesia and analgesia

A short isoflurane anesthesia was induced using a Plexiglas chamber (4% isoflurane in a 30% oxygen/70% air mixture, 30s) and buprenorphine (0.1 mg/kg) was injected intraperitoneally 30 minutes before surgery in order to reduce pain memory. For surgery, anesthesia was induced in an anesthesia chamber with 3-5% isoflurane in 30% oxygen/ 70% air mixture, until the blink reflex and pain reflexes were abolished. Anesthesia was then continued via a face mask in spontaneously breathing animals at 1-1.5% isoflurane. After surgery, buprenorphine (0.1 mg/ kg) was injected every 8 hours for 3 days to reduce perioperative pain. For MRI scanning, anesthesia was induced with inhalation of isoflurane in 30% oxygen/70% air mixture (4% for 60s and 1-1.5% throughout scanning). For transcardial perfusion, animals were terminally anesthetized with medetomidine (0.5 mg/kg body weight), midazolam (5 mg/kg), and fentanyl (0.05 mg/kg).

2.2.8 Experimental traumatic brain injury model– Controlled Cortical Impact (CCI) model

The controlled cortical impact model is a widely used model for experimental TBI, which produces a highly standardized cortical contusion. It was first reported in ferrets by James W. Lighthall in 1988 [217] and has been translated to other animal species subsequently. Our group has more than 15 years of experience with this technique in mice [218]. For the model, a custom-built, pressure operated CCI device (Mouse-Katjuscha 2000, L. Kopacz, University of Mainz, Germany, Figure 8 A) was used; it has a micrometer tip allowing for exact adjustment of impact depth as well as a speed microsensor located at the tip of the instrument for exact determination of impact velocity and contact time.

After induction of anesthesia, mice were placed in the prone position using a stereotaxic frame (Model 900 Small Animal Stereotaxic Instrument, David KOPF Instruments®, Tujunga, California, USA) and fixed with a nasal clamp (Model 926 Mouse Adaptor, David KOPF Instruments®, Tujunga, California, USA). Mice were placed on a feedback-controlled heating pad with a rectal temperature probe in order to keep the core body temperature at 37°C; eyes were protected from exsiccation by application of ointment. A 2 cm longitudinal incision was performed on the scalp and the galea aponeurotica and the periosteum were removed. Using an operation microscope, a 5x5 mm craniotomy was performed between the right coronal and lambdoid suture (see Figure 8 B for schematic drawing) with a high-speed drill (Rewatronik® Products, Wald-Michelbach GmbH, Germany; drill head GD890R, diameter 0.6 mm, Aesculap, Tuttlingen, Germany) under continuous cooling with physiological saline to avoid heat damage. Careful precautions were taken not to damage the dura mater. After partial removal of the skull plate, the mouse was positioned under the impact tip of the CCI machine. The impactor stamp was carefully placed on the dura mater within the craniotomy. Afterwards, CCI was performed with an impact depth of 1 mm, an impact duration of 150 ms, and an impact velocity of 8 m/s. Immediately after the impact, the skull was resealed and the scalp was sutured. For

sham operation, only a craniotomy was performed. After wound closure, isoflurane was discontinued and the animal was allowed to wake up. Animals were administered 100% oxygen until they fully regained consciousness and motor function. Afterwards, operated mice were placed in a heating chamber at 34°C and 55% humidity for one hour in order to avoid postoperative hypothermia. After complete recovery, mice were housed separately in a standard cage.

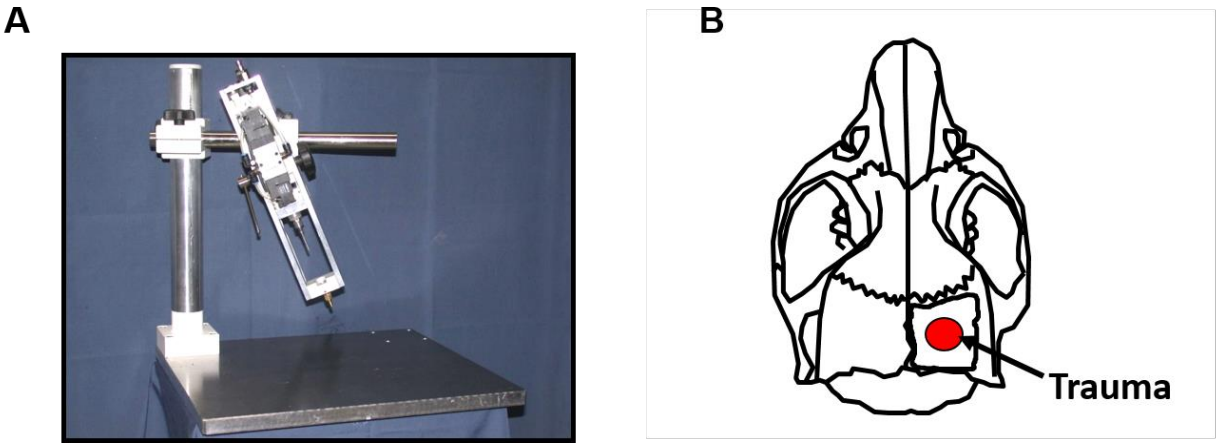

Figure 8: (A) Picture of the CCI device used in this study (B) Location of the CCI craniotomy

2.2.9 Body weight

Body weight, a parameter of general wellbeing, was evaluated daily starting 3 days before surgery. After CCI, body weight was measured daily during the first week, then on days 14, 60, 90, 180, 270, and 360 after surgery using a precision electrical scale (OHAUS®, Waagendienst Winkler GmbH, Munich, Germany) with movement correction.

2.2.10 Behavioral tests

2.2.10.1 Evaluation of motor function - Beam Walk test

Using the method detailed above, the CCI model leads to contusional brain injury within the right motor cortex which controls motor function of the left side of the body, especially the left hind paw. The beam walk test was used to evaluate the motor function

and gait changes post-TBI. In previous studies using the CCI-model, it was demonstrated that the Beam Walk test was able to detect a dysfunction of strength and fine motor skills in a highly sensitive way, also in the chronic phase after trauma, i. e. when fine motor skills recovered to a high degree [219]. In order to perform the test, both sides of a wooden beam (1 cm width, 100 cm length) were fixed in 1m height, and an escape cube was put close to one terminal side of the beam (see Figure 9 for photograph of the setup). Animals were then positioned at the starting end of the beam and observed during crossing of the beam. Time needed to cross the beam and missteps (or slipping of the hind paw) for the left hind paw were then recorded and counted. If a mouse fell off, it received the maximum deficit score. If a mouse jumped off the beam, the test was performed again. If a mouse was not able to cross the beam within 2 minutes, the test was stopped and the animal received the maximum deficit score. The beam walk test was carried out 3 days before surgery and on days 1, 3, 7, 14, 60, 90, 180, 270, and 360 post CCI.

Figure 9: Setup of Beam walk

2.2.10.2 Evaluation of depression-like behavior – the Tail Suspension test

The Tail Suspension test is a widely used behavioral test for the evaluation of depression-like behavior in rodents [220]. For the test, animals are put in a head down position by affixing them by the tail. As this is an undesirable position for the animals, they try to avoid this position by moving/climbing upwards. It has been previously reported that the time spent active correlates to normal impetus and mood whereas immobility was a sign for reduced impetus and, thus, depression-like behavior [221, 222]. For the test, tails of the animals were placed in Plexiglas cylinders (4 cm length, 1.6 cm outside diameter, 1.2 cm inside diameter) in order to avoid immediate reversal of the head-down position. Then the tail of the mouse was fixed with tape to a plastic frame in order to suspend the animal in the test position (see Figure 10 for a photograph of the setup). The animals´ reaction was recorded for three minutes with a high-resolution camera placed in front of the frame. The results (calculation of mobility and immobility time) were automatically analyzed by software-based video analysis (EthoVision®XT, Noldus Information Technology, Wageningen, Netherlands). The test was performed on days 60, 90, 180, 270, and 360 after TBI.

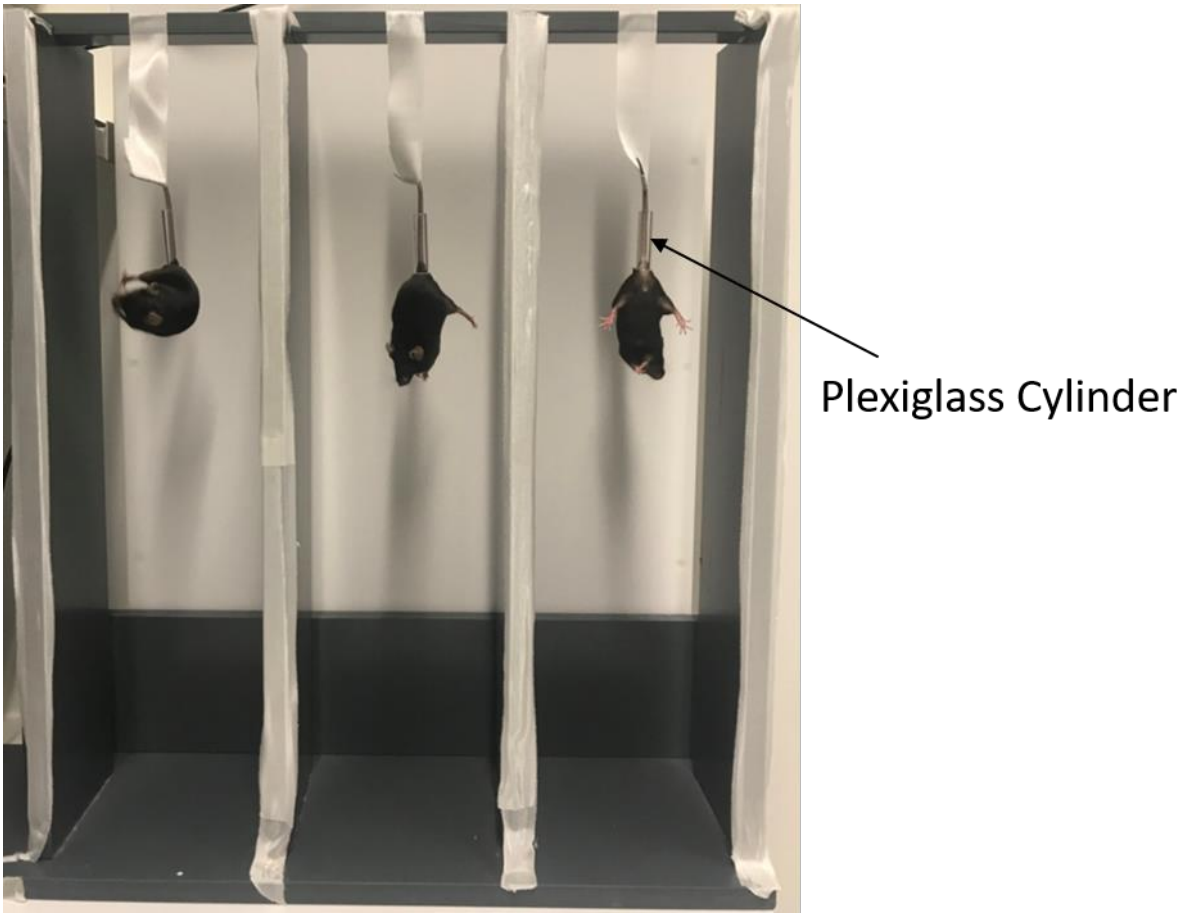

Figure 10: Set-up for the Tail Suspension test

2.2.10.3 Evaluation of spatial learning and memory behavior – the Barnes Maze test

The Barnes Maze is a well-known test paradigm for the evaluation of spatial learning and memory of rodents [223-226]. For performance of the test, a brightly lit circular metal platform (diameter 100 cm) with 20 identical holes (diameter 10 cm) equally distributed around the perimeter edge was fixed on a table (at 95 cm height) (Figure 11 A) with a high-resolution camera (4.5 – 12.5 mm, 1: 1.2) installed over the platform to record the activity of mice. A closed box (the so-called “home-box” or “home-cage”, dimensions 20 X 5 X 3 cm) was placed under a specific hole of the platform in order to provide cover from the brightly lit open space of the disk. As mice tend to avoid open and brightly lit spaces, they usually seek to take cover within the home cage as quickly as possible. For the test,

animals were trained to find the home cage for four consecutive days (with one session in the morning and one in the afternoon) before the probe day. On the first training day, in the morning, a mouse was positioned in the center of the platform under a glass cylinder (12 cm diameter, 22 cm height) for 120 seconds. Then, a researcher slowly moved the cylinder toward the escape box to show the home-box position to the mouse; afterwards the animal was left within the home-box for approximately 20 seconds. After a four to five hour long interval, i. e. in the afternoon session, the procedure was repeated, but the cylinder was lifted after 10 seconds in order to allow the animal to locate the home-cage by itself. If the animal failed to locate the escape box, the trial was stopped after three minutes. On the second day, the training procedures were repeated. On training days three and four, only the afternoon session was carried out. After a one-day long interval, the actual experimental trial was performed in the afternoon (time line depicted in Figure 11 B). The pre-test training was performed on days 55-58, 85-88, 175-178, 265-268, and 255-258 post-TBI, the actual testing was carried out on days 60, 90, 180, 270, and 360 post-TBI, respectively. The distance travelled to reach the home-cage, the time needed to reach the home-cage (latency), and the speed with which the home-cage was reached were automatically calculated. Furthermore, cumulative images of the mouse trace (heat-maps) were automatically recorded.

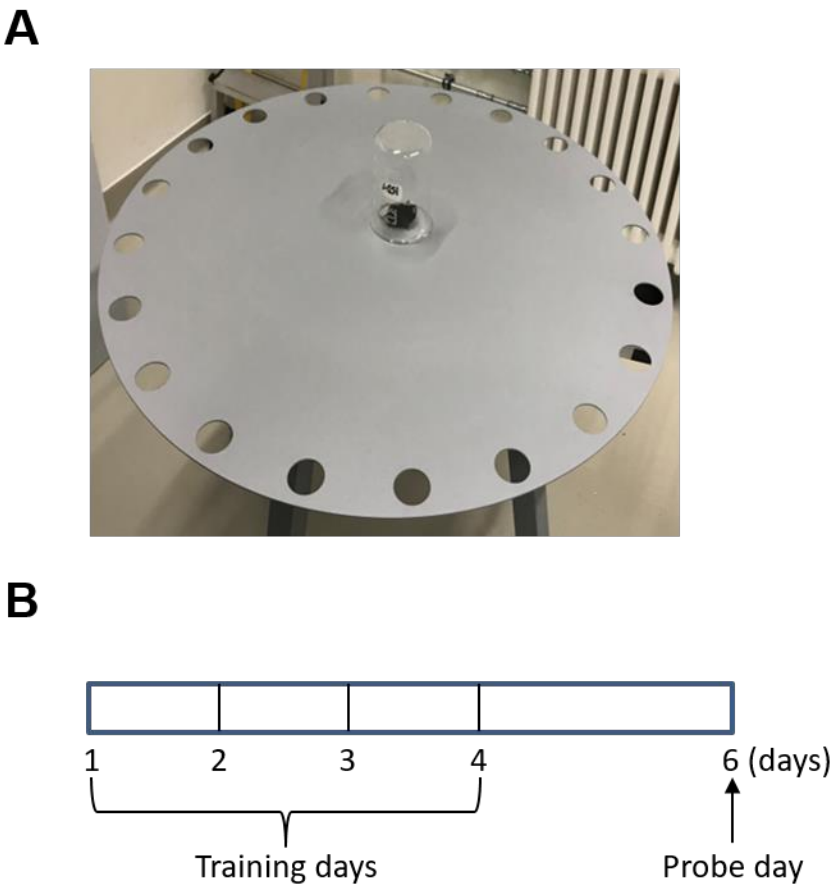

Figure 11: (A) Set-up of Barnes Maze (B) Time line of Barnes Maze test

2.2.11 Evaluation of lesion progression - Magnetic Resonance Image （MRI）

Lesion size progression after TBI was assessed longitudinally in the same animal using a 3T Nanoscan MRI (Mediso Medical Imaging Systems, Hungary) (Figure 12 A). Scanning was performed 14, 60, 90, and 180 days following TBI. For this, animals were lightly anesthetized using gas-based anesthesia (see chapter 2.2.5). Body temperature of the mouse was maintained at 37°C by a water blanket connected to the MRI. A respiratory monitoring pad was placed underneath the chest of the mouse to measure respiratory rate. A total of 19 coronal slices (0.5 mm each) were acquired for each animal using a T2-weighted (T2W) sequence. Both hemispheres were manually outlined in 13 serial slices (from 2 mm anterior to 4 mm posterior to bregma) of T2W (Figure 12 B) and analyzed by an image software (InterView™ FUSION 2, Mediso Medical Imaging Systems, Budapest,

Hungary) automatically. Lesion volume was calculated by subtracting the ipsilateral hemisphere volume from the contralateral hemisphere volume.

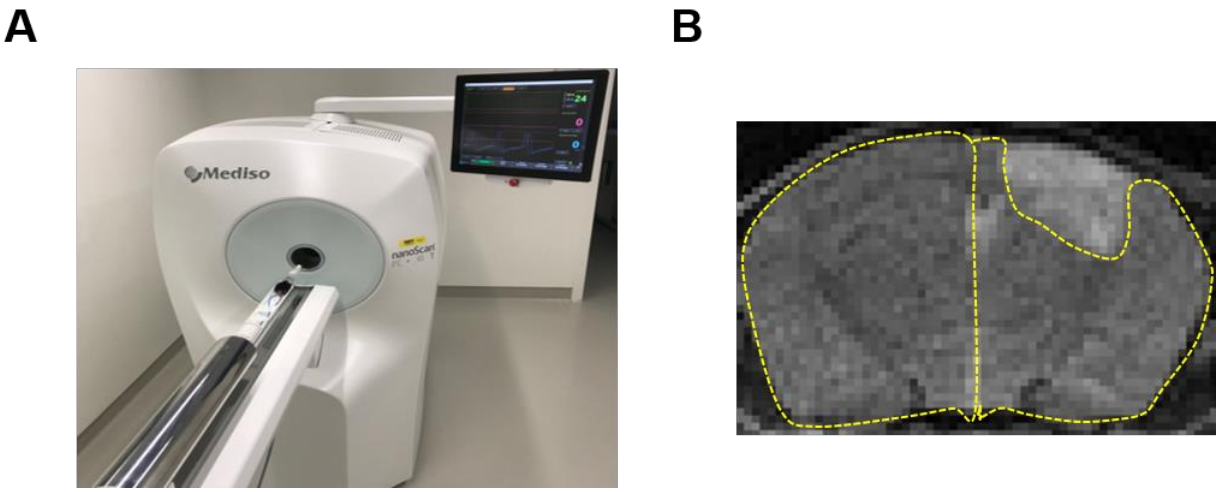

Figure 12: (A) Small Animal Magnetic Resonance Imaging (MRI) (B) Evaluation of hemispheres in images from T2W

2.2.12 Determination of brain edema formation – measurement of brain water content

Brain water content, a parameter for brain edema formation, was measured in each hemisphere separately by the wet weight-dry weight method 24h after TBI [227]. After sacrifice, the brain of the mouse was carefully removed and hemispheres were separated. Olfactory bulb and cerebellum were then removed using a metal brain matrix. The isolated hemispheres were weighed directly after preparation (wet weight). Afterwards both hemispheres were dried at 100°C for 24 h and, after cooling down to room temperature, weighed again in order to obtain the dry weight. The brain water content was then calculated in percent of total weight using the following formula: (wet weight-dry weight)/wet weight × 100%.

2.2.13 Histological analysis post-traumatic brain injury

2.2.13.1 Perfusion fixation

After induction of deep anesthesia the heart was exposed. A needle (21G, Safety-Multifly®-Needle) was inserted into the left ventricle. The mouse was then perfused using a pressure-controlled perfusion machine with 30 ml of physiological saline over 2 minutes at 120 mmHg, followed by 50 ml of 4% paraformaldehyde (PFA) over 3 minutes at 120 mmHg. The brain was then carefully dissected and fixed in 4% paraformaldehyde (PFA) at 4°C for about 24 hours; it then was immersed in PBS for storing.

2.2.13.2 Nissl staining of brain sections

After embedding the brains in 4% agarose, 50 µm thick coronal sections were cut with a vibratome at a speed of 0.9 mm/s and an amplitude of 0.8 mm. Starting 1000 micrometers behind the olfactory bulb, 12-14 sequential coronal sections were collected on glass slides. The specimens were then stained according to Nissl using the following protocol:

2 min	Fix sections with 70% Ethanol Cresyl violet solution
10-15 min	Rinse shortly with fresh water (2 x)
2 min	Ethanol 70%
2 min	Ethanol 96%
2 min	Ethanol 100%
2 min	Isopropanol
5 min	Rotihistol I
5 min	Rotihistol II

Afterwards, specimens were sealed using an embedding medium (Eukitt) and stored in a dry and dark place until analysis.

2.2.14 Histological quantification of post-traumatic brain damage parameters

2.2.14.1 Analysis of lesion volume

Nissl stained sections were positioned under the microscope (Zeiss Axio Imager M2, Carl Zeiss Microscopy GmbH, Munich, Germany), then digital photos were taken at 12.5 X magnification by a camera attached to the microscope. The photos were then analyzed using an image analysis software (AxioVision LE 4.8, Carl Zeiss Microscopy GmbH, Munich, Germany). The areas of the non-traumatic hemisphere (A) and residual traumatic hemisphere (B) were outlined in each slice (Figure 13) and measured using the software. The lesion area (C) was calculated according to the following formula:

Lesion area (C) = A-B

Then, lesion volume was determined by the following formula:

Lesion volume =0.5 mm*(C1/2+ C2+…… + Cn/2)

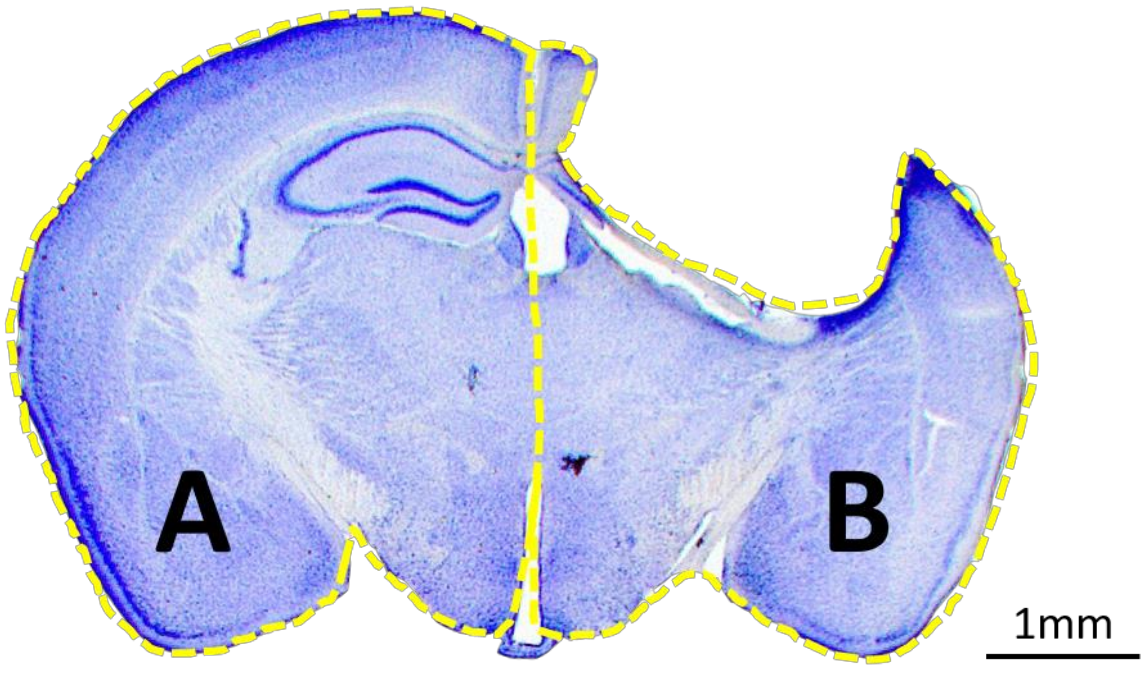

Figure 13: Histological evaluation of lesion volume

2.2.14.2 Determination of Hippocampus lesion

Using the method described above, six slices (0.5 mm interval) from 1.5 mm to 4 mm posterior to the bregma were used. The area of the hippocampus of the non-traumatic hemisphere (A) and the traumatic hemisphere (B) (Figure 14) were digitally outlined. The lesion volume was analyzed as follows:

Non-traumatic hemisphere hippocampus volume (E) = 0.5mm*(A1/2+ A2+…… + An/2)

Traumatic hemisphere hippocampus volume (F) = 0.5 mm*(B1/2+ B2+…… + Bn/2)

Hippocampus volume ratio (ipsilateral / contralateral volume) = F/E*100

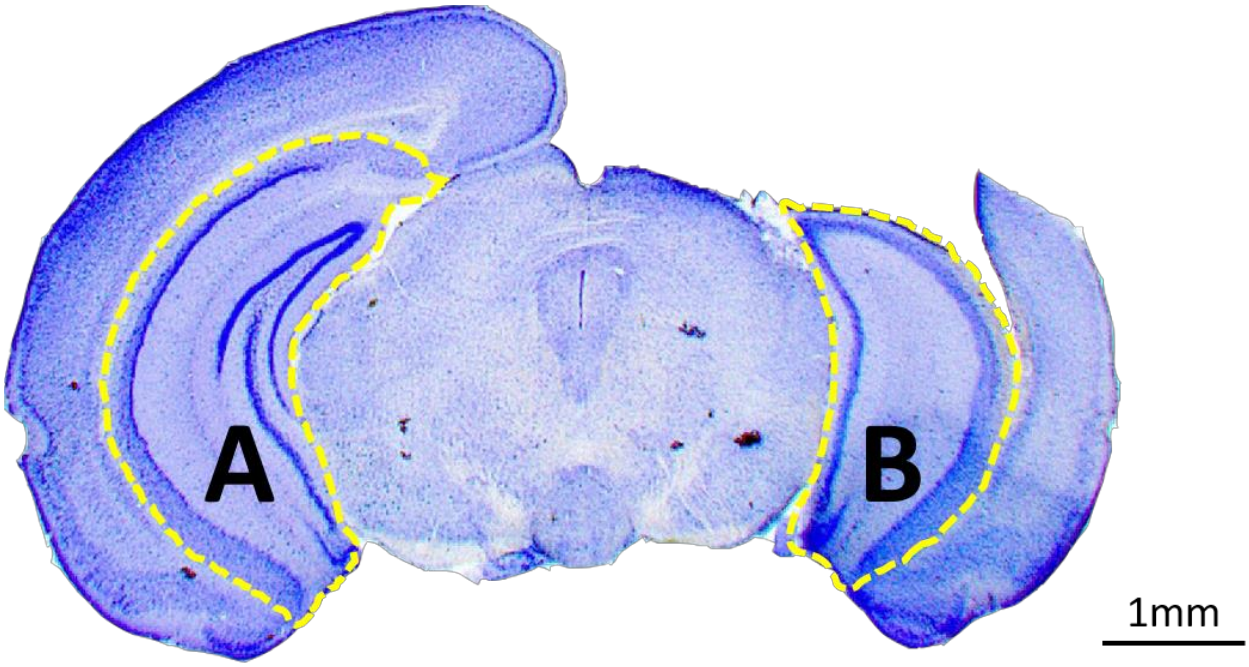

Figure 14: Histological evaluation of hippocampal defect

2.2.15 Statistical analysis

Statistical analysis was performed using Sigma plot 13.0 (Systat Software, California, USA). Due to a sample size of less than 25 per group, non-parametrical tests were used even when data passed the normality test. The Mann–Whitney test was used for two group comparisons. Kruskal–Wallis analysis followed by Dunn's post-hoc test was used for

multiple-group comparisons. For correlation between lesion volume from T2w and histology, the Pearson test was used. Survival rate was analyzed by Log Rank test. Differences between groups were considered significant at $P<0.05$. All data is expressed as mean ± standard deviation.

3. Results

3.1 Effect of Bradykinin-1-receptor knockout on the chronic outcome after experimental traumatic brain injury

3.1.1 Survival rate and changes in body weight after TBI

One WT, one $B1^{+/-}$, and two $B1^{-/-}$ mice died during surgery and were excepted from further analysis. 11 WT, 11 $B1^{+/-}$, and 10 $B1^{-/-}$ mice were included in the observation period. After surgery, one mouse in the WT group, one $B1^{+/-}$, and one $B1^{-/-}$ animal died at on the first day after CCI. One $B1^{+/-}$ mouse died at 3d and one $B1^{-/-}$ mouse died at 7d. Two more $B1^{-/-}$ mice died at 120d. One $B1^{+/-}$ mouse died at 280d, two WT mice died at 330d. In the end one $B1^{+/-}$and one $B1^{-/-}$ animals died at 370d after TBI, all remaining mice (WT group: 8, $B1^{+/-}$ group: 7, and $B1^{-/-}$ group: 5) survived until the end of the observatinon period (no significant difference, Figure 15 A).

Before surgery, there was no significant difference in body weight of WT (25.8 ± 3.22 g), heterozygous (24.63 ± 2.18 g), or homozygous mice (26 ± 1.89 g). The body weight of all traumatized mice dramatically dropped by nearly 3g on the first day after surgery, then recovered within two months and increased gradually up to one year after TBI. At 360 days after TBI, the body weight of mice was 29.7 ± 2.4 g (WT), 27.6 ± 2.6 g ($B1^{+/-}$), and 30.1 ± 2.3 g ($B1^{-/-}$), respectively. There was no significant difference between groups at any time point (Figure 15 B), indicating that Bradykinin-1-receptor deficiency does not influence general wellbeing after experimental TBI.

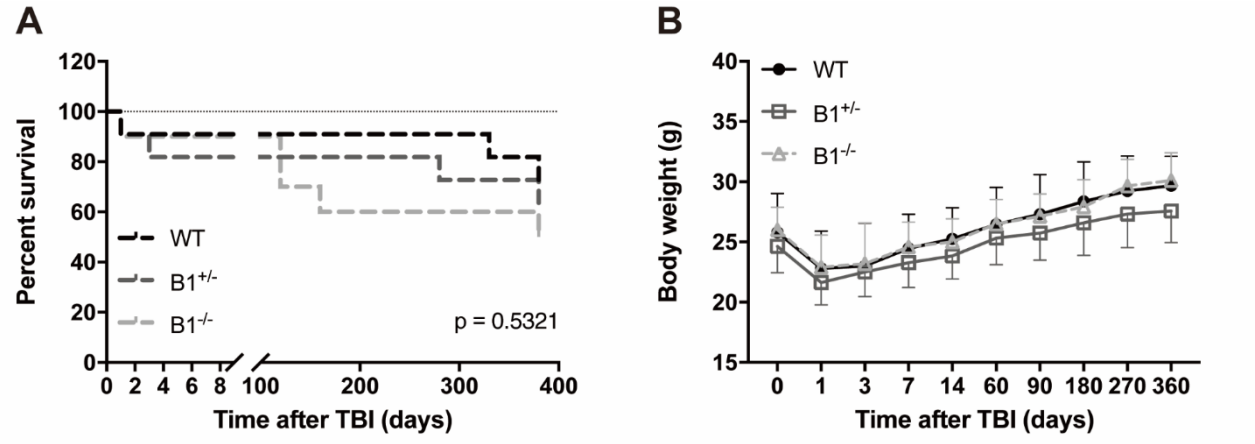

Figure 15: Survival rate and body weight after TBI. (A) There was no significant difference between genotypes (Log Rank analysis). (B) The body weight of mice dropped at the first day after CCI (p=0.423), then increased gradually up to 1 year after TBI. There was no significant difference between groups at any time point. Mean ± SD, n=5-8.

3.1.2 Effect of B1 receptor deficiency on the long-term recovery of motor function (Beam Walk Test)

Before CCI, it took 8.8 ± 3.0 s (WT), 9.1 ± 3.6 s ($B1^{+/-}$), and 10.6 ± 2.1 s ($B1^{-/-}$) for the mice to cross the beam (p=0.483). The crossing time significantly increased after CCI, peaking at day one after surgery: In the WT group, time to cross (62.1 ± 43.1 s, $p < 0.001$ vs baseline) tended to be longer compared with $B1^{+/-}$ (53.4 ± 29.8 s, $p < 0.001$ vs baseline) or $B1^{-/-}$ mice (35.44 ± 22.41 s, p = 0.008 vs baseline). However, there was no significant difference (p=0.731) between groups. Crossing time then gradually decreased over the first two months and reached a plateau (WT: 16.6 ± 4.6 s, $B1^{+/-}$: 14 ± 3.3 s, and $B1^{-/-}$: 14.7 ± 5.2 s) from 60 days after TBI on. At 360 days after TBI, all animals recovered significantly but there was still a significant difference of crossing time compared to the respective pre-trauma baseline (WT: 20.9 ± 9.4 s, p=0.003 vs baseline; $B1^{+/-}$: 17.9 ± 10.1 s, p=0.037 vs baseline; and $B1^{-/-}$: 24.4 ± 8.4 s, p=0.019 vs baseline). There was no significant difference between the genotypes (Figure 16 A).

Before TBI, there were no missteps observed in any group. One day after TBI, animals made a very high number of missteps. While the number of missteps in the WT and homozygous B1 mice (WT: 23.5 ± 11.2; $B1^{-/-}$: 24.1 ± 6.8) reached a maximum at day one after CCI, the missteps in the heterozygous B1-group peaked at three days after TBI (24.4 ± 6.7, p=0.788); there was, however, no difference between the maximum number of missteps between groups. Within the subsequent 360 days the number of missteps dropped in all genotypes over time, but remained elevated as compared to baseline in all groups indicating that a slight motor deficiency remained long-term. At the end of the observation period, the number of missteps in the $B1^{+/-}$ group (8.8 ± 6.5) was slightly lower than in the wild type (11.9 ± 5.6) or the $B1^{-/-}$ group (13.6 ± 6.8). Again, there was no significant difference between groups (p=0.607) (Figure 16 B).

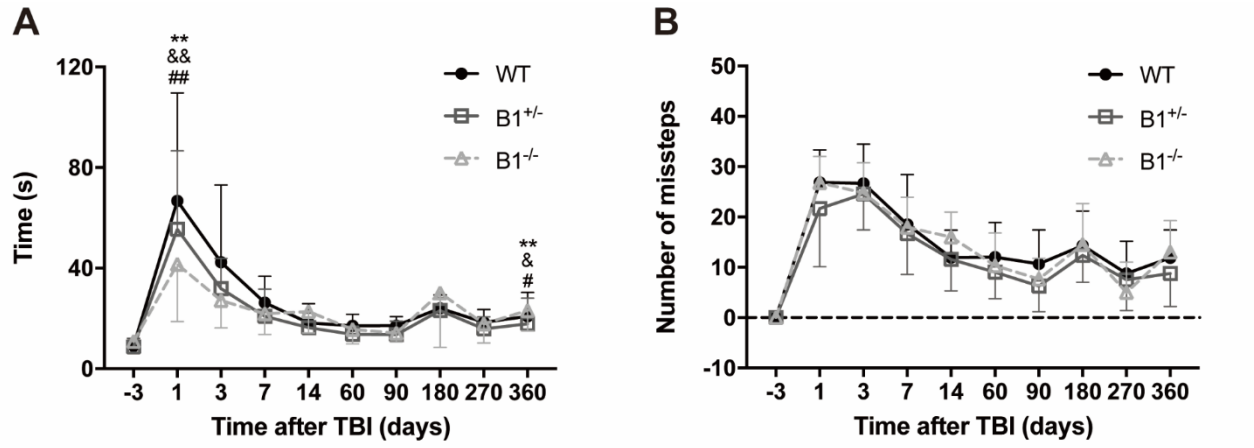

Figure 16: Effect of B1 deficiency on changes of motor function up to one year after TBI. (A) Time needed to cross the beam and (B) Number of missteps are significantly elevated directly after trauma and recover over time; at one year after CCI, a slight but significant impairment of motor function remains compared to pre-trauma values while there was no difference between genotypes for both parameters. Mean ± SD, n=5-8. & $p < 0.05$, $B1^{+/-}$ vs baseline; # $p < 0.05$, $B1^{-/-}$ vs baseline; ** $p < 0.01$, WT vs baseline; && $p < 0.01$, $B1^{+/-}$ vs baseline; ## $p < 0.01$, $B1^{-/-}$ vs baseline.

3.1.3 Effect of deficiency of B1 receptor on depressive-like behavior after TBI

Sixty days after TBI, the mobility time assessed in the tail suspension test was 111.9 ± 13.9 s in the WT group, 117.2 ± 14.8 s in heterozygous B1, and 103.52 ± 21.04 s in homozygous B1-deficient mice. While there were some slight fluctuations over time at the time points assessed (60, 90, and 180 days after CCI), there never was a significant change of mobility time within any group or between genotypes (Figure 17), indicating that the B1 receptor does not affect depression-like behavior.

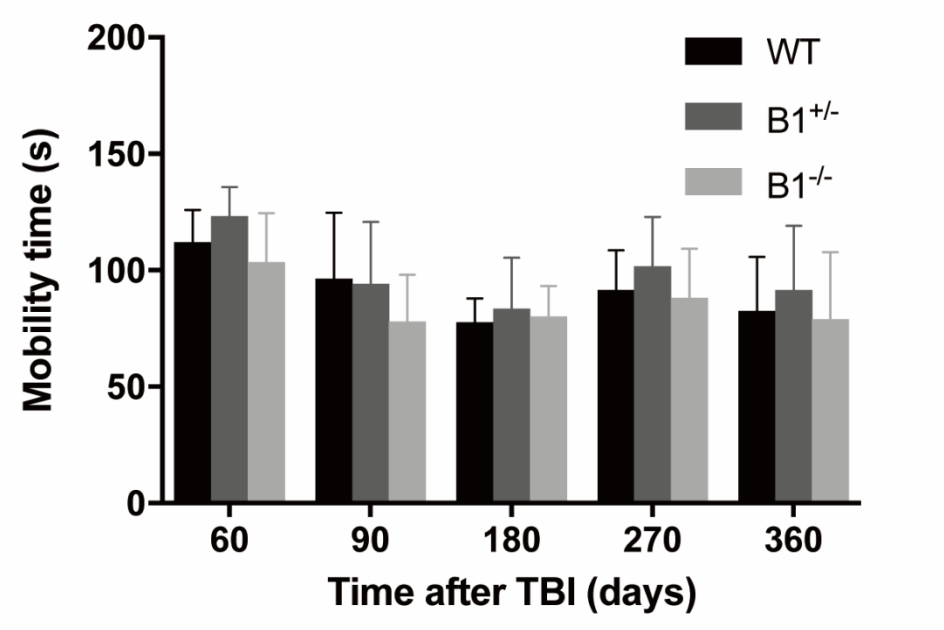

Figure 17: Effect of disruption of B1 receptor on chronic progression of depression-like behavior after TBI. Mobility time did not show significant alterations over time. Mean ± SD, n=5-8.

3.1.4 Effect of B1 receptor deficiency on memory function and learning behavior after TBI (Barnes Maze test)

The long-term cognitive function of mice after TBI was assessed by the Barnes Maze test. Figure 18 A shows representative heat-map images obtained 360 days after TBI. While latency to goal tended to increase over time, there was no significant difference compared to baseline nor any difference between genotypes over time (Figure 18 B). The distance

to goal decreased within 6 months, then increased up to one year after TBI. There was no significant difference between groups at any time (Figure 19 A). The velocity of mice increased over time, but still did not reach statistical difference between groups at any time point (Figure 19 B).

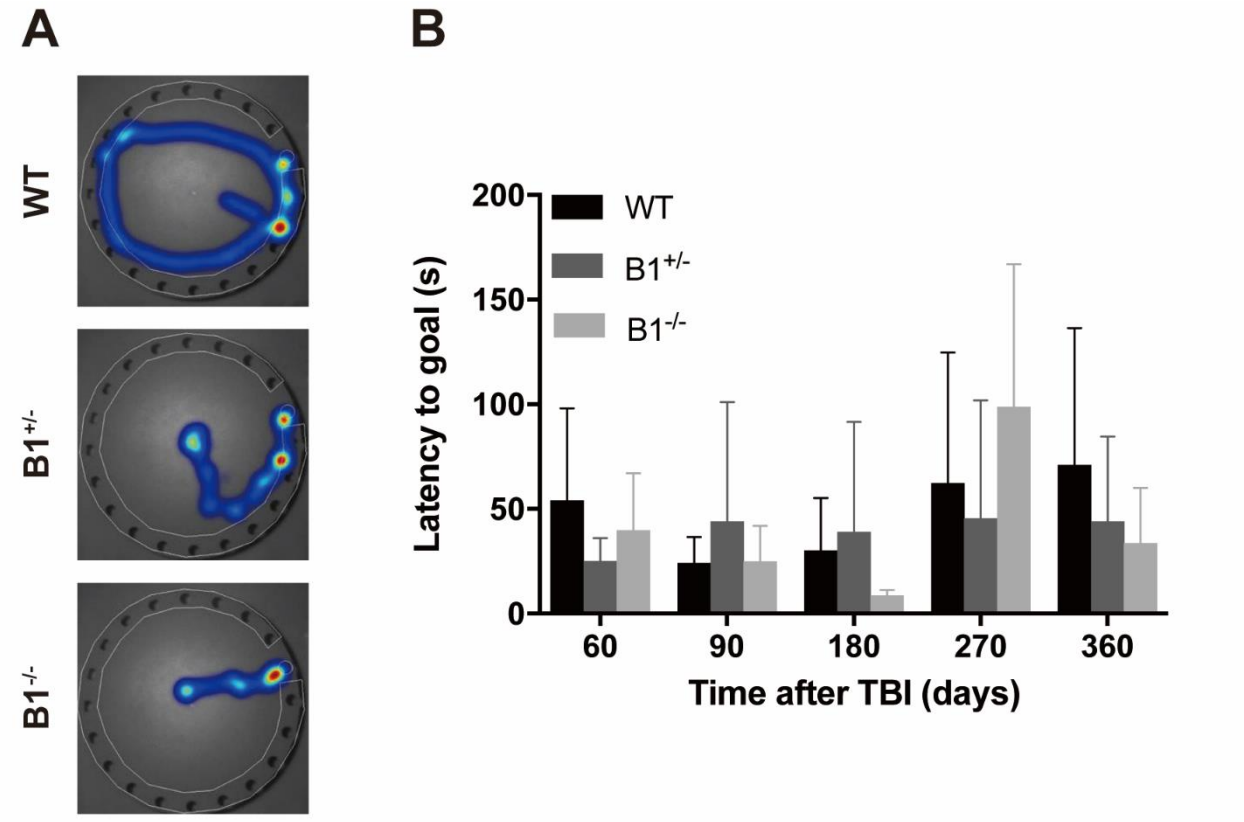

Figure 18: Effect of B1 receptor deficiency on memory and learning behavior after experimental TBI. (A) Representative heat maps at 360 days after TBI. (B) Latency to goal did not significantly change over time, furthermore there was no significant difference between groups. Mean ± SD, n=5-8.

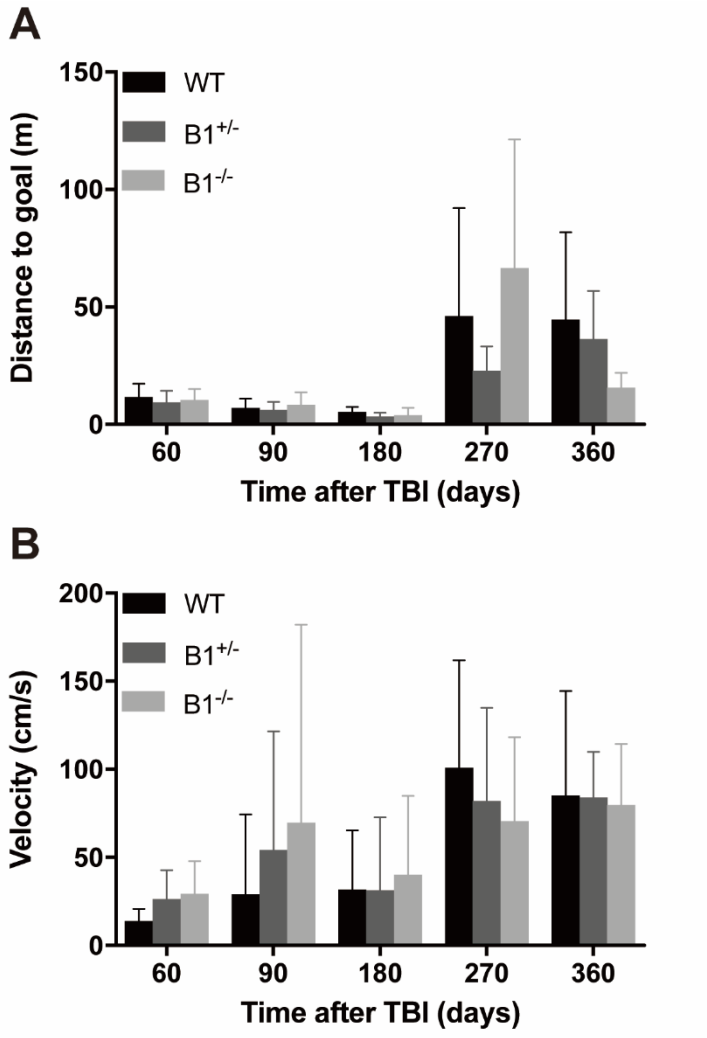

Figure 19: Effect of B1 receptor deficiency on distance (A) and velocity to goal (B) in the Barnes test. There was no significant difference between groups for both parameters. Mean ± SD, n=5-8.

3.1.5 Effect of B1 receptor deficiency on lesion size and chronic lesion progression after TBI

Lesion size was assessed longitudinally in serial MRI scans at 60, 90, 180, 270 days up to one year after CCI. Figure 20 A shows representative T2-weighted axial images obtained 360 days after TBI. In wild type animals (black bars), lesion volume steadily increased over time peaking one year after experimental TBI. Heterozygous B1 animals had significantly lower lesion volumes compared to WT mice at all-time points assessed (60 days: 15.6 ±

4.9 mm^3 vs 24.86 ± 8.97 mm^3, p=0.03; 90 days: 16.1 ± 4.3 mm^3 vs 23.7 ± 7.3 mm^3, p=0.047; 180 days: 21.7 ± 6.3 mm^3 vs 32.5 ± 5.9 mm^3, p=0.019; 270 days: 23.9 ± 7.9 mm^3 vs 34.2 ± 6.5 mm^3, p=0.041; 360 days: 23.5 ± 8.6 mm3 vs 37.6 ± 5.7 mm3, p=0.004). Lesion volume of homozygous B1 mice (60 days: 18.2 ± 5.2 mm^3, 90 days: 18.7 ± 5.4 mm^3, 180 days: 28.8 ± 6.8 mm^3, 270 days: 28.2 ± 8.6 mm^3, 360 days: 29.4 ± 7.8 mm^3) tended to be lower than those of the WT group, but there was no significant difference at any time (Figure 20 B).

Histological lesion volume assessment (see exemplary Nissl stained slices in Figure 21 A) corroborated this finding (Figure 21 B): compared to lesion volume of the WT group (37.3 ± 5.3 mm^3), $B1^{+/-}$ animals had significantly lower lesion volumes (28.1 ± 3.9 mm^3), while B1 homozygous mice had only a slight, non-significant reduction (33.6 ± 6.3 mm^3, p=0.029, $B1^{+/-}$ vs WT).

Lesion volume as assessed in T2 weighed imaging and by histology correlated significantly (Figure 22) indicating that MRI-based lesion volume determination is a valuable and accurate method for assessing posttraumatic brain damage in this setup.

In summary, these results suggest that partial depletion of the B1 receptor in heterozygous B1-mice confers significant neuroprotection, but that this effect is lost when the B1-receptor was completely abolished.

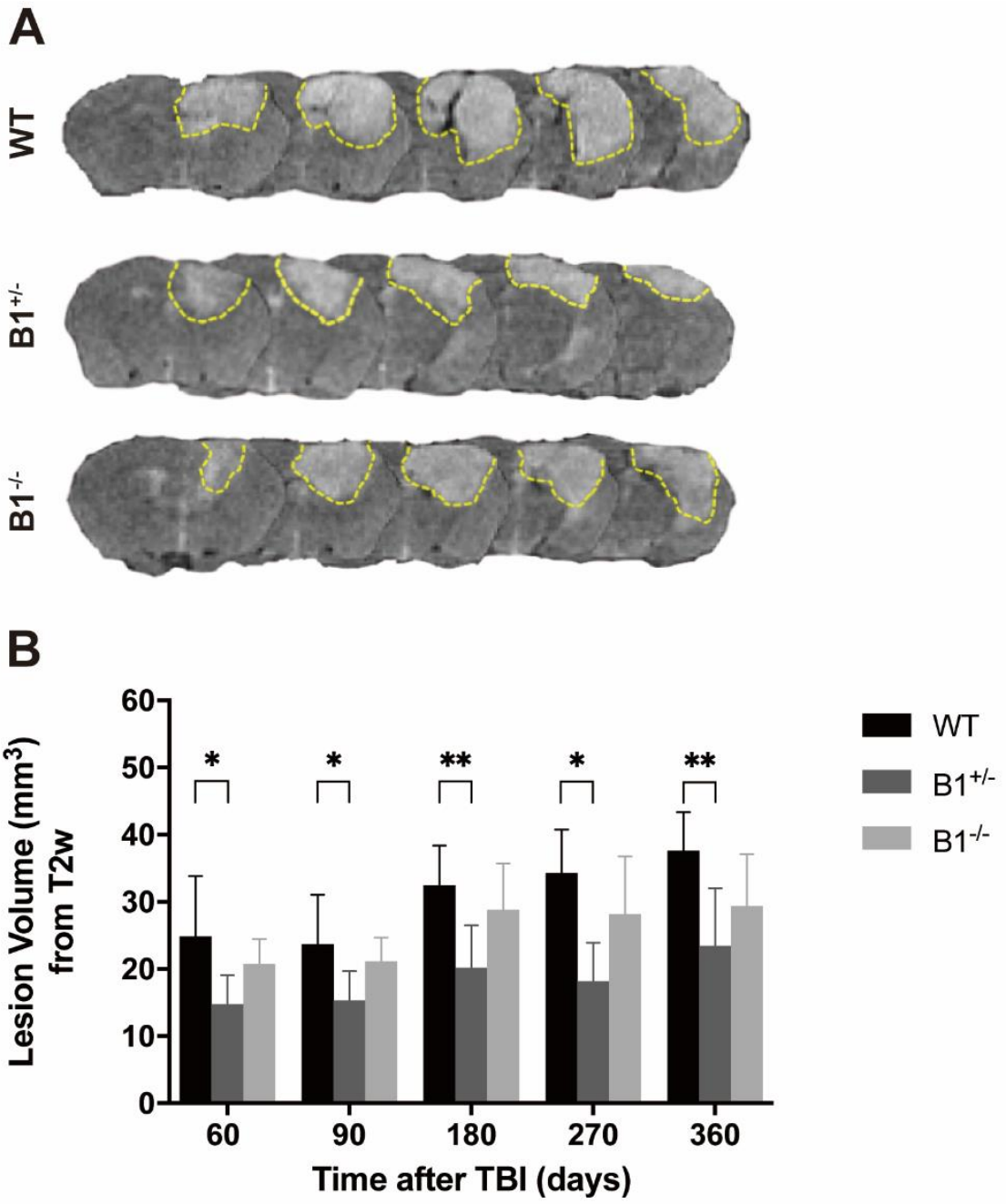

Figure 20: Effect of B1 deficiency on lesion progression as assessed by serial MRI scans after TBI. (A) Representative MRI images obtained 360 days after CCI from WT, $B1^{+/-}$, and $B1^{-/-}$ mice, respectively. (B) Lesion volume increased up to one year after TBI. $B1^{+/-}$ animals had significantly lower lesion volumes while homozygously deficient mice showed only a small reduction by trend. Mean ± SD, n=5-8.

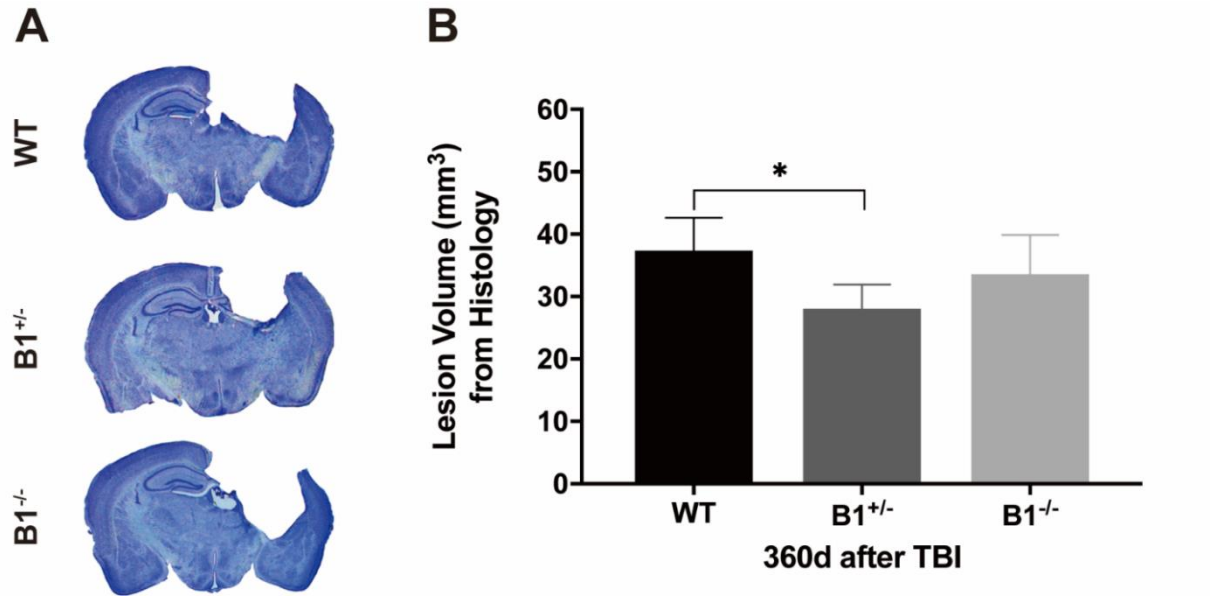

Figure 21: Histological assessment of lesion volume over time (A) Representative Nissl stained sections from WT, $B1^{+/-}$, and $B1^{-/-}$ mice at 360 days after CCI, respectively. (B) Lesion volume of WT mice was significantly larger than $B1^{+/-}$ at 360 days after TBI. Mean ± SD, n=5-8. *p<0.05, **p<0.01.

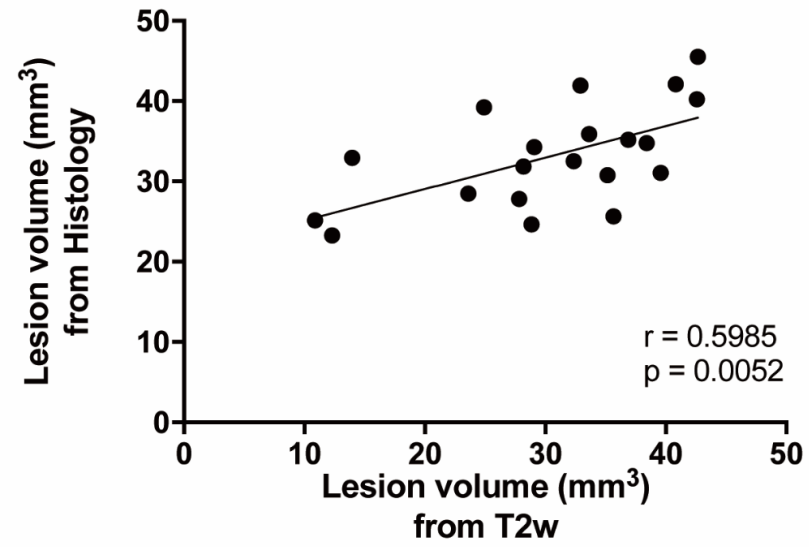

Figure 22: Lesion volume quantified by histology correlated with that measured by MRI. Pearson correlation test.

3.1.6 Effect of B1 receptor deficiency on hippocampal damage after TBI

Hippocampal damage was assessed histomorphometrically in Nissl stained sections (ipsilateral/traumatized vs. contralateral/non-traumatized). Representative brain sections of the dorsal hippocampus were obtained at 360d after TBI (Figure 23 A). While in WT mice, the ipsilateral hippocampus was significantly lesioned (35.1 ± 6.4 % of the contralateral side), it was significantly better preserved in $B1^{+/-}$ mice (50.1 ± 10.3%, p =0.011). Again, homozygous B1 mice showed some protection (48.2± 13.5 %), but no significant difference compared to wild-type littermates (Figure 23 B).

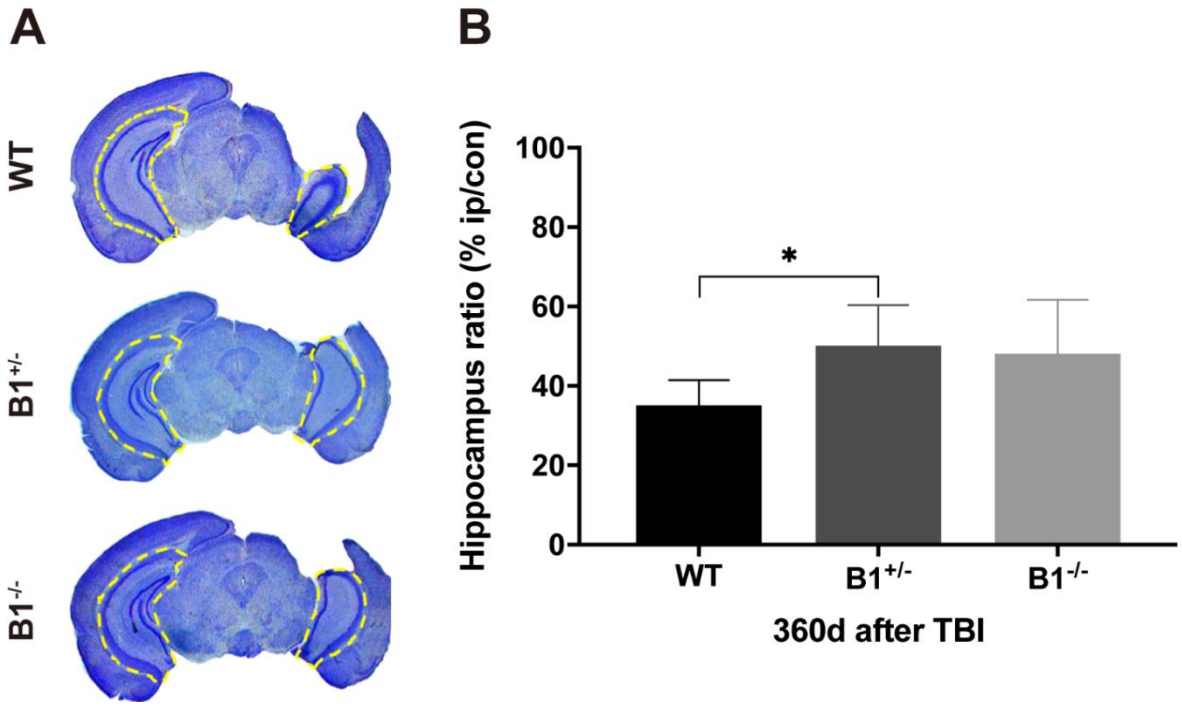

Figure 23: Effect of B1 receptor deficiency on hippocampal damage after TBI. (A) Representative Nissl stained hippocampus sections from WT, $B1^{+/-}$ and $B1^{-/-}$ mice. (B) B1 heterozygous mice had significantly less hippocampal damage compared to wild-type littermate. Mean ± SD, n=5-8. *p<0.05.

3.2 Effect of the Asic 1a channel on chronic posttraumatic brain damage and outcome after experimental traumatic brain injury

3.2.1 Survival rate and body weight after TBI

After CCI, two animals in the WT group, three in the Asic $1a^{+/-}$, and three in the Asic $1a^{-/-}$ group died within seven days; in the further course of the experiment, three WT animals, two Asic $1a^{+/-}$, and one Asic $1a^{-/-}$ mice died between 180 and 190 days after trauma. There was no significant difference between groups (P = 0.613) (Figure 24 A). Before surgery, body weight was 27.9 ± 4.1 g in the WT group, 28.2 ± 3.5 in the Asic $1a^{+/-}$, and 26.9 ± 3.1 in the Asic $1a^{-/-}$ group, respectively, there was no significant difference between groups. Body weight of all mice robustly decreased by about 13% at day one after TBI, but there was no significant difference among groups; it then recovered back to baseline at the end of the observation period. At 180d after CCI, the body weight of mice in the WT group, the Asic $1a^{+/-}$ group, and the Asic $1a^{-/-}$ group was 28.5 ± 3.5 g, 28.7 ± 3.4 g and 26.6 ± 3.3 g, respectively (p = 0.278). There was no difference between genotypes at any time during the experiment (Figure 24 B).

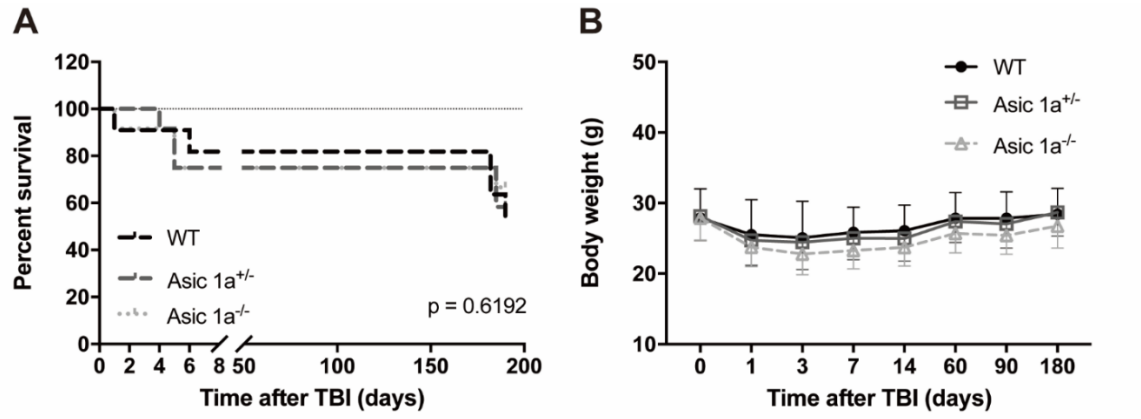

Figure 24: Survival rate and changes in body weight after TBI in Asic 1a transgenic animals. (A) Survival curve (Log Rank analysis). (B) Body weight of all mice dropped early after TBI, then recovered up to the end of the observation period. Mean ± SD, n = 9.

3.2.2 Effect of the Asic 1a on brain edema formation 24h after TBI

In sham operated animals, there was no difference in brain water content between genotypes. Twenty-four hours after TBI, brain water content of WT animals was significantly elevated compared to non-traumatized animals of both groups. Homozygous Asic $1a^{-/-}$ animals (76.8 ± 1.0%) had significantly lower brain water content than WT littermates (80.2 ± 3.0%, p=0.04, Asic $1a^{-/-}$ vs WT) indicating significantly reduced brain edema formation (Figure 25).

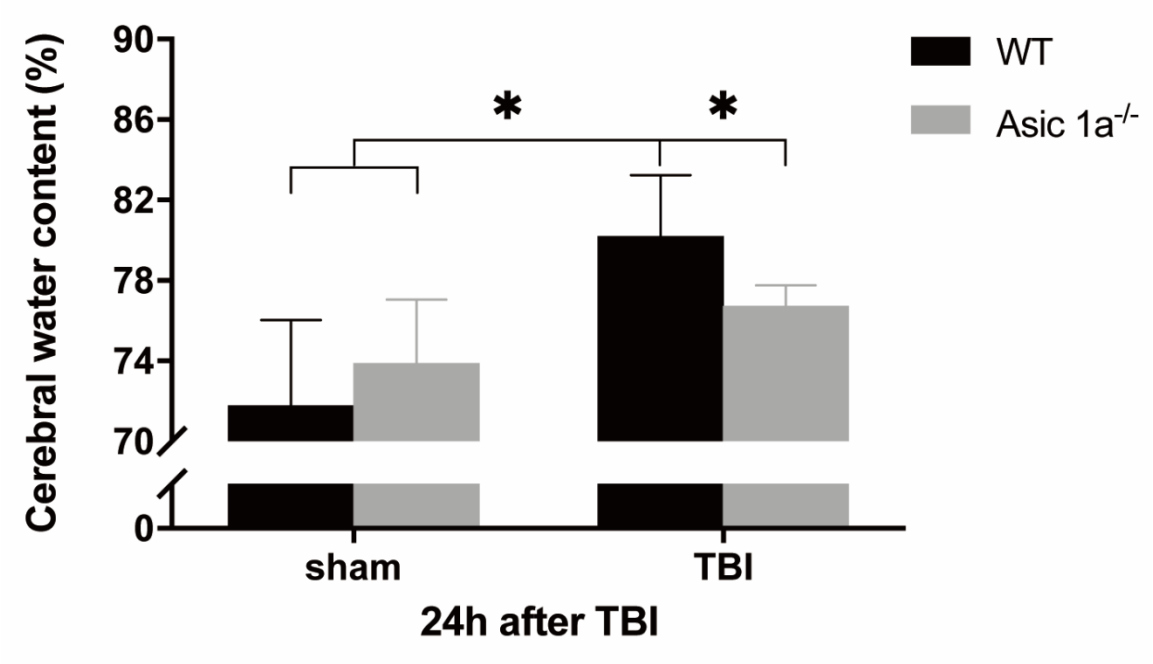

Figure 25: Effect of Asic 1a deficiency on brain edema formation 24h after TBI. While WT mice showed approximately 9% increase in brain water content compared to sham-operated animals, brain water content in Asic $1a^{-/-}$ mice was approximately 60% lower than that. Mean ± SD, n=4-8. * p<0.05.

3.2.3 Effect of Asic 1a on long-term recovery of motor function

Before TBI, all groups managed to cross the beam equally fast (WT: 12.6 ± 5.2 s, Asic $1a^{+/-}$: 14.6 ± 8.7 s, Asic $1a^{-/-}$: 11.7 ± 1.2 s). On day one, motor function significantly deteriorated compared to pre-trauma values (WT: 95.1 ± 31.2 s, p<0.001 vs baseline; Asic $1a^{+/-}$: 95.1 ±

33.1 s, p < 0.001 vs baseline; Asic $1a^{-/-}$: 73.2 ± 41.7 s, p<0.001 vs baseline). The increase was more pronounced in the WT group (95.13 ± 31.26 s) compared to heterozygous (88.33 ± 35.89 s) and homozygous (73.22 ± 42.70 s) Asic 1a animals, but there was no significant difference between groups. On days three and seven, crossing times (3d: WT: 70.2 ± 42.7 s, p<0.001 vs baseline; Asic $1a^{+/-}$: 62 ± 41.4 s, p=0.019 vs baseline; Asic $1a^{-/-}$: 48.6 ± 32.3 s, p=0.005 vs baseline; 7d: WT: 40.2 ± 31.7 s, p=0.004 vs baseline; Asic $1a^{-/-}$: 36.7 ± 19.6 s, p=0.02 vs baseline) were still significantly longer compared to pre-trauma values. Within the first two weeks after TBI, animals´ performance recovered (WT: 23.1 ± 19.7 s; Asic $1a^{+/-}$: 19.6 ± 12.5 s; Asic $1a^{-/-}$: 19.3 ± 11.9 s) then stayed stable until the end of the observation period, traumatized mice did not recover back to the pre-trauma level. There was no difference between groups at any time point (Figure 26 A). Prior to surgery, no missteps were observed. Immediately after TBI, the number of missteps (WT: 38 ± 10.1 s, p=0.001 vs baseline; Asic $1a^{+/-}$: 41.7 ± 6.8 s, p<0.001 vs baseline; Asic $1a^{-/-}$: 34.7 ± 5.5 s, p<0.001 vs baseline) significantly increased compared to baseline, but did not reach statistical significance between groups. From posttraumatic day three on, the mice´s performance improved, but did not return to pre-trauma values at the end of the observation period (WT: 7.89 ± 4.51, Asic $1a^{+/-}$: 9.44 ± 5.94, Asic $1a^{-/-}$: 7.89± 4.46), there was no significant difference between groups (Figure 26 B).

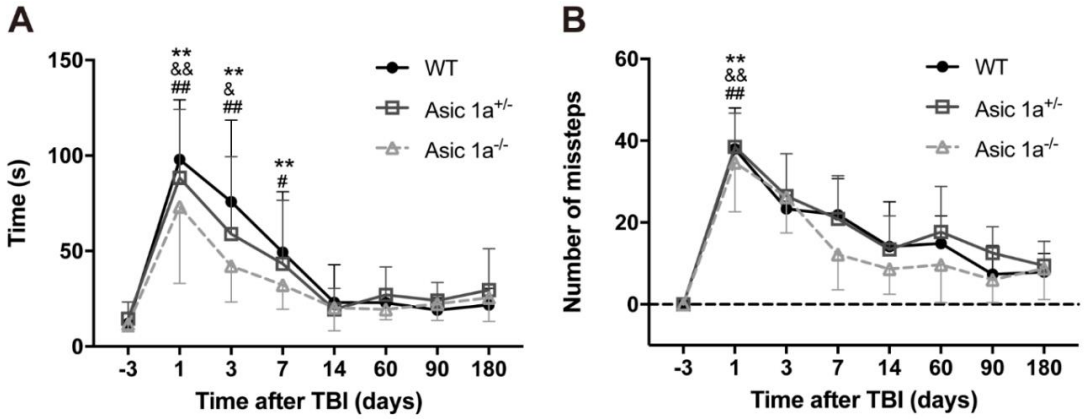

Figure 26: Effect of Asic 1a on long-term recovery of motor function. (A) Time needed to cross the beam (B) Number of missteps. &p < 0.05, Asic 1a $^{+/-}$ vs baseline; #p < 0.05, Asic 1a$^{-/-}$ vs baseline; **p < 0.01, WT vs baseline; &&p < 0.01, Asic 1a$^{+/-}$ vs baseline; ## p < 0.01, Asic 1a$^{-/-}$ vs baseline. Mean ± SD, n=9.

3.2.4 Effect of Asic 1a on depression-like behavior after TBI

At all-time points assessed, Asic1a$^{-/-}$ animals showed significantly higher mobility times than their heterozygous and wild type littermates (60 d: WT: 90.5 ± 26.5 s, Asic 1a$^{+/-}$: 100.6 ± 23.9 s, Asic 1a$^{-/-}$: 139.9 ± 18.3 s, p<0.01, Asic 1a$^{-/-}$ vs WT, Asic 1a$^{+/-}$; 90d: WT: 84.7 ± 13.6 s, Asic 1a$^{+/-}$: 89.6 ± 16.1 s, Asic 1a$^{-/-}$: 120.8 ± 20.5 s, p<0.01, Asic 1a$^{-/-}$ vs WT, Asic 1a$^{+/-}$; 180d: WT: 88.2 ± 21.4 s, Asic 1a$^{+/-}$: 103.2 ± 14.6 s, Asic 1a$^{-/-}$: 132.1 ± 16.1 s, p<0.01 ,Asic 1a$^{-/-}$ vs WT, Asic 1a$^{+/-}$), indicating that Asic 1a significantly influences the development of neurobehavioral disturbances after TBI (Figure 27).

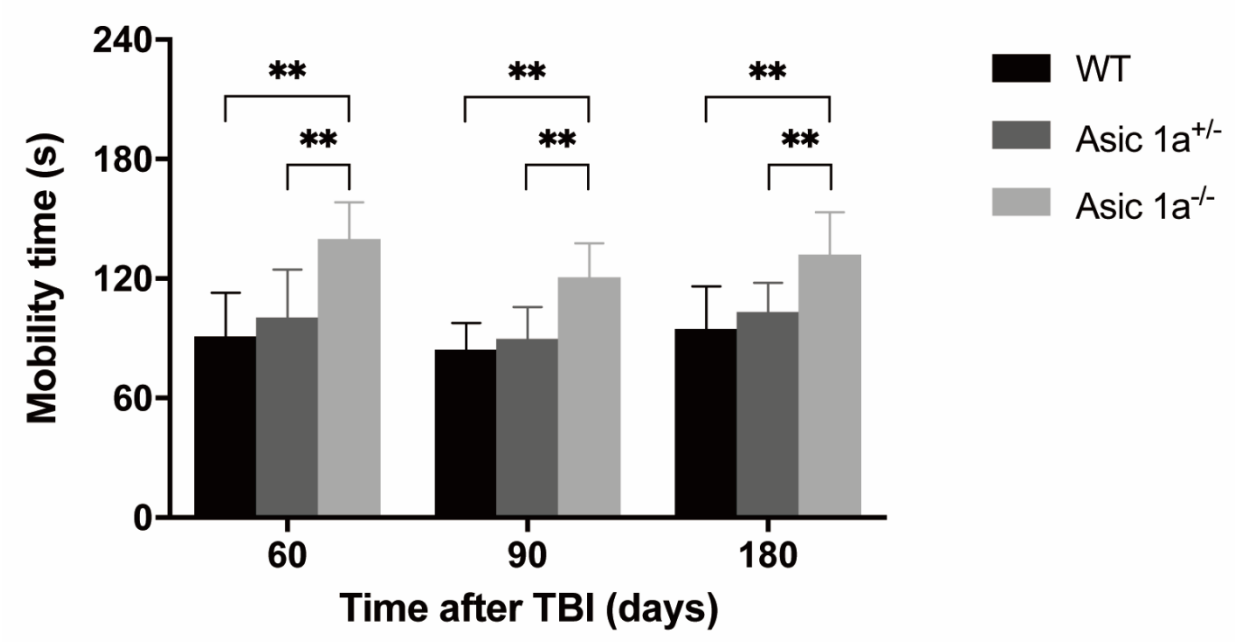

Figure 27: Effect of Asic 1a in depression-like behavior after TBI: Mobility time as assessed by the tail suspension test. Mean ± SD, n=9. **p<0.01.

3.2.5 Effect of Asic 1a on memory and learning behavior cognitive function after TBI

Exemplary heat maps from the WT, the Asic 1a $^{+/-}$, and the Asic 1a $^{-/-}$ group are presented in Figure 28 A. While latency (Figure 28 B) in all groups decreased over time (60 d: WT: 88.8 ± 70.8 s, Asic 1a$^{+/-}$: 142.6 ± 45.9 s, Asic 1a$^{-/-}$: 49.9 ± 59.1 s; 90 d: 48.9 ± 51.1 s, Asic 1a$^{+/-}$: 78.8 ± 60.2 s, Asic 1a$^{-/-}$: 22.4 ± 8.6 s; 180d: WT: 39.9 ± 26.7 s, Asic 1a$^{+/-}$: 52.4 ± 50.5 s, Asic 1a$^{-/-}$: 18.4 ± 23.4 s), it was significantly shorter in the Asic 1a$^{-/-}$ group compared to heterozygous Asic 1a mice and wild type littermates (at 180 days, p=0.026, Asic 1a$^{-/-}$ vs WT; p=0.025, Asic 1a$^{-/-}$ vs Asic 1a$^{+/-}$).

The distance travelled to reach the home-cage was not different between groups at 60 (WT: 73.3 ± 67.2 m, Asic 1a$^{+/-}$: 85.5 ± 58.6 m, Asic 1a$^{-/-}$: 42.6 ± 33.6 m) and 90 days (WT: 42.5 ± 23.4 m, Asic 1a$^{+/-}$: 99.4 ± 99.6 m, Asic 1a$^{-/-}$: 34.7 ± 15.1 m) after trauma; at the last testing session 180 days after CCI, the WT group´s distance (45.09 ± 35.43 m) was

significantly longer than in the Asic $1a^{-/-}$ group (23.17 ± 30.34 m, p=0.048, Asic $1a^{-/-}$ vs WT) (Figure 29 A).

The velocity to get the home cage slightly fluctuated over time (60 d: WT: 97.9 ± 41.6 cm/s, Asic $1a^{+/-}$: 67.9 ± 48.1 cm/s, Asic $1a^{-/-}$: 117.2 ± 38.2 cm/s; 90 d: 106.5 ± 38.2 cm/s, Asic $1a^{+/-}$: 35 ± 26.6 s, Asic $1a^{-/-}$: 154.2 ± 35.9 s; 180d: WT: 112.7 ± 32.8 s, Asic $1a^{+/-}$: 86.2 ± 32.6 s, Asic $1a^{-/-}$: 134.7 ± 32.9 s) (Figure 29 B), but there was no statistical difference at any time. These results indicate that Asic1a deficiency significantly improves cognitive deficits after TBI.

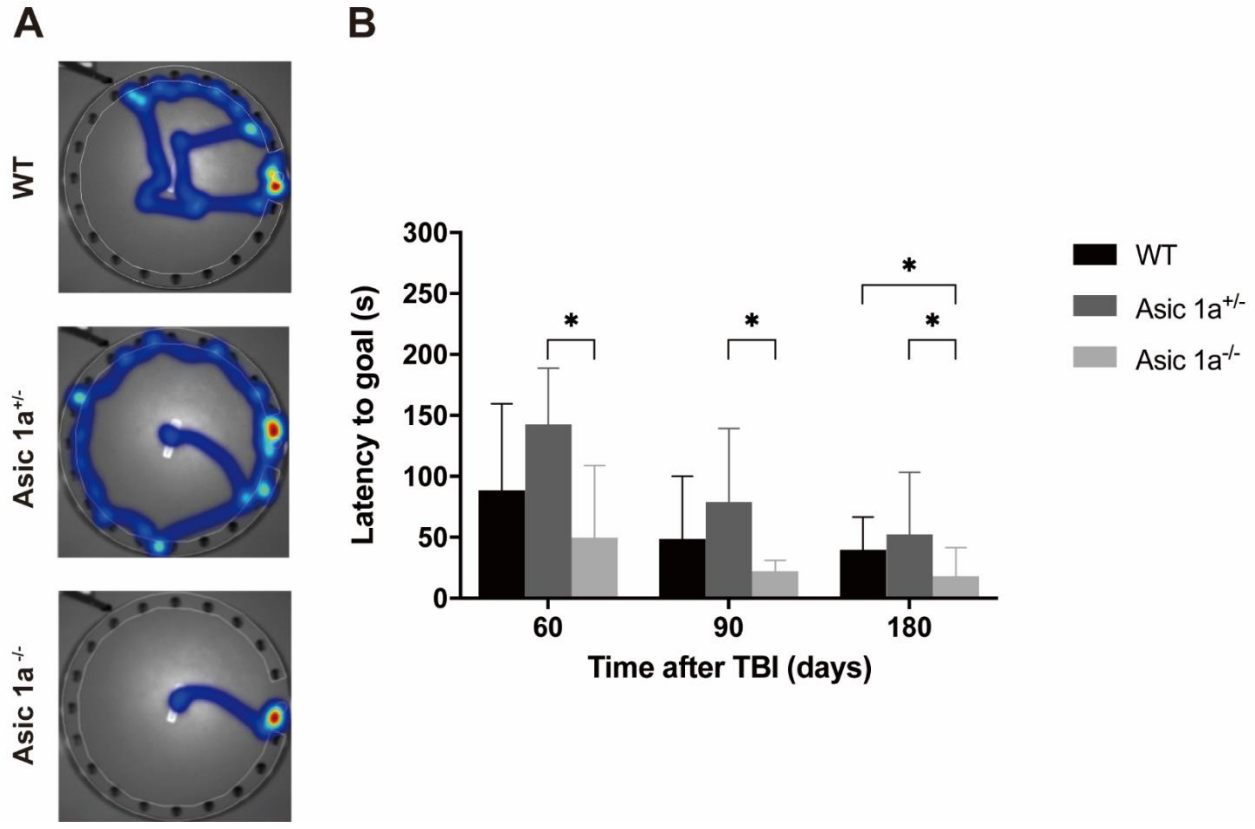

Figure 28: Effect of Asic1a on neurocognitive deficits after TBI. (A) Representative heat maps from WT, Asic $1a^{+/-}$, and Asic $1a^{-/-}$ mice at 180d after TBI. (B) Latency to goal. Mean ± SD, n=9. *p<0.05.

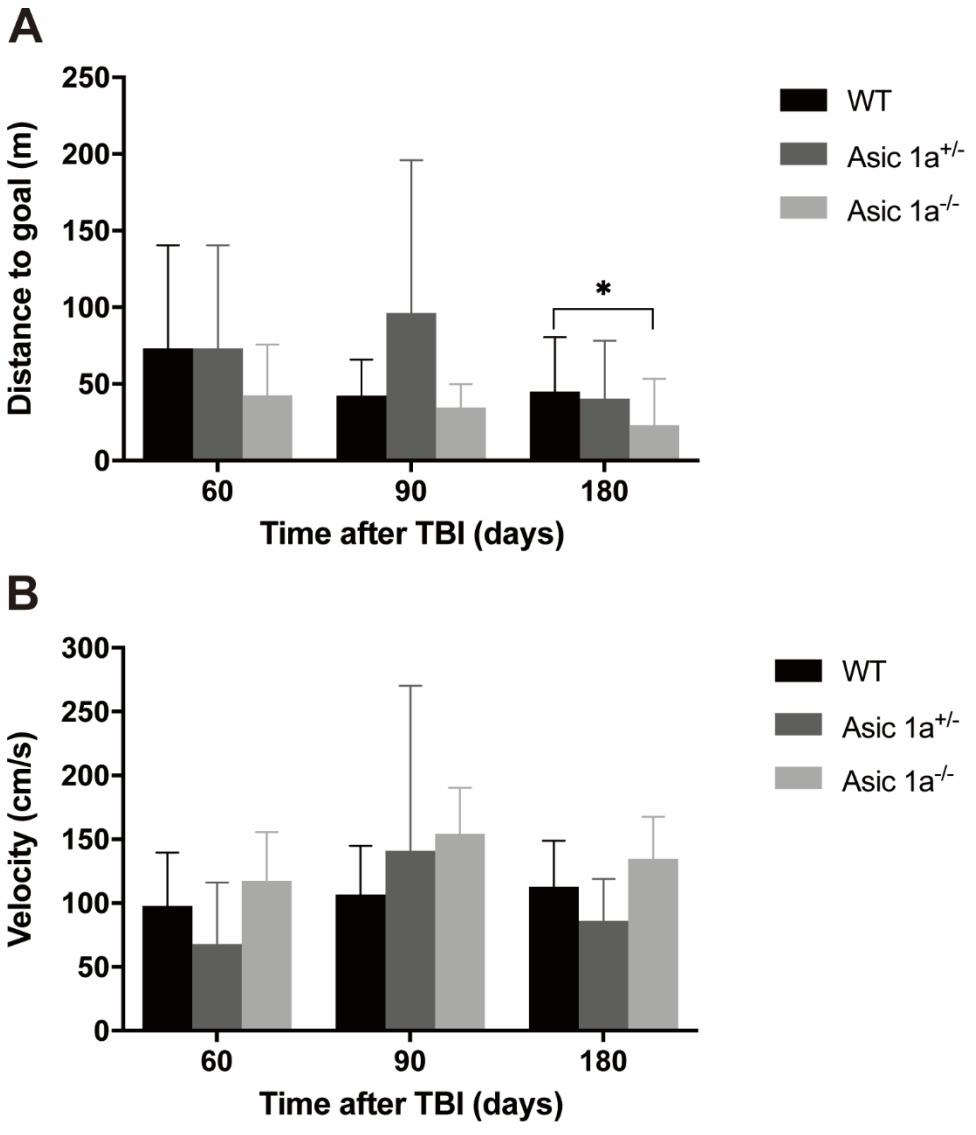

Figure 29**:** Effect of Asic 1a on distance and velocity to goal in the Barnes Maze test after TBI. (A) Distance to goal. (B) Velocity to goal. Mean ± SD, n=9. *p<0.05.

3.2.6 Effect of Asic 1a on lesion progression after experimental TBI

Exemplary images of T2 weight MRI scans from the WT, the Asic $1a^{+/-}$, and the Asic $1a^{-/-}$ group obtained at 180d post-TBI are provided in Figure 30 A. In WT animals, lesion volume steadily increased over time up to 180 days after TBI (32.3 ± 5.2 mm^3, p=0.011, 180 days vs 14 days). In Asic 1a transgenic animals, lesion size remained relatively stable, there was no obvious lesion progression from day 14 to day 180 after CCI. At later time points (60, 90, and 180 days after TBI), lesion size of Asic1a transgenic animals was significantly

smaller compared to wild-type littermates (60 days: WT: 24.6 ± 8.3 mm^3, Asic $1a^{+/-}$: 15.2 ± 4.6 mm^3, Asic $1a^{-/-}$: 17.4 ± 2.9 mm^3, $p<0.01$, Asic $1a^{+/-}$ vs WT; $p<0.05$, Asic $1a^{-/-}$ vs WT; 90 days: WT: 26.2 ± 8.1 mm^3, Asic $1a^{+/-}$: 17.8 ± 5.2 mm^3, Asic $1a^{-/-}$: 18.2 ± 4.2 mm^3, $p<0.05$, Asic$1a^{+/-}$, Asic $1a^{-/-}$ vs WT; 180 days: WT: 32.3 ± 5.1 mm^3, Asic $1a^{+/-}$: 19.2 ± 4.5 mm^3, Asic $1a^{-/-}$: 20.4 ± 2.4 mm^3, $p<0.01$, Asic $1a^{+/-}$, Asic $1a^{-/-}$ vs WT). There was, however, no difference between homozygous and heterozygous Asic 1a mice (Figure 30 B).

MRI results were then correlated with histology (obtained at 180 days after TBI). Figure 31 A contains representative Nissl stained brain sections for each genotype. Histomorphologically assessed lesion volume was significantly larger in the WT group (37.0± 5.1 mm^3) compared to the Asic $1a^{+/-}$ (26.9 ± 3.3 mm^3) and the Asic $1a^{-/-}$ group (25.8 ± 3.9 mm^3, $p<0.01$, Asic $1a^{+/-}$, Asic $1a^{-/-}$ vs WT), respectively (Figure 31 B).

Histopathologically obtained results strongly correlated ($r = 0.8266$, $P < 0.0001$, Figure 32) with lesion volume measured in MRI indicating the MRI measurements are a reliable way to quantify posttraumatic brain damage. This data indicates that Asic1a deficiency significantly influences long-term lesion progression after TBI.

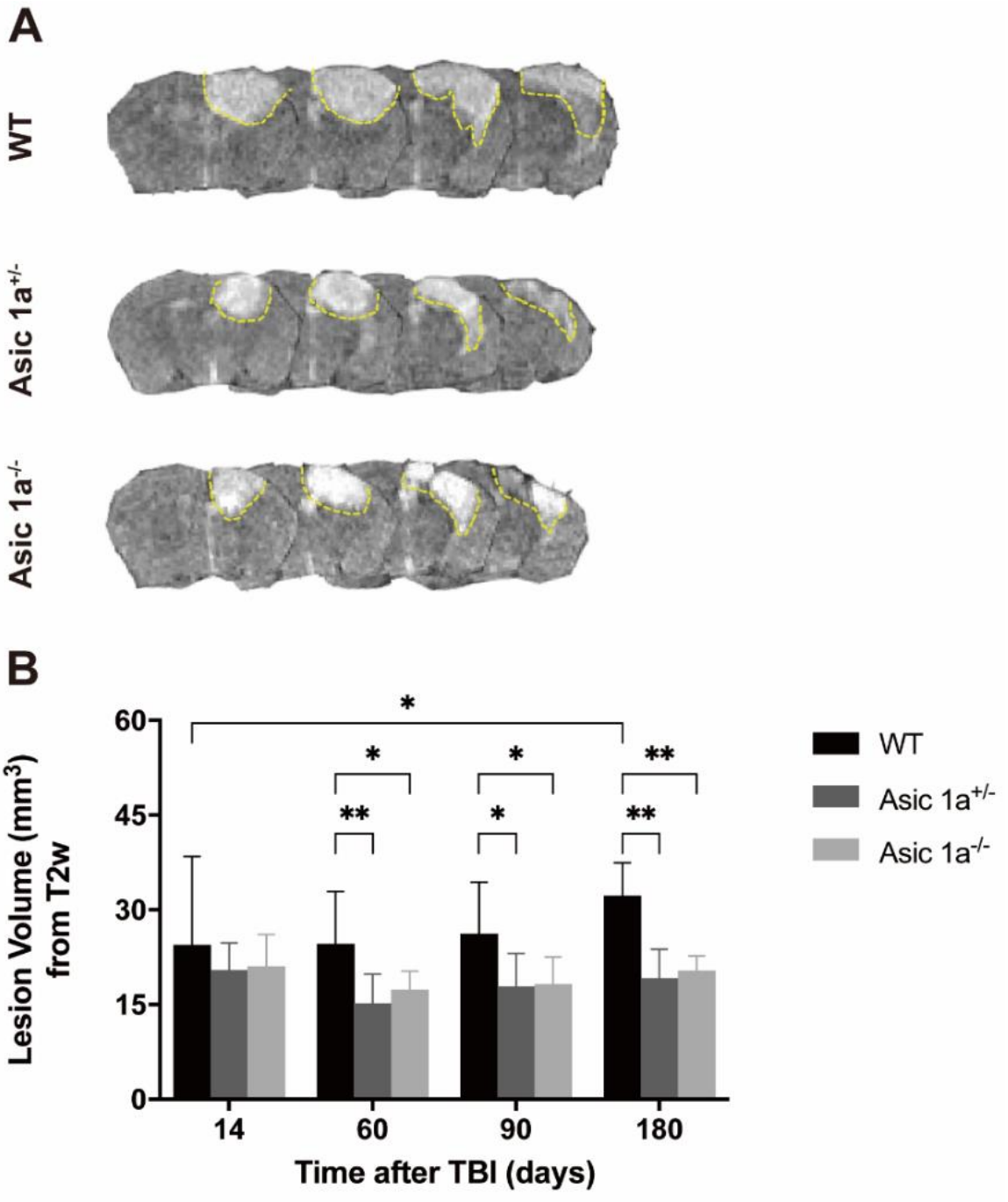

Figure 30: Effect of Asic1a deficiency on lesion progression after TBI assessed by MRI. (A) Representative MRI images from WT, Asic 1a $^{+/-}$, and Asic 1a $^{-/-}$ mice at 180d post-TBI, respectively. (B) Lesion volume over time. Mean ± SD, n=9. *p<0.05, **p<0.01.

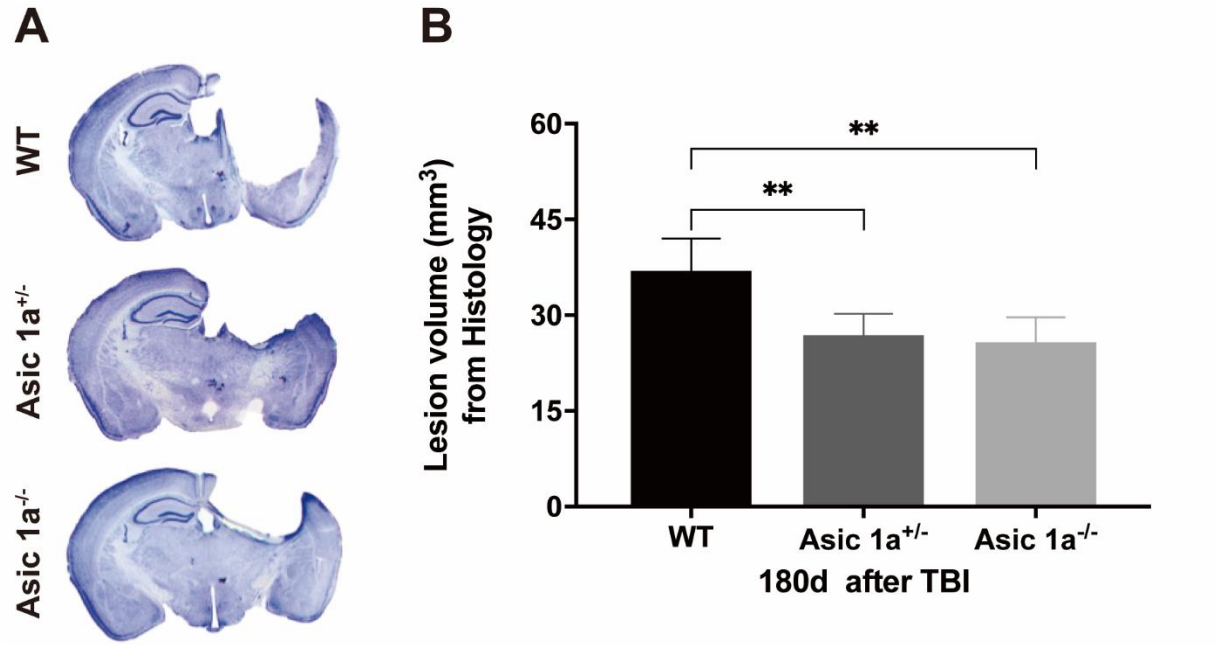

Figure 31**:** Lesion volume 180 days after TBI. Mean ± SD, n=6-8. **p<0.01.

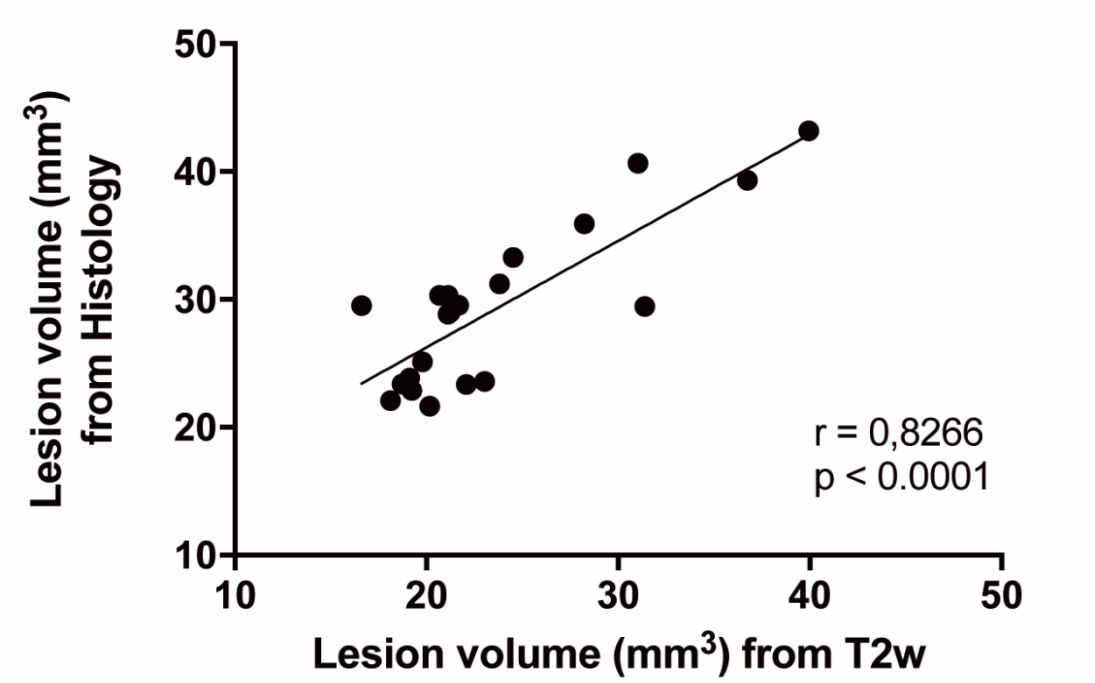

Figure 32: Lesion volume quantified by histology strongly correlates with that measured by MRI. Pearson correlation test.

3.2.7 Effect of Asic 1a on hippocampal damage after TBI

Figure 33 A shows representative brain sections used for hippocampus evaluation. In the WT group, hippocampal volume (26.27 ± 4.04 % of non-traumatized side) was significantly more reduced than in the Asic $1a^{+/-}$ (44.24 ± 13.11 %) and the Asic $1a^{-/-}$ (45.40 ± 4.82 %) group, where the hippocampal region was significantly better preserved (Figure 33 B). The reduction of hippocampal damage in the chronic phase after TBI may explain the improved performance of Asic1a deficient animals in memory tasks.

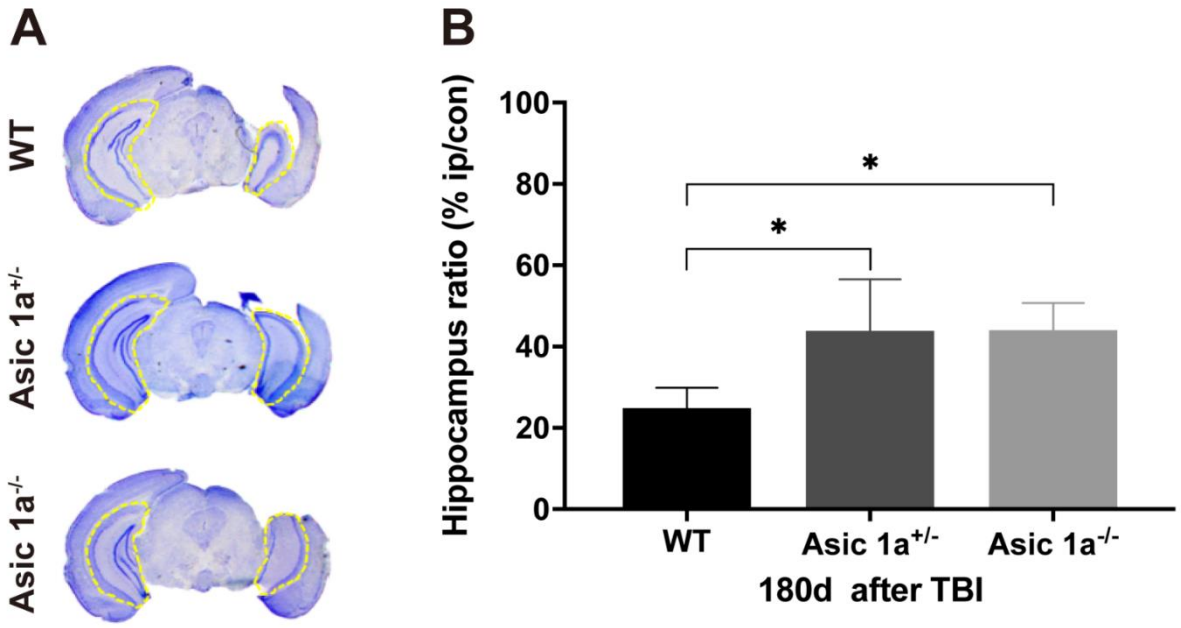

Figure 33: Effect of Asic 1a in hippocampal damage after TBI. (A) Representative Nissl stained section used for evaluation (B) Ratio of ipsilateral versus contralateral hippocampus volume. Mean ± SD, n=6-8. *p<0.05.

4. Discussion

4.1 Discussion of methods

4.1.1 Selection of traumatic brain injury model

Pathology and pathophysiology in humans is inhomogeneous after traumatic brain injury and may result in contusion, DAI, laceration, hemorrhage, or a combination thereof. In the past decades, three TBI animal models, namely the weight drop (WD) [228], the fluid percussion injury (FPI) [229], and the controlled cortical impact (CCI) model have been widely used in experimental studies [230] in order to model and investigate posttraumatic brain damage. Every model has advantages and disadvantages.

In the WD model, TBI is induced by a weight falling from a designated height onto the exposed skull with resulting in shearing forces causing brain injury [228, 231]. The injury severity is determined through adjustment of dropping height and weight of the mass. This model closely mimics clinical TBI and the application of the mechanical force is direct and simple [232]. The disadvantages of this model consist in re-hits [233], high mortality, and variable severity of brain injury [232]. In the FPI model, diffuse brain injury is induced by a fluid driven pendulum applied through a fluid-filled tube positioned over a craniotomy in a parasagittal, parietal, or frontal location [234, 235]. In this model, the placement of the craniotomy and the fluid pressure determine the pattern of brain injury, which – among other things – results in extensive contusions without skull fractures. This model causes widespread brain injury with characteristics of DAI and allows for induction of scalable lesion size with an acceptable rate of mortality. However, this model should be performed carefully, including precise craniotomy (size, position, and shape), accurate placement of tube over the opening skull, and complete removal of residual air in the tube. If not performed with utmost precaution, extent and type of brain injury is highly variable making this model hard to reproduce.

The CCI model causes a focal parenchymal contusion caused by the impact of a solid piston onto the dura mater through a cranial window [236-238]. The parameters (e.g. impact depth, duration, and velocity) of CCI can be accurately controlled to produce a reproducible, highly consistent focal brain injury. Adjustment of impact depth and velocity allows for variation of TBI severity (mild, moderate and severe), in combination with a low mortality. Furthermore, surgery for the CCI model is comparatively easy, making CCI a widely applied and accepted model for experimental TBI studies [236, 237, 239]. The model was routinely utilized in our laboratory in the past decades [74, 176, 219, 240-243]. In this model, the extent of cortical deformation is strongly correlated with histological brain damage [244], and neurological outcome [245, 246]. Even though CCI does not routinely induce DAI, it creates contusion injury and mimics several key components of human pathology after TBI [57], e. g. intracranial hypertension and cerebral hyperperfusion. Furthermore, the CCI model has been shown to be suitable for long-term investigation of posttraumatic brain damage as it also induces long-term changes comparable to those found in humans. Loane et al. reported that progressive lesion and persistent inflammatory responses up to one year in a rodent CCI model [247]. Progressive lesion expansion, white matter damage, and cognitive dysfunction were related to persistent inflammation up to one year in a single CCI model [248]. Xenon improved chronic neurological outcome associated with reduction of histological damage and chronic inflammatory responses up to 20 months after TBI [249]. Based on these characteristics of CCI, the model seemed an adequate choice for the present study.

4.1.2 Evaluation of posttraumatic brain damage

Since its introduction, magnetic resonance imaging is widely used in clinical and experimental brain research [250-253]. High-resolution MRI allows for exact assessment and tracking of anatomical and structural changes and may help to visualize and determine a variety of pathological changes [254]. Functional MRI can also detect cerebral blood flow changes and changes in lesion volume after TBI at the same time [255]. MRI

scanning is a noninvasive and time-saving method to observe brain injury at multiple time points in the same animal, giving information about the progression of a lesion over time which is not possible using histological methods, i.e. determination of lesion volume in histological specimens (e.g. Nissl staining), as this requires terminal tissue sampling. Therefore, MRI scanning significantly reduces the number of animals needed for studies with multiple time-points. Furthermore, histological assessment requires chemical treatment of the specimens with may result in tissue damage, especially in and around the contusion where tissue is necrotic and therefore hard to preserve. However, due to its low resolution, MRI scanning may be considered imprecise. In the present study we therefore correlated the results of lesion volumes obtained by MRI with histopathology at one chronic time-point after TBI and found a very high correlation. Therefore, lesion volumes determined by MRI seem to be reliable thereby making MRI the method of choice for long-term longitudinal studies after TBI.

4.1.3 Assessment of neurological outcome

After TBI, humans often present a variety of sequelae, e. g. motor and gait disturbances, depressive behavior, and neurocognitive abnormalities [256-258]. Neuropsychiatric symptoms are among the main reasons for impairment of quality of life in TBI patients and often prevent patients from leading an independent life and returning to their previous jobs [259, 260]. However, these symptoms can be challenging to diagnose and quantify in patients and even more so in experimental animals. In the present study, we decided to focus on three main symptom complexes: long-term changes in motor function (Beam walk test), learning and memory performance (Barnes Maze test), and depression-like behavior (Tail suspension test).

Various methods to assess motor function in rodents have been described, among them the beam walk test, the rotarod test [261], and the grid walking test [262]. The beam walk test can be performed in a highly standardized fashion with inexpensive equipment and is easily learnable; when combined with video monitoring also the evaluation is

standardized and less investigator-dependent, therefore the test is extensively used in rodent TBI models [263, 264]. The beam walk test has been validated to be an efficient test that was sensitive to the severity of injury, injury lateralization, and pharmacological administration in a cohort of TBI models, including CCI and lateral FP in rats and acceleration induced injury in mice [265-267]. Then grid walk, a test where animals are placed on an elevated metal square grid and their motor performance/missteps are recorded with a camera [268], sensibly shows forelimb dysfunction. However, in some studies, the beam walk test was more sensitive to hind limb motor deficits [269]. In this study, the injury position located in the right motor cortex controlling hind paw function on the left. Therefore, we chose the beam walk test for evaluation of motor dysfunction after TBI.

In order to diagnose and assess cognitive function, especially learning and memory deficits, the Water Morris Maze test (WMM) [270] and the Barnes Maze (BM) test [271] are commonly used. For the WMM, a home-cage platform is positioned in a circular pool filled with opaque water; animals then are trained to remember the location of the platform. The WMM, introduced by Robert Morris in 1982, was first applied to detect spatial memory deficits in rats with hippocampal lesions [272]. Later, the WMM was extensively used in order to detect and assess TBI-induced cognitive abnormalities [273, 274]. The BM was developed by Dr. Carol Barnes in 1979 [271] as a dry-land alternative to WWM. The BM has also been widely applied in experimental TBI [275, 276]. Compared to the MWM, animals were shown to have less averseness, anxiety, and stress compared to the MWM [271, 277]. Furthermore, neurochemical changes including serotonergic responses [278] were seen during MWM testing and have been shown to influence the results in cognitive function tests. In addition, swimming may lead to hypothermia, which may interfere with test results [279] and may be especially problematic in the setting of TBI where hypothermia was found to be neuroprotective [280]. Therefore, the BW test was chosen for assessing cognitive function in the present study.

Depression-like behavior is frequently tested using the forced swim test (FST) [281] and the tail suspension test [220, 282] in experimental (rodent) studies. In FST, the mouse is forced to swim in a cylinder filled with water and recorded by a camera for two minutes. Vigorous swimming motions are considered a physiological response, mobility time is calculated and recorded; immobility shows a reduced impetus indicating depressive behavior [283]. Again, hypothermia can be induced due to contact with water in the FST, interfering with the results [284]. The tail suspension test was described as a new model for testing anti-depressant drugs in 1985 [220]. In comparison to the FST, in the tail suspension test animals are suspended in a frame without induction of hypothermia. The experiment is considered less stressful for the animals. Furthermore, more animals can be tested simultaneously. In particular, this test is thought to be more sensitive in transgenic animals [222]. Therefore, the tail suspension test was used it in present study.

4.2 Discussion of the results

4.2.1 Effect of B1R deficiency on chronic post-traumatic brain damage

Bradykinin plays a crucial role in the acute phase after TBI, but its effect in the chronic phase in unclear. In the present study, we investigated the effect of the B1 receptor on long-term outcome after experimental TBI. We demonstrated that deficiency of B1R did not affect survival rate and body weight after TBI. Also, B1R deficit did not influence motor dysfunction, depression-like behavior, and cognitive function in a model of experimental traumatic brain injury. However, heterozygous B1R deficiency ameliorated lesion growth and hippocampal damage.

Motor dysfunction is a common sequela after severe traumatic brain injury. In a longitudinal study, motor abnormalities, including persistence of abnormal tandem gait, was observed up to two years after the TBI in a large number of subjects [285]; motor impairment was shown to persist from three months [286] up to five years post-TBI [287]. In the present investigation, motor dysfunction reached a peak at day one after TBI, then

recovered quickly and reached a plateau within two weeks. However, abnormal motor function persisted up to the end of the observation period of one year, which is consistent with previous studies [248, 288]. B1 deficiency did not alter the development of motor function compared to WT mice. According to previous data of our group, B1 receptor deficiency did not notably reduce brain edema in the acute phase [176], which may explain this result. Body weight is another parameter that reflects recovery after TBI. Loss of body weight results from a decrease of food intake and changes in metabolism [289]; in this study, it declined drastically on the first day after TBI and slightly recovered over time. This tendency was in accordance with previous investigations using the CCI model [248, 290]. B1R deficiency did not affect changes in bodyweight of mice after TBI. Some papers report that an increase in bodyweight can worsen motor function in long term studies post-TBI [291, 292], but in the present study body weight did not correlate with motor function.

In summary, B1R knockout did not show improvement of motor function or reduction of weight loss in the chronic phase after TBI.

Psychiatric disorders are common complications of traumatic brain injury and may present as depression, psychosis, mania and many more [293]. 15 to 33% of patients were diagnosed with a major depressive episode after TBI [294, 295]. According to a one-year longitudinal study on patients with TBI, about 40% of patients suffered from depression [296]. The highest rates of depression in patients with TBI were recorded within the first year after TBI [297], but depression onset was observed up to decades post-TBI [298]. In experimental TBI, depression-like behavior was noted to occur up to three months after brain injury [299-301]. There is little experimental data beyond this time point. In the present study, the mobility time declined from 60 days to one year post-TBI indicating that depression-like behavior aggravated over time and that three months may be too short to fully assess the frequency and severity of depression. Viana at al. found that inhibition of the B1 receptor did improve depression-like behavior in stressed mice 24 hours after

LPS injection [302] suggesting an involvement of bradykinin/ B1 receptors in the development of depression. In the present investigation, a deficit of B1R did not affect depressive behavior after experimental traumatic brain injury. The mechanisms of the development of depressive behavior in TBI is complicated. Development of depression post-TBI maybe is associated with disruption of biogenic amine containing fibers [296], furthermore is seems to be associated with grey matter atrophy, e. g. in the left pre-frontal cortex [303], the right frontal, left occipital, and left temporal lobes [304]. B1 deficiency alone was not sufficient to alter depression-like behavior independently. The B1 receptor therefore does not seem to play a major role in the development of depressive behavior after TBI.

Cognitive disorders are frequently diagnosed and may persist long-term in patients with traumatic brain injury regardless of injury severity [305-307] in form of – among others - attention deficits, memory disorders, and impairment of executive functions [308-311]. Cognitive abnormalities were described from three weeks after TBI [312] on. A review reported that nearly 50% of patients with penetrating, moderate, and severe TBI presented cognitive abnormalities six months and longer post-injury [308]. In several experimental studies, cognitive impairments were shown to persist up to one year after TBI [313-315]. In line with clinical and previous experimental data, our results indicate that cognitive dysfunction of mice persists up to one year after TBI, but was not altered by B1R deficiency. Of note, cognitive disorders do not just depend on axonal injury [136]; impaired synaptic plasticity and neurotransmitter systems (e.g., cholinergic, and catecholamine) may as well play pivotal roles [316]. Blocking of B1R facilitated recovery of cognitive deficits in a murine Alzheimer model [317] but while plaque formation is described to occur after TBI the pathophysiology most probably is fundamentally different to trauma-induced cognitive dysfunction.

Lesion volume progressively increased over time after TBI, which was in line with previous results using the CCI model [247]. Dixon showed that lesion volume at one year almost

doubled compared to that measured by histology at three weeks after TBI [318]. In the histological analysis 360 days after TBI, the result was similar to that observed with MRI at the same time point. The lesion volume assessed by MRI and histology correlated well, which is in accordance with the results obtained by Pischiutta et al. [248]. Homozygous B1R deficiency did not significantly reduce lesion progression compared to WT mice but heterozygous B1R knockout animals slowed smaller lesions from two months up to one year after TBI. It was previously reported that inhibition [178] or genetic depletion of the B1 receptor [179] confers neuroprotection after traumatic brain injury. Our previous results, however, indicate that B1 deficiency did not reduce lesion volume at 24h post-trauma [176]. Furthermore, lesion volume was only assessed in the acute phase so far, i.e. 24 hours after injury. In the present study, it was observed up to one year after trauma with changes visible only at later stages indicating that partial deficiency of the B1 receptor may have an influence long term. Additional studies are needed to further clarify this interesting effect. Our results also underline the need for long-term assessments following experimental traumatic brain injury.

In the present study, hippocampal damage was reduced in heterozygous B1 animals. Smith showed that hippocampal atrophy was associated with persistent memory dysfunction [319]. The changes in the neuronal circuitry of the hippocampus might be the neurological substrate of cognitive abnormalities frequently noted after TBI in humans [320-322]. Also, cognitive deficits correlated with hippocampal injury in an experimental rat model [323]. In the present study, no effect on memory function was detected despite reduction of hippocampal atrophy in B1 heterozygous animals. Neuronal loss in the hippocampus, however, was not specifically addressed. Furthermore, the Barnes Maze test may not be sensitive enough to detect slight differences. These data indicate that the relationship between cognitive function and hippocampus volume is more complex and needs further evaluation.

4.2.2 Effect of Asic 1a deficiency on chronic post-traumatic brain damage

In the present study, we investigated the effect of Asic 1a on the long-term outcome in a mouse model of traumatic brain injury. We demonstrated that deficiency of Asic 1a significantly reduced brain damage in the early phase after CCI. Chronically, it attenuated progression of lesion volume up to 6 months and hippocampus loss at 6 months after trauma. Furthermore, Asic 1a knockout remarkably ameliorated depressive behavior and cognitive dysfunction at 6 months post-TBI, but did not improve motor function.

Asic 1a is expressed on the postsynaptic membrane in both the central and peripheral nervous system [324] and activated by acidosis, resulting in influx of Na^+ and Ca^{2+}, ultimately inducing neuronal pathology [187]. After TBI, there is an increase in intracranial pressure (ICP) [325, 326], which may lead to ischemia; this is usually followed by lactate accumulation, causing acidosis and a decrease in pH [327-329]. When Asic 1a is activated by acidosis the subsequent influx of Na^+ and Ca^{2+} in the cell causes cytotoxic edema [187], it contributes to neuronal apoptosis and necrosis after ischemic stroke [330] and has been implied in H_2O_2-induced cortical neuronal death in vitro [331]. Asic 1a plays an important role in the development of posttraumatic brain damage in the acute phase after TBI [214] and has been demonstrated to reduce neuronal death in hippocampus early after TBI [214], but its effect on the chronic posttraumatic phase has not been investigated.

In the present study, lesion volume of Asic 1a deficient mice was significantly smaller than in the WT group in the chronic phase after TBI; also, hippocampal damage was significantly reduced. These changes may help to explain the improvement in cognitive dysfunction (see below) as hippocampal damage was shown to be related to the extent of hippocampus lesions [323, 332].

Motor deficit is a common sequel in humans with severe TBI [285]. Severe motor dysfunction notably improved within six weeks, however, persisted for years post-trauma in human [333]. In experimental TBI models, motor abnormalities improve significantly

within three months but persisting deficits were detected one year after TBI [248, 334]. In the present study, the motor deficit assessed by beam walk testing peaked on the first day after trauma then quickly declined within two weeks and recovered gradually over time but did not reach baseline levels in all genotypes. Homozygous Asic 1a mice tended to perform slightly better but there was no significant difference among groups. McCarthy et al. demonstrated that pharmacological inhibition of Asic 1a improved motor function in a model of ischemic stroke [335], indicating Asic 1a may be involved in motor function. However, while the pathophysiology of stroke and TBI shares many similarities there are also marked differences. In ischemic stroke, brain injury includes infarct core lesion and penumbra, the location of injury is different from TBI, and the lesion develops significantly slower than after TBI [336].

Humans with TBI frequently present with psychiatric disorders, including depression [337-339], obsessive-compulsive disorder, and posttraumatic stress disorder [295]. Approximately a third of patients show depressive symptoms within the first year after TBI [257], in 17% of patients even three to five year after TBI [340]. In experimental studies, depression-like behavior was observed in the chronic phase after TBI [341-343]. Development of depression was shown to be related to neural disconnection among prefrontal cortex, amygdala, hippocampus, basal ganglia, and thalamus [344]. In present study, Asic 1a deficient animals had significantly less structural brain damage than wild type littermates which may explain the difference in depressive behavior post-trauma on the anatomical level. The improvement of posttraumatic depressive behavior observed in the present study is in line with previous results indicating that genetic disruption and pharmacological inhibition of Asic 1a alleviated depression-like behavior in stressed mice [345]. Cognitive disorders (including memory and learning deficits) are also often diagnosed in TBI patients [311, 346, 347], starting as early as three weeks after injury [312] and persisting chronically in 15% of patients [348]. Cognitive impairment can also be reliably detected from two days and up to one year in rodent TBI models [263, 349-351];

it was shown to correlate to structural and functional changes within the white matter (e.g., diffuse axonal injury) as well as to alterations in neurotransmitter activity [352, 353]. It was previously shown that depletion of Asic in normal mice may impair spatial memory and learning [186]. In the present study, however, we did not detect changes between Asic 1a and wild type mice during baseline assessment. Yin et al. demonstrated that loss of Asic 1a attenuated cognitive impairment associated neuron degeneration five days post-injury in a FPI model [214], there is, however, no data on time points beyond the acute phase. Homozygous Asic 1a mice performed significantly better in the Barnes Maze test indicating reduced long-term cognitive impairments after TBI. In the future, synaptic, axonal and neuronal degeneration should be assessed to further characterize the potential mechanism of Asic 1a induced cognitive decline after TBI.

In summary, Asic 1a deficiency significantly attenuated brain edema in the acute phase and posttraumatic brain damage (lesion volume and hippocampus damage) in the chronic phase post-TBI. This translated into improvement of neurological outcome (depression-like behavior, cognitive dysfunction), but did not affect motor deficits. Asic 1a therefore seems to plays a pivotal role in the development of posttraumatic brain damage and neurocognitive and behavioral deficits long-term, which makes Asic 1a a potential therapeutic target for the treatment of traumatic brain injury.

5. Summary

5.1 English summary

Traumatic brain injury is a major public health problem worldwide with high morbidity and mortality. So far, little is known about the long-term pathophysiology and the mechanisms of chronic posttraumatic brain damage. In addition, there are no specific therapies targeting posttraumatic brain damage. The present study aims to detect whether bradykinin 1 receptors (B1R) or acid sensing ion channels 1a (Asic 1a) are involved in the development of long-term deficits after experimental TBI. B1R and Asic 1a deficient mice and their wild type littermates were subjected to experimental TBI by controlled cortical impact (CCI) and observed one year and six months post-trauma, respectively. Brain edema formation, lesion volume and functional outcome were repeatedly assessed longitudinally over time in a strict randomized and blinded manner. Homozygous B1R deficiency did not affect posttraumatic brain damage (lesion volume and hippocampus damage) or neurological outcome (motor function, depressive behavior, and cognitive function) up to one year after TBI. Homozygous Asic 1a deficiency significantly reduced brain edema formation in the acute phase and ameliorated depressive behavior and cognitive dysfunction up to six months after TBI. Asic 1a transgenic animals were shown to have reduced posttraumatic brain damage up to six months post-trauma which translated into an improvement of posttraumatic neurocognitive and neurobehavioral deficits. Hence, Asic 1a deficiency resulted in neuroprotection after TBI and could be a potential target for the treatment of chronic posttraumatic brain damage.

5.2 Zusammenfassung

Das Schädel-Hirn-Trauma (SHT) ist weltweit einer der häufigsten Todesursachen im Kinder- und jungen Erwachsenenalter; zudem kann ein einmaliges SHT auch noch Jahre nach dem eigentlichen Unfall zu progredienten neurokognitiven Beeinträchtigungen führen und scheint ein Risikofaktor für die Entwicklung demenzieller Syndrome zu sein. Die Pathomechanismen dieser chronischen posttraumatischen Hirnschädigung sind

jedoch bisher weitgehend unbekannt, eine spezifische oder kausale Therapie für die im chronischen Verlauf zunehmende Schädigung existiert deswegen nicht. Sowohl das Kallikrein-Kinin-System mit seinem Haupt-Mediator Bradykinin als auch durch Azidose aktivierte Ionen-Kanäle (Acid-sensing ion channels, Asic) spielen in der Frühphase nach SHT eine wichtige Rolle bei der Entwicklung der Traumaläsion. Über ihre Bedeutung im längerfristigen Verlauf nach SHT ist für beide Entitäten bisher allerdings nichts bekannt. In der vorliegenden Arbeit wurde die Rolle des Bradykinin-1-Rezeptors (B1R) und des Acid-sensing-Ionen-Kanals 1a (Asic 1a) auf die Entwicklung des posttraumatischen Hirnschadens bis zu sechs Monate nach experimentellem Schädel-Hirn-Trauma in einem transgenen Maus-Modell untersucht. Hierfür wurde das in der Arbeitsgruppe seit langem etablierte Controlled Cortical Impact (CCI) - Modell verwendet; transgene Mauslinien für den Bradykinin-1-Rezeptor und Asic 1a wurden hiernach bis sechs Monate nach Trauma mittels multimodaler funktioneller und neurokognitiver Tests untersucht, die Entwicklung des strukturellen Hirnschadens wurde mittels longitudinaler Magnet-Resonanz-Tomographie (MRT) -Untersuchungen und histologisch gemessen. Alle Experimente wurden randomisiert und verblindet durchgeführt. Bradikinin-1-Rezeptor-Defizienz hatte keinen Einfluss auf den Allgemeinzustand oder das funktionelle Outcome nach SHT; heterozygote B1-R-defiziente Mäuse boten zwar eine Reduktion des mittels MRT und Histologie gemessenen strukturellen Hirnschadens, diese geringere Läsion führte jedoch zu keiner messbaren Verbesserung depressiver Symptome oder der posttraumatischen Gedächtnis- und Orientierungsstörung. Knockout von Asic 1a führte im Gegenteil hierzu zu einer signifikanten Reduktion des akuten posttraumatischen Hirnödems (24h nach CCI). Im weiteren Verlauf boten ASIC 1a transgene Tiere bessere Leistungen im Barnes-Maze-Test zur Beurteilung von Lernverhalten und Orientierung sowie weniger ausgeprägtes depressives Verhalten. In Bezug auf den posttraumatischen Hirnschaden war sowohl bei heterozygoten als auch bei homozygoten Tieren eine signifikant geringere Läsion im längerfristigen Verlauf nachweisbar. Hierbei war vor allem die Schädigung im Bereich des Hippocampus deutlich geringer ausgeprägt, einer anatomischen Struktur, die vor allem

für Gedächtnisprozesse wichtig ist. Während also der Bradykinin-1-Rezeptor für den längerfristigen Verlauf des posttraumatischen Hirnschadens keine relevante Rolle zu spielen scheint, scheint der Acid-sensing-Ionen-Kanal 1a einen wichtigen Einfluss auf die Entwicklung des chronischen Hirnschadens und funktioneller sowie neurokognitiver Defizite im längerfristigen Verlauf nach Schädel-Hirn-Trauma zu haben. Asic 1a könnte deswegen ein vielversprechender Ansatzpunkt möglicher neuroprotektiver Therapiestrategien sein und sollte deswegen weiter untersucht werden.

6. References

1. Hyder, A.A., et al., *The impact of traumatic brain injuries: a global perspective.* NeuroRehabilitation, 2007. 22(5): p. 341-53.

2. Engberg Aa, W. and T.W. Teasdale, *Traumatic brain injury in Denmark 1979-1996. A national study of incidence and mortality.* Eur J Epidemiol, 2001. 17(5): p. 437-42.

3. Kassi, A.A.Y., et al., *Enduring Neuroprotective Effect of Subacute Neural Stem Cell Transplantation After Penetrating TBI.* Front Neurol, 2018. 9: p. 1097.

4. Tagliaferri, F., et al., *A systematic review of brain injury epidemiology in Europe.* Acta Neurochir (Wien), 2006. 148(3): p. 255-68; discussion 268.

5. Dewan, M.C., et al., *Estimating the global incidence of traumatic brain injury.* J Neurosurg, 2018: p. 1-18.

6. Taylor, C.A., et al., *Traumatic Brain Injury-Related Emergency Department Visits, Hospitalizations, and Deaths - United States, 2007 and 2013.* MMWR Surveill Summ, 2017. 66(9): p. 1-16.

7. Peeters, W., et al., *Epidemiology of traumatic brain injury in Europe.* Acta Neurochir (Wien), 2015. 157(10): p. 1683-96.

8. Brazinova, A., et al., *Epidemiology of Traumatic Brain Injury in Europe: A Living Systematic Review.* J Neurotrauma, 2018.

9. Ilie, G., et al., *Prevalence and correlates of traumatic brain injuries among adolescents.* JAMA, 2013. 309(24): p. 2550-2.

10. Filer, W. and M. Harris, *Falls and traumatic brain injury among older adults.* N C Med J, 2015. 76(2): p. 111-4.

11. Gerber, L.M., et al., *Impact of falls on early mortality from severe traumatic brain injury.* J Trauma Manag Outcomes, 2009. 3: p. 9.

12. Centers for Disease, C. and Prevention, *Traumatic brain injury--Colorado, Missouri, Oklahoma, and Utah, 1990-1993.* MMWR Morb Mortal Wkly Rep, 1997. 46(1): p. 8-11.

13. Oseni, A., et al., *Outcome of traumatic brain injury at a neurocritical care unit: A review of 189 patients.* Southern African Journal of Critical Care, 2019. 35(1): p. 31-33.

14. Kerr, Z.Y., et al., *The epidemiology of traumatic brain injuries treated in emergency departments in North Carolina, 2010-2011.* N C Med J, 2014. 75(1): p. 8-14.

15. Kuo, K.W., L.M. Bacek, and A.R. Taylor, *Head Trauma.* Vet Clin North Am Small Anim Pract, 2018. 48(1): p. 111-128.

16. Caldicott, D.G. and N. Edwards, *Traumatic brain injury after a motor vehicle accident: fact or "fantasy"?* Emerg Med J, 2001. 18(6): p. 458-9.

17. Langlois, J.A., W. Rutland-Brown, and M.M. Wald, *The epidemiology and impact of traumatic brain injury: a brief overview.* The Journal of head trauma rehabilitation, 2006. 21(5): p. 375-378.

18. Wong, P.P., et al., *Statistical profile of traumatic brain injury: a Canadian rehabilitation population.* Brain Inj, 1993. 7(4): p. 283-94.

19. Ommaya, A.K., et al., *Causation, incidence, and costs of traumatic brain injury in the U.S. military medical system.* J Trauma, 1996. 40(2): p. 211-7.

20. Teasdale, G. and B. Jennett, *Assessment of coma and impaired consciousness. A practical scale.* Lancet, 1974. 2(7872): p. 81-4.

21. Yamamoto, S., D.S. DeWitt, and D.S. Prough, *Impact & Blast Traumatic Brain Injury: Implications for Therapy.* Molecules, 2018. 23(2).

22. Kashani, E., H.M. Ziarat, and A. Tajabadi, *Critique of the Glasgow Coma Scale (GCS).* 2019.

23. Fay, T.B., et al., *Predicting longitudinal patterns of functional deficits in children with traumatic brain injury.* Neuropsychology, 2009. 23(3): p. 271-82.

24. Wells, R., P. Minnes, and M. Phillips, *Predicting social and functional outcomes for individuals sustaining paediatric traumatic brain injury.* Dev Neurorehabil, 2009. 12(1): p. 12-23.

25. Saatman, K.E., et al., *Classification of traumatic brain injury for targeted therapies.* J Neurotrauma, 2008. 25(7): p. 719-38.

26. Marshall, L., et al., *The diagnosis of head injury requires a classification based on computed axial tomography.* Journal of neurotrauma, 1992. 9: p. S287-92.

27. Munakomi, S., *A comparative study between Marshall and Rotterdam CT scores in predicting early deaths in patients with traumatic brain injury in a major tertiary care hospital in Nepal.* Chinese Journal of Traumatology, 2016. 19(1): p. 25-27.

28. *Consensus conference. Rehabilitation of persons with traumatic brain injury. NIH Consensus Development Panel on Rehabilitation of Persons With Traumatic Brain Injury.* JAMA, 1999. 282(10): p. 974-83.

29. Gean, A.D. and N.J. Fischbein, *Head trauma.* Neuroimaging Clinics, 2010. 20(4): p. 527-556.

30. Johnson, V.E., et al., *Inflammation and white matter degeneration persist for years after a single traumatic brain injury.* Brain, 2013. 136(1): p. 28-42.

31. Farrell, D. and A.A. Bendo, *Perioperative Management of Severe Traumatic Brain Injury: What Is New?* Curr Anesthesiol Rep, 2018. 8(3): p. 279-289.

32. Maas, A.I., N. Stocchetti, and R. Bullock, *Moderate and severe traumatic brain injury in adults.* The Lancet Neurology, 2008. 7(8): p. 728-741.

33. Ragaisis, V., *[Brain contusion: morphology, pathogenesis and treatment].* Medicina (Kaunas), 2002. 38(3): p. 243-9; quiz 354.

34. Pudenz, R.H. and C.H. Shelden, *The lucite calvarium; a method for direct observation of the brain; cranial trauma and brain movement.* J Neurosurg, 1946. 3(6): p. 487-505.

35. Hilmer, L.V., et al., *Cerebral Contusion: An Investigation of Etiology, Risk Factors, Related Diagnoses, and the Surgical Management at a Major Government Hospital in Cambodia.* Asian J Neurosurg, 2018. 13(1): p. 23-30.

36. Iaccarino, C., et al., *Patients with brain contusions: predictors of outcome and relationship between radiological and clinical evolution.* J Neurosurg, 2014. 120(4): p. 908-18.

37. Chen, K.T., T.K. Lin, and T.C. Hsieh, *Isolated Internuclear Ophthalmoplegia After Massive Supratentorial Epidural Hematoma: A Case Report and Review of the Literature.* World Neurosurg, 2017. 100: p. 712 e5-712 e13.

38. Nasi, D., et al., *Surgical management of traumatic supra and infratentorial extradural hematomas: our experience and systematic literature review.* Neurosurg Rev, 2019.

39. Fernandes-Cabral, D.T., et al., *Surgical Management of Vertex Epidural Hematoma: Technical Case Report and Literature Review.* World Neurosurg, 2017. 103: p. 475-483.

40. Hamm, J., et al., *Cranial epidural hematomas: A case series and literature review of this rare complication associated with sickle cell disease.* Pediatr Blood Cancer, 2017. 64(3).

41. Pearl, G.S., *Traumatic neuropathology.* Clinics in laboratory medicine, 1998. 18(1): p. 39-64.

42. Vezina, G., *Assessment of the nature and age of subdural collections in nonaccidental head injury with CT and MRI.* Pediatric radiology, 2009. 39(6): p. 586-590.

43. Scotti, G., et al., *Evaluation of the age of subdural hematomas by computerized tomography.* J Neurosurg, 1977. 47(3): p. 311-315.

44. Alvis-Miranda, H., S.M. Castellar-Leones, and L.R. Moscote-Salazar, *Decompressive craniectomy and traumatic brain injury: a review.* Bulletin of Emergency & Trauma, 2013. 1(2): p. 60.

45. Sehba, F.A. and J.B. Bederson, *Mechanisms of acute brain injury after subarachnoid hemorrhage.* Neurol Res, 2006. 28(4): p. 381-398.

46. Modi, N.J., M. Agrawal, and V.D. Sinha, *Post-traumatic subarachnoid hemorrhage: A review.* Neurol India, 2016. 64(7): p. 8.

47. Gan, Y.-C. and M.S. Choksey, *Rebleed in traumatic subarachnoid haemorrhage.* Injury Extra, 2006. 37(12): p. 484-486.

48. Mesfin, F.B. and S.C. Dulebohn, *Diffuse Axonal Injury (DAI)*, in *StatPearls [Internet]*. 2018, StatPearls Publishing.

49. Gennarelli, T.A., *Mechanisms of brain injury.* J Emerg Med, 1993. 11: p. 5-11.

50. Adams, J.H., et al., *Diffuse axonal injury in head injury: definition, diagnosis and grading.* Histopathology, 1989. 15(1): p. 49-59.

51. Tang-Schomer, M.D., et al., *Mechanical breaking of microtubules in axons during dynamic stretch injury underlies delayed elasticity, microtubule disassembly, and axon degeneration.* The FASEB Journal, 2010. 24(5): p. 1401-1410.

52. Izzy, S., et al., *Revisiting grade 3 diffuse axonal injury: not all brainstem microbleeds are prognostically equal.* Neurocrit Care, 2017. 27(2): p. 199-207.

53. Levin, H.S. and R.R. Diaz-Arrastia, *Diagnosis, prognosis, and clinical management of mild traumatic brain injury.* The Lancet Neurology, 2015. 14(5): p. 506-517.

54. Moen, K.G., et al., *A longitudinal MRI study of traumatic axonal injury in patients with moderate and severe traumatic brain injury.* J Neurol Neurosurg Psychiatry, 2012. 83(12): p. 1193-1200.

55. Sullivan, P.G., et al., *Dose-response curve and optimal dosing regimen of cyclosporin A after traumatic brain injury in rats.* Neuroscience, 2000. 101(2): p. 289-95.

56. Ramlackhansingh, A.F., et al., *Inflammation after trauma: microglial activation and traumatic brain injury.* Ann Neurol, 2011. 70(3): p. 374-83.

57. Werner, C. and K. Engelhard, *Pathophysiology of traumatic brain injury.* BJA: British Journal of Anaesthesia, 2007. 99(1): p. 4-9.

58. Hayyan, M., M.A. Hashim, and I.M. AlNashef, *Superoxide Ion: Generation and Chemical Implications.* Chem Rev, 2016. 116(5): p. 3029-85.

59. Ladak, A.A., S.A. Enam, and M.T. Ibrahim, *A review of the molecular mechanisms of Traumatic Brain Injury.* World Neurosurg, 2019.

60. Cornelius, C., et al., *Traumatic brain injury: oxidative stress and neuroprotection.* Antioxid Redox Signal, 2013. 19(8): p. 836-53.

61. Ikonomidou, C. and L. Turski, *Why did NMDA receptor antagonists fail clinical trials for stroke and traumatic brain injury?* Lancet Neurol, 2002. 1(6): p. 383-6.

62. Ascenzi, P., et al., *Hemoglobin and heme scavenging.* IUBMB Life, 2005. 57(11): p. 749-59.

63. Ishii, T., *[Basic principles clinical biochemistry].* Rinsho Byori, 1967. 15(4): p. 265-8.

64. Pun, P.B., J. Lu, and S. Moochhala, *Involvement of ROS in BBB dysfunction.* Free Radic Res, 2009. 43(4): p. 348-64.

65. Hanafy, K.A. and M.H. Selim, *Antioxidant strategies in neurocritical care.* Neurotherapeutics, 2012. 9(1): p. 44-55.

66. Sullivan, P.G., et al., *Mitochondrial permeability transition in CNS trauma: cause or effect of neuronal cell death?* J Neurosci Res, 2005. 79(1-2): p. 231-9.

67. Lozano, D., et al., *Neuroinflammatory responses to traumatic brain injury: etiology, clinical consequences, and therapeutic opportunities.* Neuropsychiatr Dis Treat, 2015. 11: p. 97.

68. Wang, K., D. Cui, and L. Gao, *Traumatic brain injury: a review of characteristics, molecular basis and management.* Front Biosci (Landmark Ed), 2016. 21: p. 890-9.

69. Choi, D.W., *Ionic dependence of glutamate neurotoxicity.* J Neurosci, 1987. 7(2): p. 369-79.

70. Mbye, L.H., et al., *Attenuation of acute mitochondrial dysfunction after traumatic brain injury in mice by NIM811, a non-immunosuppressive cyclosporin A analog.* Exp Neurol, 2008. 209(1): p. 243-53.

71. Kolaczkowska, E. and P. Kubes, *Neutrophil recruitment and function in health and inflammation.* Nat Rev Immunol, 2013. 13(3): p. 159-75.

72. Carlos, T.M., et al., *Expression of endothelial adhesion molecules and recruitment of neutrophils after traumatic brain injury in rats.* J Leukoc Biol, 1997. 61(3): p. 279-85.

73. Walko III, T.D., et al., *Cerebrospinal fluid mitochondrial DNA–a novel DAMP in pediatric traumatic brain injury.* Shock (Augusta, Ga.), 2014. 41(6): p. 499.

74. Schwarzmaier, S.M., et al., *In vivo temporal and spatial profile of leukocyte adhesion and migration after experimental traumatic brain injury in mice.* Journal of neuroinflammation, 2013. 10(1): p. 808.

75. Plesnila, N., *The immune system in traumatic brain injury.* Current opinion in pharmacology, 2016. 26: p. 110-117.

76. Corps, K.N., T.L. Roth, and D.B. McGavern, *Inflammation and neuroprotection in traumatic brain injury.* JAMA Neurol, 2015. 72(3): p. 355-62.

77. Szmydynger-Chodobska, J., et al., *Posttraumatic invasion of monocytes across the blood-cerebrospinal fluid barrier.* J Cereb Blood Flow Metab, 2012. 32(1): p. 93-104.

78. Soares, H.D., et al., *Inflammatory leukocytic recruitment and diffuse neuronal degeneration are separate pathological processes resulting from traumatic brain injury.* Journal of Neuroscience, 1995. 15(12): p. 8223-8233.

79. Whalen, M.J., et al., *Neutrophils do not mediate blood-brain barrier permeability early after controlled cortical impact in rats.* J Neurotrauma, 1999. 16(7): p. 583-94.

80. Kenne, E., et al., *Neutrophil depletion reduces edema formation and tissue loss following traumatic brain injury in mice.* Journal of neuroinflammation, 2012. 9(1): p. 17.

81. Weaver, L.C., et al., *CD11d integrin blockade reduces the systemic inflammatory response syndrome after traumatic brain injury in rats.* Experimental neurology, 2015. 271: p. 409-422.

82. Semple, B.D., et al., *Neutrophil elastase mediates acute pathogenesis and is a determinant of long-term behavioral recovery after traumatic injury to the immature brain.* Neurobiol Dis, 2015. 74: p. 263-80.

83. Jassam, Y.N., et al., *Neuroimmunology of traumatic brain injury: time for a paradigm shift.* Neuron, 2017. 95(6): p. 1246-1265.

84. Hailer, N.P., A. Grampp, and R. Nitsch, *Proliferation of microglia and astrocytes in the dentate gyrus following entorhinal cortex lesion: a quantitative bromodeoxyuridine-labelling study.* Eur J Neurosci, 1999. 11(9): p. 3359-64.

85. Bachstetter, A.D., et al., *Microglial p38α MAPK is a key regulator of proinflammatory cytokine up-regulation induced by toll-like receptor (TLR) ligands or beta-amyloid (Aβ).* Journal of neuroinflammation, 2011. 8(1): p. 79.

86. Fenn, A.M., et al., *Methylene blue attenuates traumatic brain injury-associated neuroinflammation and acute depressive-like behavior in mice.* Journal of neurotrauma, 2015. 32(2): p. 127-138.

87. Shlosberg, D., et al., *Blood-brain barrier breakdown as a therapeutic target in traumatic brain injury.* Nat Rev Neurol, 2010. 6(7): p. 393-403.

88. Thal, S.C. and W. Neuhaus, *The blood-brain barrier as a target in traumatic brain injury treatment.* Arch Med Res, 2014. 45(8): p. 698-710.

89. Abdul-Muneer, P.M., N. Chandra, and J. Haorah, *Interactions of oxidative stress and neurovascular inflammation in the pathogenesis of traumatic brain injury.* Mol Neurobiol, 2015. 51(3): p. 966-79.

90. Lou, N., et al., *Purinergic receptor P2RY12-dependent microglial closure of the injured blood-brain barrier.* Proc Natl Acad Sci U S A, 2016. 113(4): p. 1074-9.

91. Roth, T.L., et al., *Transcranial amelioration of inflammation and cell death after brain injury.* Nature, 2014. 505(7482): p. 223-8.

92. Nagamoto-Combs, K., et al., *Prolonged microgliosis in the rhesus monkey central nervous system after traumatic brain injury.* J Neurotrauma, 2007. 24(11): p. 1719-42.

93. Rice, R.A., et al., *Elimination of microglia improves functional outcomes following extensive neuronal loss in the hippocampus.* Journal of Neuroscience, 2015. 35(27): p. 9977-9989.

94. Cherry, J.D., J.A. Olschowka, and M.K. O'Banion, *Neuroinflammation and M2 microglia: the good, the bad, and the inflamed.* Journal of neuroinflammation, 2014. 11(1): p. 98.

95. Wang, G., et al., *Microglia/macrophage polarization dynamics in white matter after traumatic brain injury.* J Cereb Blood Flow Metab, 2013. 33(12): p. 1864-74.

96. Donat, C.K., et al., *Microglial activation in traumatic brain injury.* Frontiers in aging neuroscience, 2017. 9: p. 208.

97. Nagamoto-Combs, K., et al., *Long-term gliosis and molecular changes in the cervical spinal cord of the rhesus monkey after traumatic brain injury.* Journal of neurotrauma, 2010. 27(3): p. 565-585.

98. Donkin, J.J. and R. Vink, *Mechanisms of cerebral edema in traumatic brain injury: therapeutic developments.* Curr Opin Neurol, 2010. 23(3): p. 293-9.

99. Klatzo, I., *Presidental address. Neuropathological aspects of brain edema.* J Neuropathol Exp Neurol, 1967. 26(1): p. 1-14.

100. Hudak, A.M., et al., *Cytotoxic and vasogenic cerebral oedema in traumatic brain injury: assessment with FLAIR and DWI imaging.* Brain Inj, 2014. 28(12): p. 1602-9.

101. Unterberg, A.W., et al., *Edema and brain trauma.* Neuroscience, 2004. 129(4): p. 1021-9.

102. Chen, M. and J.M. Simard, *Cell swelling and a nonselective cation channel regulated by internal Ca2+ and ATP in native reactive astrocytes from adult rat brain.* Journal of Neuroscience, 2001. 21(17): p. 6512-6521.

103. Jayakumar, A.R., et al., *Na－K－Cl cotransporter－1 in the mechanism of cell swelling in cultured astrocytes after fluid percussion injury.* Journal of neurochemistry, 2011. 117(3): p. 437-448.

104. Simard, J.M., et al., *Sulfonylurea receptor 1 in central nervous system injury: a focused review.* Journal of Cerebral Blood Flow & Metabolism, 2012. 32(9): p. 1699-1717.

105. Stokum, J.A., V. Gerzanich, and J.M. Simard, *Molecular pathophysiology of cerebral edema.* J Cereb Blood Flow Metab, 2016. 36(3): p. 513-38.

106. Shohami, E. and A. Biegon, *Novel approach to the role of NMDA receptors in traumatic brain injury.* CNS & Neurological Disorders-Drug Targets (Formerly Current Drug Targets-CNS & Neurological Disorders), 2014. 13(4): p. 567-573.

107. Jha, R.M., P.M. Kochanek, and J.M. Simard, *Pathophysiology and treatment of cerebral edema in traumatic brain injury.* Neuropharmacology, 2019. 145(Pt B): p. 230-246.

108. Schilling, L. and M. Wahl, *Brain edema: pathogenesis and therapy.* Kidney International Supplement, 1997(59).

109. Ballabh, P., A. Braun, and M. Nedergaard, *The blood–brain barrier: an overview: structure, regulation, and clinical implications.* Neurobiology of disease, 2004. 16(1): p. 1-13.

110. Chodobski, A., B.J. Zink, and J. Szmydynger-Chodobska, *Blood-brain barrier pathophysiology in traumatic brain injury.* Transl Stroke Res, 2011. 2(4): p. 492-516.

111. Simon, D.W., et al., *The far-reaching scope of neuroinflammation after traumatic brain injury.* Nat Rev Neurol, 2017. 13(9): p. 572.

112. Woodcock, T.M., et al., *The scavenging chemokine receptor ACKR2 has a significant impact on acute mortality rate and early lesion development after traumatic brain injury.* PLoS One, 2017. 12(11): p. e0188305.

113. Corrigan, F., et al., *Neurogenic inflammation after traumatic brain injury and its potentiation of classical inflammation.* Journal of neuroinflammation, 2016. 13(1): p. 264.

114. Murakami, T., E.A. Felinski, and D.A. Antonetti, *Occludin phosphorylation and ubiquitination regulate tight junction trafficking and vascular endothelial growth factor-induced permeability.* J Biol Chem, 2009. 284(31): p. 21036-46.

115. Zhang, S., et al., *Distinct roles for metalloproteinases during traumatic brain injury.* Neurochem Int, 2016. 96: p. 46-55.

116. Rangel-Castillo, L. and C.S. Robertson, *Management of intracranial hypertension.* Crit Care Clin, 2006. 22(4): p. 713-32; abstract ix.

117. Neff, S. and R.P. Subramaniam, *Monro-Kellie doctrine.* J Neurosurg, 1996. 85(6): p. 1195.

118. Rosner, M.J. and I.B. Coley, *Cerebral perfusion pressure, intracranial pressure, and head elevation.* J Neurosurg, 1986. 65(5): p. 636-41.

119. Round, R. and J.R. Keane, *The minor symptoms of increased intracranial pressure: 101 patients with benign intracranial hypertension.* Neurology, 1988. 38(9): p. 1461-4.

120. Rehman, T., et al., *Rapid progression of traumatic bifrontal contusions to transtentorial herniation: A case report.* Cases J, 2008. 1(1): p. 203.

121. Trivedi, M.A., et al., *Longitudinal changes in global brain volume between 79 and 409 days after traumatic brain injury: relationship with duration of coma.* J Neurotrauma, 2007. 24(5): p. 766-71.

122. Bendlin, B.B., et al., *Longitudinal changes in patients with traumatic brain injury assessed with diffusion-tensor and volumetric imaging.* Neuroimage, 2008. 42(2): p. 503-14.

123. Sidaros, A., et al., *Diffusion tensor imaging during recovery from severe traumatic brain injury and relation to clinical outcome: a longitudinal study.* Brain, 2008. 131(Pt 2): p. 559-72.

124. Kumar, A. and D.J. Loane, *Neuroinflammation after traumatic brain injury: opportunities for therapeutic intervention.* Brain Behav Immun, 2012. 26(8): p. 1191-201.

125. Smith, C., et al., *The neuroinflammatory response in humans after traumatic brain injury.* Neuropathol Appl Neurobiol, 2013. 39(6): p. 654-66.

126. Aungst, S.L., et al., *Repeated mild traumatic brain injury causes chronic neuroinflammation, changes in hippocampal synaptic plasticity, and associated cognitive deficits.* J Cereb Blood Flow Metab, 2014. 34(7): p. 1223-32.

127. Mouzon, B.C., et al., *Chronic neuropathological and neurobehavioral changes in a repetitive mild traumatic brain injury model.* Ann Neurol, 2014. 75(2): p. 241-54.

128. Levin, H.S., et al., *Ventricular enlargement after closed head injury.* Archives of Neurology, 1981. 38(10): p. 623-629.

129. Ariza, M., et al., *Hippocampal head atrophy after traumatic brain injury.* Neuropsychologia, 2006. 44(10): p. 1956-1961.

130. Gale, S., et al., *Trauma–induced degenerative changes in brain injury: a morphometric analysis of three patients with preinjury and postinjury MR scans.* The Journal of Head Trauma Rehabilitation, 1996. 11(6): p. 100.

131. Papadopoulos, V. and L. Lecanu, *Translocator protein (18 kDa) TSPO: an emerging therapeutic target in neurotrauma.* Exp Neurol, 2009. 219(1): p. 53-7.

132. Erturk, A., et al., *Interfering with the Chronic Immune Response Rescues Chronic Degeneration After Traumatic Brain Injury.* J Neurosci, 2016. 36(38): p. 9962-75.

133. Rodgers, K.M., et al., *Reversal of established traumatic brain injury-induced, anxiety-like behavior in rats after delayed, post-injury neuroimmune suppression.* J Neurotrauma, 2014. 31(5): p. 487-97.

134. Byrnes, K.R., et al., *Delayed mGluR5 activation limits neuroinflammation and neurodegeneration after traumatic brain injury.* Journal of neuroinflammation, 2012. 9(1): p. 43.

135. Mannix, R., et al., *Clinical correlates in an experimental model of repetitive mild brain injury.* Ann Neurol, 2013. 74(1): p. 65-75.

136. Walker, K.R. and G. Tesco, *Molecular mechanisms of cognitive dysfunction following traumatic brain injury.* Frontiers in aging neuroscience, 2013. 5: p. 29.

137. Iqbal, K., C.-X. Gong, and F. Liu, *Hyperphosphorylation-induced tau oligomers.* Frontiers in neurology, 2013. 4: p. 112.

138. Cowan, C.M. and A. Mudher, *Are tau aggregates toxic or protective in tauopathies?* Frontiers in neurology, 2013. 4: p. 114.

139. Martland, H.S., *Punch drunk.* Journal of the American Medical Association, 1928. 91(15): p. 1103-1107.

140. Omalu, B.I., et al., *Chronic traumatic encephalopathy in a National Football League player.* Neurosurgery, 2005. 57(1): p. 128-134.

141. Omalu, B.I., et al., *Chronic traumatic encephalopathy in a professional American wrestler.* Journal of forensic nursing, 2010. 6(3): p. 130-136.

142. McKee, A.C., et al., *The first NINDS/NIBIB consensus meeting to define neuropathological criteria for the diagnosis of chronic traumatic encephalopathy.* Acta neuropathologica, 2016. 131(1): p. 75-86.

143. Cherry, J.D., et al., *Microglial neuroinflammation contributes to tau accumulation in chronic traumatic encephalopathy.* Acta neuropathologica communications, 2016. 4(1): p. 112.

144. Sacramento, C.B., et al., *Anti-phospho-tau Gene Therapy for Chronic Traumatic Encephalopathy.* Human gene therapy, 2019(ja).

145. Abelous, J., *Les substances hypotensives de l'urine humaine normale.* CR Soc Biol., 1909. 66: p. 511-512.

146. Hillmeister, P. and P.B. Persson, *The Kallikrein-Kinin system.* Acta Physiol (Oxf), 2012. 206(4): p. 215-9.

147. Trautschold, I., *Assay methods in the kinin system*, in *Bradykinin, Kallidin and Kallikrein*. 1970, Springer. p. 52-81.

148. e Silva, M.R., W.T. Beraldo, and G. Rosenfeld, *Bradykinin, a hypotensive and smooth muscle stimulating factor released from plasma globulin by snake venoms and by trypsin.* American Journal of Physiology-Legacy Content, 1949. 156(2): p. 261-273.

149. Regoli, D. and J. Barabe, *Pharmacology of bradykinin and related kinins.* Pharmacological reviews, 1980. 32(1): p. 1-46.

150. Schachter, M., *Kinins--a group of active peptides.* Annual Review of Pharmacology, 1964. 4(1): p. 281-292.

151. Fink, E., et al., *Cellular expression of plasma prekallikrein in human tissues.* Biological chemistry, 2007. 388(9): p. 957-963.

152. Marcondes, S. and E. Antunes, *The plasma and tissue kininogen-kallikrein-kinin system: role in the cardiovascular system.* Current Medicinal Chemistry-Cardiovascular & Hematological Agents, 2005. 3(1): p. 33-44.

153. Kashuba, E., et al., *The kinin–kallikrein system: physiological roles, pathophysiology and its relationship to cancer biomarkers.* Biomarkers, 2013. 18(4): p. 279-296.

154. Chung, D.W., et al., *Human plasma prekallikrein, a zymogen to a serine protease that contains four tandem repeats.* Biochemistry, 1986. 25(9): p. 2410-2417.

155. Borgono, C.A., I.P. Michael, and E.P. Diamandis, *Human tissue kallikreins: physiologic roles and applications in cancer.* Molecular cancer research, 2004. 2(5): p. 257-280.

156. MacDonald, R.J., H.S. Margolius, and E.G. Erdos, *Molecular biology of tissue kallikrein.* Biochem J, 1988. 253(2): p. 313-21.

157. Erdös, E. *Enzyme inhibitors of the kallikrein and renin systems: introduction*. in *Federation proceedings*. 1979.

158. Colman, R.W., *Activation of plasminogen by human plasma kallikrein.* Biochemical and biophysical research communications, 1969. 35(2): p. 273-279.

159. Okamoto, H., et al., *Fibroblasts synthesize kininogen in response to inflammatory mediators.* Immunopharmacology, 1996. 32(1-3): p. 28-33.

160. Mann, E.A. and J.B. Lingrel, *Developmental and tissue-specific expression of rat T-kininogen.* Biochemical and biophysical research communications, 1991. 174(2): p. 417-423.

161. Chao, J., et al., *Regulation of kininogen gene expression and localization in the lung after monocrotaline-induced pulmonary hypertension in rats.* Proceedings of the Society for Experimental Biology and Medicine, 1993. 203(2): p. 243-250.

162. Iwai, N., et al., *Detection of low molecular kininogen messenger RNA in human kidney.* Journal of hypertension. Supplement: official journal of the International Society of Hypertension, 1988. 6(4): p. S399-400.

163. Sainz, I.M., R.A. Pixley, and R.W. Colman, *Fifty years of research on the plasma kallikrein-kinin system: from protein structure and function to cell biology and in-vivo pathophysiology.* Thrombosis and haemostasis, 2007. 98(07): p. 77-83.

164. Moreau, M.E., et al., *The kallikrein-kinin system: current and future pharmacological targets.* Journal of pharmacological sciences, 2005. 99(1): p. 6-38.

165. Marceau, F. and D. Regoli, *Bradykinin receptor ligands: therapeutic perspectives.* Nature reviews Drug discovery, 2004. 3(10): p. 845.

166. Kuoppala, A., et al., *Inactivation of bradykinin by angiotensin-converting enzyme and by carboxypeptidase N in human plasma.* American Journal of Physiology-Heart and Circulatory Physiology, 2000. 278(4): p. H1069-H1074.

167. Golias, C., et al., *The kinin system-bradykinin: biological effects and clinical implications. Multiple role of the kinin system-bradykinin.* Hippokratia, 2007. 11(3): p. 124.

168. Albert-Weissenberger, C., A.-L. Sirén, and C. Kleinschnitz, *Ischemic stroke and traumatic brain injury: the role of the kallikrein–kinin system.* Progress in neurobiology, 2013. 101: p. 65-82.

169. Albert-Weissenberger, C., et al., *Role of the kallikrein–kinin system in traumatic brain injury.* Frontiers in cellular neuroscience, 2014. 8: p. 345.

170. Prado, G.N., et al., *Mechanisms regulating the expression, self-maintenance, and signaling-function of the bradykinin B2 and B1 receptors.* J Cell Physiol, 2002. 193(3): p. 275-86.

171. Marceau, F., et al., *Bifunctional ligands of the bradykinin B2 and B1 receptors: An exercise in peptide hormone plasticity.* Peptides, 2018. 105: p. 37-50.

172. Marceau, F., J.F. Hess, and D.R. Bachvarov, *The B1 receptors for kinins.* Pharmacol Rev, 1998. 50(3): p. 357-86.

173. Leeb-Lundberg, L.F., et al., *International union of pharmacology. XLV. Classification of the kinin receptor family: from molecular mechanisms to pathophysiological consequences.* Pharmacological reviews, 2005. 57(1): p. 27-77.

174. Auer, L., et al., *Proteolytic enzyme activity in patients with severe head injury and the effect of a proteinase inhibitor.* Acta neurochirurgica, 1979. 49(3-4): p. 207-217.

175. Unterberg, A., et al., *The kallikrein-kinin system as mediator in vasogenic brain edema: Part 3: Inhibition of the kallikrein-kinin system in traumatic brain swelling.* Journal of neurosurgery, 1986. 64(2): p. 269-276.

176. Trabold, R., et al., *The role of bradykinin B1 and B2 receptors for secondary brain damage after traumatic brain injury in mice.* Journal of Cerebral Blood Flow & Metabolism, 2010. 30(1): p. 130-139.

177. Hellal, F., et al., *Detrimental role of bradykinin B2 receptor in a murine model of diffuse brain injury.* Journal of neurotrauma, 2003. 20(9): p. 841-851.

178. Albert-Weissenberger, C., et al., *Blocking of bradykinin receptor B1 protects from focal closed head injury in mice by reducing axonal damage and astroglia activation.* J Cereb Blood Flow Metab, 2012. 32(9): p. 1747-56.

179. Raslan, F., et al., *Inhibition of bradykinin receptor B1 protects mice from focal brain injury by reducing blood-brain barrier leakage and inflammation.* J Cereb Blood Flow Metab, 2010. 30(8): p. 1477-86.

180. Dong-Creste, K.E., et al., *Kinin B1 receptor mediates memory impairment in the rat hippocampus.* Biol Chem, 2016. 397(4): p. 353-64.

181. Krishtal, O., *The ASICs: signaling molecules? modulators?* Trends in neurosciences, 2003. 26(9): p. 477-483.

182. Waldmann, R., et al., *A proton-gated cation channel involved in acid-sensing.* Nature, 1997. 386(6621): p. 173.

183. Hanukoglu, I., *ASIC and ENaC type sodium channels: conformational states and the structures of the ion selectivity filters.* The FEBS journal, 2017. 284(4): p. 525-545.

184. Duan, B., et al., *Extracellular spermine exacerbates ischemic neuronal injury through sensitization of ASIC1a channels to extracellular acidosis.* Journal of Neuroscience, 2011. 31(6): p. 2101-2112.

185. Lingueglia, E., et al., *A modulatory subunit of acid sensing ion channels in brain and dorsal root ganglion cells.* Journal of Biological Chemistry, 1997. 272(47): p. 29778-29783.

186. Wemmie, J.A., et al., *The acid-activated ion channel ASIC contributes to synaptic plasticity, learning, and memory.* Neuron, 2002. 34(3): p. 463-477.

187. Gründer, S. and M. Pusch, *Biophysical properties of acid-sensing ion channels (ASICs).* Neuropharmacology, 2015. 94: p. 9-18.

188. Chen, C.-C., et al., *A sensory neuron-specific, proton-gated ion channel.* Proceedings of the National Academy of Sciences, 1998. 95(17): p. 10240-10245.

189. Lai, C., et al., *Sequence and transmembrane topology of MEC-4, an ion channel subunit required for mechanotransduction in Caenorhabditis elegans.* The Journal of cell biology, 1996. 133(5): p. 1071-1081.

190. Jasti, J., et al., *Structure of acid-sensing ion channel 1 at 1.9 Å resolution and low pH.* Nature, 2007. 449(7160): p. 316.

191. Noël, J., et al., *Current perspectives on acid-sensing ion channels: new advances and therapeutic implications.* Expert review of clinical pharmacology, 2010. 3(3): p. 331-346.

192. Benson, C.J., et al., *Heteromultimers of DEG/ENaC subunits form H+-gated channels in mouse sensory neurons.* Proceedings of the National Academy of Sciences, 2002. 99(4): p. 2338-2343.

193. Chu, X.-P., K.A. Grasing, and J.Q. Wang, *Acid-sensing ion channels contribute to neurotoxicity.* Translational stroke research, 2014. 5(1): p. 69-78.

194. Chen, X., H. Kalbacher, and S. Gründer, *Interaction of acid-sensing ion channel (ASIC) 1 with the tarantula toxin psalmotoxin 1 is state dependent.* The Journal of general physiology, 2006. 127(3): p. 267-276.

195. Hoagland, E.N., et al., *Identification of a calcium permeable human acid-sensing ion channel 1 transcript variant.* Journal of Biological Chemistry, 2010. 285(53): p. 41852-41862.

196. Askwith, C.C., et al., *Acid-sensing ion channel 2 (ASIC2) modulates ASIC1 H+-activated currents in hippocampal neurons.* Journal of Biological Chemistry, 2004. 279(18): p. 18296-18305.

197. Babinski, K., et al., *Mammalian ASIC2a and ASIC3 subunits co-assemble into heteromeric proton-gated channels sensitive to Gd3+.* Journal of Biological Chemistry, 2000. 275(37): p. 28519-28525.

198. Zha, X.-m., *Acid-sensing ion channels: trafficking and synaptic function.* Molecular brain, 2013. 6(1): p. 1.

199. Wemmie, J.A., et al., *Acid-sensing ion channel 1 is localized in brain regions with high synaptic density and contributes to fear conditioning.* Journal of Neuroscience, 2003. 23(13): p. 5496-5502.

200. Du, J., et al., *Protons are a neurotransmitter that regulates synaptic plasticity in the lateral amygdala.* Proceedings of the National Academy of Sciences, 2014. 111(24): p. 8961-8966.

201. Price, M.P., et al., *The mammalian sodium channel BNC1 is required for normal touch sensation.* Nature, 2000. 407(6807): p. 1007.

202. Page, A.J., et al., *Different contributions of ASIC channels 1a, 2, and 3 in gastrointestinal mechanosensory function.* Gut, 2005. 54(10): p. 1408-1415.

203. Lu, Y., et al., *The ion channel ASIC2 is required for baroreceptor and autonomic control of the circulation.* Neuron, 2009. 64(6): p. 885-897.

204. Gannon, K.P., et al., *Impaired pressure-induced constriction in mouse middle cerebral arteries of ASIC2 knockout mice.* American Journal of Physiology-Heart and Circulatory Physiology, 2008. 294(4): p. H1793-H1803.

205. Omerbašić, D., et al., *ASICs and mammalian mechanoreceptor function.* Neuropharmacology, 2015. 94: p. 80-86.

206. Xiong, Z.G., et al., *Neuroprotection in ischemia: blocking calcium-permeable acid-sensing ion channels.* Cell, 2004. 118(6): p. 687-98.

207. Pignataro, G., R.P. Simon, and Z.-G. Xiong, *Prolonged activation of ASIC1a and the time window for neuroprotection in cerebral ischaemia.* Brain, 2006. 130(1): p. 151-158.

208. Pignataro, G., et al., *ASIC1a contributes to neuroprotection elicited by ischemic preconditioning and postconditioning.* International journal of physiology, pathophysiology and pharmacology, 2011. 3(1): p. 1.

209. Friese, M.A., et al., *Acid-sensing ion channel-1 contributes to axonal degeneration in autoimmune inflammation of the central nervous system.* Nat Med, 2007. 13(12): p. 1483-9.

210. Arias, R.L., et al., *Amiloride is neuroprotective in an MPTP model of Parkinson's disease.* Neurobiology of disease, 2008. 31(3): p. 334-341.

211. Wong, H.K., et al., *Blocking acid-sensing ion channel 1 alleviates Huntington's disease pathology via an ubiquitin-proteasome system-dependent mechanism.* Human molecular genetics, 2008. 17(20): p. 3223-3235.

212. Chu, X.-P., et al., *Modulation of acid-sensing ion channels: molecular mechanisms and therapeutic potential.* International journal of physiology, pathophysiology and pharmacology, 2011. 3(4): p. 288.

213. Veenith, T.V., et al., *Pathophysiologic Mechanisms of Cerebral Ischemia and Diffusion Hypoxia in Traumatic Brain Injury.* JAMA Neurol, 2016. 73(5): p. 542-50.

214. Yin, T., et al., *Loss of Acid sensing ion channel-1a and bicarbonate administration attenuate the severity of traumatic brain injury.* PLoS One, 2013. 8(8): p. e72379.

215. Li, M.H., et al., *Modulation of Acid-sensing Ion Channel 1a by Intracellular pH and Its Role in Ischemic Stroke.* J Biol Chem, 2016. 291(35): p. 18370-83.

216. Pesquero, J.B., et al., *Hypoalgesia and altered inflammatory responses in mice lacking kinin B1 receptors.* Proceedings of the National Academy of Sciences, 2000. 97(14): p. 8140-8145.

217. Lighthall, J.W., *Controlled cortical impact: a new experimental brain injury model.* J Neurotrauma, 1988. 5(1): p. 1-15.

218. Krieg, S.M., R. Trabold, and N. Plesnila, *Time-Dependent Effects of Arginine-Vasopressin V1 Receptor Inhibition on Secondary Brain Damage after Traumatic Brain Injury.* J Neurotrauma, 2017. 34(7): p. 1329-1336.

219. Zweckberger, K., et al., *Effect of decompression craniotomy on increase of contusion volume and functional outcome after controlled cortical impact in mice.* Journal of neurotrauma, 2003. 20(12): p. 1307-1314.

220. Steru, L., et al., *The tail suspension test: a new method for screening antidepressants in mice.* Psychopharmacology, 1985. 85(3): p. 367-370.

221. Dunn, A.J., *Animal models of depressive illness and sickness behavior.* Cancer Symptom Science: Measurement, Mechanisms, and Management, 2010: p. 82.

222. Castagné, V., et al., *Rodent models of depression: forced swim and tail suspension behavioral despair tests in rats and mice.* Current Protocols in Neuroscience, 2011. 55(1): p. 8.10 A. 1-8.10 A. 14.

223. Rosenfeld, C.S. and S.A. Ferguson, *Barnes maze testing strategies with small and large rodent models.* J Vis Exp, 2014(84): p. e51194.

224. McLay, R.N., S.M. Freeman, and J.E. Zadina, *Chronic corticosterone impairs memory performance in the Barnes maze.* Physiology & behavior, 1998. 63(5): p. 933-937.

225. Fedorova, I., et al., *An n-3 fatty acid deficient diet affects mouse spatial learning in the Barnes circular maze.* Prostaglandins, Leukotrienes and Essential Fatty Acids, 2007. 77(5-6): p. 269-277.

226. O'leary, T.P. and R.E. Brown, *The effects of apparatus design and test procedure on learning and memory performance of C57BL/6J mice on the Barnes maze.* Journal of neuroscience methods, 2012. 203(2): p. 315-324.

227. Yang, M., et al., *Semaphorin 3A Contributes To Secondary Blood-Brain Barrier Damage After Traumatic Brain Injury.* Front Cell Neurosci, 2019. 13: p. 117.

228. Flierl, M.A., et al., *Mouse closed head injury model induced by a weight-drop device.* Nature protocols, 2009. 4(9): p. 1328.

229. Bolkvadze, T. and A. Pitkänen, *Development of post-traumatic epilepsy after controlled cortical impact and lateral fluid-percussion-induced brain injury in the mouse.* Journal of neurotrauma, 2012. 29(5): p. 789-812.

230. Terpolilli, N.A., et al., *Inhaled nitric oxide reduces secondary brain damage after traumatic brain injury in mice.* Journal of Cerebral Blood Flow & Metabolism, 2013. 33(2): p. 311-318.

231. Clark, R.S., et al., *Neutrophil accumulation after traumatic brain injury in rats: comparison of weight drop and controlled cortical impact models.* Journal of neurotrauma, 1994. 11(5): p. 499-506.

232. Zhang, Y.P., et al., *Traumatic brain injury using mouse models.* Translational stroke research, 2014. 5(4): p. 454-471.

233. Viano, D.C., et al., *Evaluation of three animal models for concussion and serious brain injury.* Annals of biomedical engineering, 2012. 40(1): p. 213-226.

234. Spain, A., et al., *Mild fluid percussion injury in mice produces evolving selective axonal pathology and cognitive deficits relevant to human brain injury.* Journal of neurotrauma, 2010. 27(8): p. 1429-1438.

235. Dixon, C.E., J.W. Lighthall, and T.E. Anderson, *Physiologic, histopathologic, and cineradiographic characterization of a new fluid-percussion model of experimental brain injury in the rat.* J Neurotrauma, 1988. 5(2): p. 91-104.

236. Hunt, R.F., S.W. Scheff, and B.N. Smith, *Posttraumatic epilepsy after controlled cortical impact injury in mice.* Experimental neurology, 2009. 215(2): p. 243-252.

237. Dixon, C.E., et al., *A controlled cortical impact model of traumatic brain injury in the rat.* Journal of neuroscience methods, 1991. 39(3): p. 253-262.

238. Schwarzmaier, S.M., et al., *Endothelial nitric oxide synthase mediates arteriolar vasodilatation after traumatic brain injury in mice.* Journal of neurotrauma, 2015. 32(10): p. 731-738.

239. Gilmer, L.K., K.N. Roberts, and S.W. Scheff, *Efficacy of progesterone following a moderate unilateral cortical contusion injury.* Journal of neurotrauma, 2008. 25(6): p. 593-602.

240. Trabold, R., et al., *Role of vasopressin V1a and V2 receptors for the development of secondary brain damage after traumatic brain injury in mice.* Journal of neurotrauma, 2008. 25(12): p. 1459-1465.

241. Schwarzmaier, S.M. and N. Plesnila, *Contributions of the immune system to the pathophysiology of traumatic brain injury–evidence by intravital microscopy.* Frontiers in cellular neuroscience, 2014. 8: p. 358.

242. Terpolilli, N.A., et al., *The novel nitric oxide synthase inhibitor 4-amino-tetrahydro-L-biopterine prevents brain edema formation and intracranial hypertension following traumatic brain injury in mice.* Journal of neurotrauma, 2009. 26(11): p. 1963-1975.

243. Zweckberger, K. and N. Plesnila, *Anatibant®, a selective non-peptide bradykinin B2 receptor antagonist, reduces intracranial hypertension and histopathological damage after experimental traumatic brain injury.* Neuroscience letters, 2009. 454(2): p. 115-117.

244. Hall, E.D., et al., *Evolution of post-traumatic neurodegeneration after controlled cortical impact traumatic brain injury in mice and rats as assessed by the de Olmos silver and fluorojade staining methods.* Journal of neurotrauma, 2008. 25(3): p. 235-247.

245. Clausen, F., et al., *Neutralization of interleukin‐1β modifies the inflammatory response and improves histological and cognitive outcome following traumatic brain injury in mice.* European Journal of Neuroscience, 2009. 30(3): p. 385-396.

246. Saatman, K.E., et al., *Differential behavioral and histopathological responses to graded cortical impact injury in mice.* Journal of neurotrauma, 2006. 23(8): p. 1241-1253.

247. Loane, D.J., et al., *Progressive neurodegeneration after experimental brain trauma: association with chronic microglial activation.* J Neuropathol Exp Neurol, 2014. 73(1): p. 14-29.

248. Pischiutta, F., et al., *Single severe traumatic brain injury produces progressive pathology with ongoing contralateral white matter damage one year after injury.* Exp Neurol, 2018. 300: p. 167-178.

249. Campos-Pires, R., et al., *Xenon improves long-term cognitive function, reduces neuronal loss and chronic neuroinflammation, and improves survival after traumatic brain injury in mice.* British journal of anaesthesia, 2019. 123(1): p. 60-73.

250. Milidonis, X., et al., *Magnetic resonance imaging in experimental stroke and comparison with histology: systematic review and meta-analysis.* Stroke, 2015. 46(3): p. 843-851.

251. Bradley, K., et al., *Serial brain MRI at 3–6 month intervals as a surrogate marker for Alzheimer's disease.* The British journal of radiology, 2002. 75(894): p. 506-513.

252. Barzó, P., et al., *Magnetic resonance imaging—monitored acute blood-brain barrier changes in experimental traumatic brain injury.* Journal of neurosurgery, 1996. 85(6): p. 1113-1121.

253. Foley, L.M., et al., *Magnetic resonance imaging assessment of macrophage accumulation in mouse brain after experimental traumatic brain injury.* Journal of neurotrauma, 2009. 26(9): p. 1509-1519.

254. Koretsky, A.P., *New developments in magnetic resonance imaging of the brain.* NeuroRx, 2004. 1(1): p. 155-164.

255. Kochanek, P., et al., *Severe controlled cortical impact in rats: Assessment of cerebral edema, blood flow, and contusion volume.* Restorative Neurology and Neuroscience, 1996. 2(10): p. 116.

256. Keren, O., J. Reznik, and Z. Groswasser, *Combined motor disturbances following severe traumatic brain injury: an integrative long-term treatment approach.* Brain injury, 2001. 15(7): p. 633-638.

257. Jorge, R.E., et al., *Major depression following traumatic brain injury.* Archives of general psychiatry, 2004. 61(1): p. 42-50.

258. Vakil, E., *The effect of moderate to severe traumatic brain injury (TBI) on different aspects of memory: a selective review.* Journal of clinical and experimental neuropsychology, 2005. 27(8): p. 977-1021.

259. Tomberg, T., et al., *Coping strategies, social support, life orientation and health-related quality of life following traumatic brain injury.* Brain Injury, 2005. 19(14): p. 1181-1190.

260. Ciurli, P., et al., *Neuropsychiatric disorders in persons with severe traumatic brain injury: prevalence, phenomenology, and relationship with demographic, clinical, and functional features.* The Journal of head trauma rehabilitation, 2011. 26(2): p. 116-126.

261. Stanley, J.L., et al., *The mouse beam walking assay offers improved sensitivity over the mouse rotarod in determining motor coordination deficits induced by benzodiazepines.* Journal of Psychopharmacology, 2005. 19(3): p. 221-227.

262. Rogers, D.C., et al., *Correlation between motor impairment and infarct volume after permanent and transient middle cerebral artery occlusion in the rat.* Stroke, 1997. 28(10): p. 2060-2066.

263. Fujimoto, S.T., et al., *Motor and cognitive function evaluation following experimental traumatic brain injury.* Neuroscience & biobehavioral reviews, 2004. 28(4): p. 365-378.

264. Dixon, C.E., et al., *A fluid percussion model of experimental brain injury in the rat.* Journal of neurosurgery, 1987. 67(1): p. 110-119.

265. Berman, R.F., B.H. Verweij, and J.P. Muizelaar, *Neurobehavioral protection by the neuronal calcium channel blocker ziconotide in a model of traumatic diffuse brain injury in rats.* Journal of neurosurgery, 2000. 93(5): p. 821-828.

266. Mikawa, S., et al., *Attenuation of acute and chronic damage following traumatic brain injury in copper, zinc—superoxide dismutase transgenic mice.* Journal of neurosurgery, 1996. 85(5): p. 885-891.

267. Yan, H.Q., et al., *Evaluation of combined fibroblast growth factor-2 and moderate hypothermia therapy in traumatically brain injured rats.* Brain research, 2000. 887(1): p. 134-143.

268. Chao, O., et al., *The grid-walking test: assessment of sensorimotor deficits after moderate or severe dopamine depletion by 6-hydroxydopamine lesions in the dorsal striatum and medial forebrain bundle.* Neuroscience, 2012. 202: p. 318-325.

269. Modo, M., et al., *Neurological sequelae and long-term behavioural assessment of rats with transient middle cerebral artery occlusion.* Journal of neuroscience methods, 2000. 104(1): p. 99-109.

270. Morris, R., *Developments of a water-maze procedure for studying spatial learning in the rat.* Journal of neuroscience methods, 1984. 11(1): p. 47-60.

271. Barnes, C.A., *Memory deficits associated with senescence: a neurophysiological and behavioral study in the rat.* Journal of comparative and physiological psychology, 1979. 93(1): p. 74.

272. Morris, R.G., et al., *Place navigation impaired in rats with hippocampal lesions.* Nature, 1982. 297(5868): p. 681.

273. Clausen, F., et al., *Correlation of hippocampal morphological changes and morris water maze performance after cortical contusion injury in rats.* Neurosurgery, 2005. 57(1): p. 154-163.

274. Floyd, C.L., et al., *Craniectomy position affects morris water maze performance and hippocampal cell loss after parasagittal fluid percussion.* Journal of neurotrauma, 2002. 19(3): p. 303-316.

275. Vink, R., et al., *Magnesium attenuates persistent functional deficits following diffuse traumatic brain injury in rats.* Neuroscience letters, 2003. 336(1): p. 41-44.

276. Nimmo, A., et al., *Neurogenic inflammation is associated with development of edema and functional deficits following traumatic brain injury in rats.* Neuropeptides, 2004. 38(1): p. 40-47.

277. Bach, M.E., et al., *Impairment of spatial but not contextual memory in CaMKII mutant mice with a selective loss of hippocampal LTP in the range of the ϑ frequency.* Cell, 1995. 81(6): p. 905-915.

278. Kirby, L.G., et al., *The effects of different stressors on extracellular 5-hydroxytryptamine and 5-hydroxyindoleacetic acid.* Brain research, 1997. 760(1-2): p. 218-230.

279. Iivonen, H., et al., *Hypothermia in mice tested in Morris water maze.* Behavioural brain research, 2003. 141(2): p. 207-213.

280. Polderman, K.H., *Induced hypothermia and fever control for prevention and treatment of neurological injuries.* The Lancet, 2008. 371(9628): p. 1955-1969.

281. Porsolt, R., A. Bertin, and M. Jalfre, *Behavioral despair in mice: a primary screening test for antidepressants.* Archives internationales de pharmacodynamie et de therapie, 1977. 229(2): p. 327-336.

282. Cryan, J.F., C. Mombereau, and A. Vassout, *The tail suspension test as a model for assessing antidepressant activity: review of pharmacological and genetic studies in mice.* Neuroscience & Biobehavioral Reviews, 2005. 29(4-5): p. 571-625.

283. Porsolt, R.D., et al., *Rodent models of depression: forced swimming and tail suspension behavioral despair tests in rats and mice.* Current protocols in neuroscience, 2001. 14(1): p. 8.10 A. 1-8.10 A. 10.

284. Taltavull, J., et al., *Severe brain hypothermia as a factor underlying behavioral immobility during cold-water forced swim.* Brain research, 2003. 975(1-2): p. 244-247.

285. Walker, W.C. and T.C. Pickett, *Motor impairment after severe traumatic brain injury: A longitudinal multicenter study.* J Rehabil Res Dev, 2007. 44(7): p. 975-82.

286. Basford, J.R., et al., *An assessment of gait and balance deficits after traumatic brain injury.* Arch Phys Med Rehabil, 2003. 84(3): p. 343-9.

287. Hillier, S.L., M.H. Sharpe, and J. Metzer, *Outcomes 5 years post-traumatic brain injury (with further reference to neurophysical impairment and disability).* Brain Inj, 1997. 11(9): p. 661-75.

288. Zanier, E.R., et al., *Fractalkine receptor deficiency is associated with early protection but late worsening of outcome following brain trauma in mice.* J Neurotrauma, 2016. 33(11): p. 1060-1072.

289. Dénes, Z., *The influence of severe malnutrition on rehabilitation in patients with severe head injury.* Disability and rehabilitation, 2004. 26(19): p. 1163-1165.

290. Joo, H., et al., *Icariin Improves Functional Behavior in a Mouse Model of Traumatic Brain Injury and Promotes Synaptic Plasticity Markers.* Planta Med, 2019. 85(3): p. 231-238.

291. Zanier, E.R., et al., *Six‐month ischemic mice show sensorimotor and cognitive deficits associated with brain atrophy and axonal disorganization.* CNS neuroscience & therapeutics, 2013. 19(9): p. 695-704.

292. Brooks, S.P. and S.B. Dunnett, *Tests to assess motor phenotype in mice: a user's guide.* Nature Reviews Neuroscience, 2009. 10(7): p. 519.

293. Kim, E., et al., *Neuropsychiatric complications of traumatic brain injury: a critical review of the literature (a report by the ANPA Committee on Research).* The Journal of neuropsychiatry and clinical neurosciences, 2007. 19(2): p. 106-127.

294. Seel, R.T., et al., *Depression after traumatic brain injury: a National Institute on Disability and Rehabilitation Research Model Systems multicenter investigation.* Arch Phys Med Rehabil, 2003. 84(2): p. 177-184.

295. Schwarzbold, M., et al., *Psychiatric disorders and traumatic brain injury.* Neuropsychiatric disease and treatment, 2008.

296. Jorge, R.E., et al., *Depression following traumatic brain injury: a 1 year longitudinal study.* J Affect Disord, 1993. 27(4): p. 233-43.

297. Jorge, R.E., et al., *Depression and anxiety following traumatic brain injury.* The Journal of neuropsychiatry and clinical neurosciences, 1993.

298. Holsinger, T., et al., *Head injury in early adulthood and the lifetime risk of depression.* Archives of general psychiatry, 2002. 59(1): p. 17-22.

299. Washington, P.M., et al., *The effect of injury severity on behavior: a phenotypic study of cognitive and emotional deficits after mild, moderate, and severe controlled cortical impact injury in mice.* J Neurotrauma, 2012. 29(13): p. 2283-2296.

300. Milman, A., et al., *DHEAS repeated treatment improves cognitive and behavioral deficits after mild traumatic brain injury.* European Neuropsychopharmacology, 2008. 18(3): p. 181-187.

301. Zohar, O., et al., *Behavioral consequences of minimal traumatic brain injury in mice.* Acta Neurobiol Exp (Wars), 2011. 71(1): p. 36-45.

302. Viana, A.F., et al., *Kinin B1 receptors mediate depression-like behavior response in stressed mice treated with systemic E. coli lipopolysaccharide.* J Neuroinflammation, 2010. 7: p. 98.

303. Jorge, R.E. and S.E. Starkstein, *Pathophysiologic aspects of major depression following traumatic brain injury.* The Journal of head trauma rehabilitation, 2005. 20(6): p. 475-487.

304. Rao, V., et al., *Neuroanatomical correlates of depression in post traumatic brain injury: preliminary results of a pilot study.* The Journal of neuropsychiatry and clinical neurosciences, 2010. 22(2): p. 231-235.

305. Whitnall, L., et al., *Disability in young people and adults after head injury: 5–7 year follow up of a prospective cohort study.* Journal of Neurology, Neurosurgery & Psychiatry, 2006. 77(5): p. 640-645.

306. Levin, H.S., et al., *Neurobehavioral outcome 1 year after severe head injury: experience of the Traumatic Coma Data Bank.* J Neurosurg, 1990. 73(5): p. 699-709.

307. Levin, H.S., R.G. Grossman, and P.J. Kelly, *Short-term recognition memory in relation to severity of head injury.* Cortex, 1976. 12(2): p. 175-182.

308. Dikmen, S.S., et al., *Cognitive outcome following traumatic brain injury.* The Journal of head trauma rehabilitation, 2009. 24(6): p. 430-438.

309. Ponsford, J. and G. Kinsella, *Attentional deficits following closed-head injury.* Journal of Clinical and Experimental Neuropsychology, 1992. 14(5): p. 822-838.

310. Levin, H. and M.F. Kraus, *The frontal lobes and traumatic brain injury.* The Journal of neuropsychiatry and clinical neurosciences, 1994.

311. Draper, K. and J. Ponsford, *Cognitive functioning ten years following traumatic brain injury and rehabilitation.* Neuropsychology, 2008. 22(5): p. 618.

312. Stenberg, M., et al., *Cognitive impairment after severe traumatic brain injury, clinical course and impact on outcome: a Swedish-Icelandic study.* Behavioural neurology, 2015. 2015.

313. Pierce, J., et al., *Enduring cognitive, neurobehavioral and histopathological changes persist for up to one year following severe experimental brain injury in rats.* Neuroscience, 1998. 87(2): p. 359-369.

314. Lindner, M.D., et al., *Dissociable long-term cognitive deficits after frontal versus sensorimotor cortical contusions.* J Neurotrauma, 1998. 15(3): p. 199-216.

315. Meehan III, W.P., et al., *Increasing recovery time between injuries improves cognitive outcome after repetitive mild concussive brain injuries in mice.* Neurosurgery, 2012. 71(4): p. 885-892.

316. McAllister, T.W., *Neurobiological consequences of traumatic brain injury.* Dialogues in clinical neuroscience, 2011. 13(3): p. 287.

317. Lacoste, B., et al., *Cognitive and cerebrovascular improvements following kinin B 1 receptor blockade in Alzheimer's disease mice.* Journal of neuroinflammation, 2013. 10(1): p. 850.

318. Dixon, C., et al., *One-year study of spatial memory performance, brain morphology, and cholinergic markers after moderate controlled cortical impact in rats.* Journal of neurotrauma, 1999. 16(2): p. 109-122.

319. Smith, D.H., et al., *Persistent memory dysfunction is associated with bilateral hippocampal damage following experimental brain injury.* Neurosci Lett, 1994. 168(1-2): p. 151-154.

320. DeKosky, S.T., et al., *Time course analysis of hippocampal nerve growth factor and antioxidant enzyme activity following lateral controlled cortical impact brain injury in the rat.* J Neurotrauma, 2004. 21(5): p. 491-500.

321. Arciniegas, D.B., et al., *Reduced hippocampal volume in association with p50 nonsuppression following traumatic brain injury.* The Journal of neuropsychiatry and clinical neurosciences, 2001. 13(2): p. 213-221.

322. Tomaiuolo, F., et al., *Gross morphology and morphometric sequelae in the hippocampus, fornix, and corpus callosum of patients with severe non-missile traumatic brain injury without macroscopically detectable lesions: a T1 weighted MRI study.* Journal of Neurology, Neurosurgery & Psychiatry, 2004. 75(9): p. 1314-1322.

323. Hicks, R., et al., *Mild experimental brain injury in the rat induces cognitive deficits associated with regional neuronal loss in the hippocampus.* J Neurotrauma, 1993. 10(4): p. 405-414.

324. Osmakov, D., Y.A. Andreev, and S. Kozlov, *Acid-sensing ion channels and their modulators.* Biochemistry (Moscow), 2014. 79(13): p. 1528-1545.

325. Smith, M., *Monitoring intracranial pressure in traumatic brain injury.* Anesthesia & Analgesia, 2008. 106(1): p. 240-248.

326. Belli, A., et al., *Metabolic failure precedes intracranial pressure rises in traumatic brain injury: a microdialysis study.* Acta Neurochir (Wien), 2008. 150(5): p. 461-470.

327. Miller, J.D., *Head injury and brain ischaemia-implications for therapy.* Br J Anaesth, 1985. 57(1): p. 120-130.

328. Rehncrona, S., I. Rosén, and B.K. Siesjö, *Brain lactic acidosis and ischemic cell damage: 1. Biochemistry and neurophysiology.* Journal of Cerebral Blood Flow & Metabolism, 1981. 1(3): p. 297-311.

329. Raichle, M.E., *The pathophysiology of brain ischemia.* Annals of Neurology: Official Journal of the American Neurological Association and the Child Neurology Society, 1983. 13(1): p. 2-10.

330. Weilinger, N.L., et al., *Ionotropic receptors and ion channels in ischemic neuronal death and dysfunction.* Acta Pharmacologica Sinica, 2013. 34(1): p. 39.

331. Wang, Y., et al., *Intracellular ASIC1a regulates mitochondrial permeability transition-dependent neuronal death.* Cell death and differentiation, 2013. 20(10): p. 1359.

332. Rosenzweig, E.S. and C.A. Barnes, *Impact of aging on hippocampal function: plasticity, network dynamics, and cognition.* Progress in neurobiology, 2003. 69(3): p. 143-179.

333. Swaine, B.R. and S.J. Sullivan, *Longitudinal profile of early motor recovery following severe traumatic brain injury.* Brain Inj, 1996. 10(5): p. 347-66.

334. Zanier, E.R., et al., *Fractalkine receptor deficiency is associated with early protection but late worsening of outcome following brain trauma in mice.* Journal of neurotrauma, 2016. 33(11): p. 1060-1072.

335. McCarthy, C.A., et al., *PcTx1 affords neuroprotection in a conscious model of stroke in hypertensive rats via selective inhibition of ASIC1a.* Neuropharmacology, 2015. 99: p. 650-7.

336. Mergenthaler, P., U. Dirnagl, and A. Meisel, *Pathophysiology of stroke: lessons from animal models.* Metab Brain Dis, 2004. 19(3-4): p. 151-67.

337. Kreutzer, J.S., R.T. Seel, and E. Gourley, *The prevalence and symptom rates of depression after traumatic brain injury: a comprehensive examination.* Brain Inj, 2001. 15(7): p. 563-576.

338. Rosenthal, M., B.K. Christensen, and T.P. Ross, *Depression following traumatic brain injury.* Arch Phys Med Rehabil, 1998. 79(1): p. 90-103.

339. Bombardier, C.H., et al., *Rates of major depressive disorder and clinical outcomes following traumatic brain injury.* JAMA, 2010. 303(19): p. 1938-1945.

340. Dikmen, S.S., et al., *Natural history of depression in traumatic brain injury.* Archives of physical medicine and rehabilitation, 2004. 85(9): p. 1457-1464.

341. Milman, A., et al., *Mild traumatic brain injury induces persistent cognitive deficits and behavioral disturbances in mice.* J Neurotrauma, 2005. 22(9): p. 1003-1010.

342. Popovitz, J.M.B., S.P. Mysore, and H. Adwanikar, *Long-term effects of traumatic brain injury on anxiety-like behaviors in mice: behavioral and neural correlates.* Frontiers in behavioral neuroscience, 2019. 13: p. 6.

343. Bajwa, N.M., et al., *Mild concussion, but not moderate traumatic brain injury, is associated with long-term depression-like phenotype in mice.* PLoS One, 2016. 11(1): p. e0146886.

344. Jorge, R.E. and S.E. Starkstein, *Pathophysiologic aspects of major depression following traumatic brain injury.* J Head Trauma Rehabil, 2005. 20(6): p. 475-87.

345. Coryell, M.W., et al., *Acid-sensing ion channel-1a in the amygdala, a novel therapeutic target in depression-related behavior.* Journal of Neuroscience, 2009. 29(17): p. 5381-5388.

346. Ponsford, J., K. Draper, and M. Schönberger, *Functional outcome 10 years after traumatic brain injury: its relationship with demographic, injury severity, and cognitive and emotional status.* Journal of the International Neuropsychological Society, 2008. 14(2): p. 233-242.

347. Kraus, M.F., et al., *White matter integrity and cognition in chronic traumatic brain injury: a diffusion tensor imaging study.* Brain, 2007. 130(10): p. 2508-2519.

348. McInnes, K., et al., *Mild Traumatic Brain Injury (mTBI) and chronic cognitive impairment: A scoping review.* PloS one, 2017. 12(4): p. e0174847.

349. Chen, Y., et al., *An experimental model of closed head injury in mice: pathophysiology, histopathology, and cognitive deficits.* J Neurotrauma, 1996. 13(10): p. 557-568.

350. Tucker, L.B., A.G. Velosky, and J.T. McCabe, *Applications of the Morris water maze in translational traumatic brain injury research.* Neuroscience & Biobehavioral Reviews, 2018. 88: p. 187-200.

351. Lindner, M.D., et al., *Dissociable long-term cognitive deficits after frontal versus sensorimotor cortical contusions.* Journal of neurotrauma, 1998. 15(3): p. 199-216.

352. Babikian, T., D. McArthur, and R.F. Asarnow, *Predictors of 1-month and 1-year neurocognitive functioning from the UCLA longitudinal mild, uncomplicated, pediatric traumatic brain injury study.* Journal of the International Neuropsychological Society, 2013. 19(2): p. 145-154.

353. Giza, C.C. and D.A. Hovda, *The new neurometabolic cascade of concussion.* Neurosurgery, 2014. 75(suppl_4): p. S24-S33.

7. List of abbreviations

AMPA	α-Amino-3-Hydroxy5-Methyl-4-Isoxazole-Propionic Acid
AQP4	Aquaporin 4
ASICs	Acid-Sensing Ion Channels
B1R	B1 receptor
B2R	B2 receptor
BBB	Blood Brain Barrier
CBF	Cerebral Blood Flow
CCI	Controlled Cortical Impact
CPP	Cerebral Perfusion Pressure
CT	Computed Tomography
CTE	Chronic Traumatic Encephalopathy
DAI	Diffuse Axonal Injury
DWI	Diffusion Weighted Imaging
GCS	Glasgow Coma Scale
ICP	Intracranial Cerebral Pressure
MAP	Mean Arterial Pressure
MMP-2	Matrix Metalloproteinase -2
MMP-9	Matrix Metalloproteinase -9
MRI	Magnetic Resonance Imaging
NKCC1	Na^+-K^+-$2Cl^-$ cotransporter
NFT	Neurofilament Tangle

NMDA	N-Methyl-D-Aspartic Acid
PFA	Paraformaldehyde
ROS	Reactive Oxygen Species
SAH	Subarachnoid Hemorrhage
SUR1- TRPM4	Sulfonylurea-Receptor 1 – Transient Receptor Potential Member 4
NaHCO3	Sodium Hydrogen Carbonate
T2W	T2-Weighted
TBI	Traumatic Brain Injury
tSAH	Traumatic Subarachnoid Hemorrhage
VEGF-A	Vascular Endothelial Growth Factor A
WHO	World Health Organization
MWM	Morris Water Maze
WT	Wild Type

8. Acknowledgments

At first, I would like to thank Prof. Dr. med. Nikolaus Plesnila for offering me the opportunity to join your research group and study in the ISD. Thank you for your excellent care and suggestions.

I also would like to thank my kind supervisor Nicole Terpolilli for your patience and scientific support.

I also would like to thank Dr. Farida Hellal and Burcu Seker Fatma for scientific discussions.

I also would like to thank Uta Mamrak and Hedwig Pietsch for your support in the laboratory.

I am really grateful to my colleagues: Susanne Schwarzmaier, Kathrin Nehrkorn, Burcu Seker Fatma, Mao Xiang, Joshua Shrouder, Eva Auffenberg, Ziyu Fan, Yue Hu, Xiangjiang Lin, Susana Valero Freitag, Rebecca Sienel, Igor Khalin, Bernhard, Wehn Antonia Clarissa, Samixa Pudasaini, Stergios Tsitos, and others in our group and the ISD, it is enjoyable for me to stay with you in past three years.

Many thanks to the Chinese Scholarship Council for offering me financial support to study in Germany.

Finally, I want to thank the most important people in my life: my parents, and my wife.

Affidavit

I, Shiqi Cheng, hereby confirm that my thesis entitled

Effect of bradykinin receptor 1 and acid-sensing ion channel 1a on outcome after experimental traumatic brain injury

is the result of my own work. I did not receive any help or support from commercial consultants. All sources and/or materials applied are listed and specified in the thesis.

Furthermore, I confirm that this thesis has not yet been submitted as part of another examination process neither in identical nor in similar form.

Place and date: Munich, 26.05.2020

Name: Shiqi Cheng